

AD-A048 881

FLORIDA UNIV GAINESVILLE COASTAL AND OCEANOGRAPHIC --ETC F/6 8/3
EVALUATION AND DEVELOPMENT OF WATER WAVE THEORIES FOR ENGINEERI--ETC(U)
NOV 74 R 6 DEAN DACW72-67-C-0009

UNCLASSIFIED

TR-14

CERC-SR-1-VOL-1

NL

1 OF 2

AD
A048881



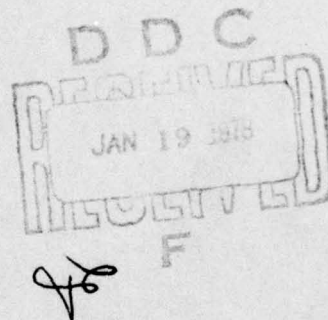
ADA04881

AD No. _____
DDC FILE COPY

①
SR - 1
OK
**Evaluation And Development Of
Water Wave Theories For
Engineering Application**

VOLUME I
Presentation Of Research Results
by
R.G. Dean

SPECIAL REPORT NO. 1
NOVEMBER 1974



Approved for public release;
distribution unlimited

Prepared for
U.S. ARMY, CORPS OF ENGINEERS
COASTAL ENGINEERING
RESEARCH CENTER

Kingman Building
Fort Belvoir, Va. 22060

Reprint or republication of any of this material shall give appropriate credit to the U.S. Army Coastal Engineering Research Center.

U.S. Army Coastal Engineering Research Center
Kingman Building
Fort Belvoir, Virginia 22060

(18) CERC

(19) SR-1-VOL-1

UNCLASSIFIED

SECURITY CLASSIFICATION OF THIS PAGE (When Data Entered)

REPORT DOCUMENTATION PAGE		READ INSTRUCTIONS BEFORE COMPLETING FORM
1. REPORT NUMBER SR-1	2. GOVT ACCESSION NO.	3. RECIPIENT'S CATALOG NUMBER
4. TITLE (and Subtitle) EVALUATION AND DEVELOPMENT OF WATER WAVE THEORIES FOR ENGINEERING APPLICATION • Volume I PRESENTATION OF RESEARCH RESULTS • VOL. II • TABULATION OF DIMENSIONLESS STREAM-FUNCTION • DEPENDENT VARIABLES		5. TYPE OF REPORT & PERIOD COVERED SPECIAL REPORT
7. AUTHOR(s) R. G. DEAN		6. PERFORMING ORG. REPORT NUMBER TECHNICAL REPORT NO. 14
(14) TR-14		8. CONTRACT OR GRANT NUMBER(s) DACW 72-67-C-0000
9. PERFORMING ORGANIZATION NAME AND ADDRESS COASTAL AND OCEANOGRAPHIC ENGINEERING LABORATORY COLLEGE OF ENGINEERING UNIVERSITY OF FLORIDA GAINESVILLE, FLORIDA 32611		10. PROGRAM ELEMENT, PROJECT, TASK AREA & WORK UNIT NUMBERS VO 4200
11. CONTROLLING OFFICE NAME AND ADDRESS DEPARTMENT OF THE ARMY COASTAL ENGINEERING RESEARCH CENTER KINGMAN BUILDING, FORT BELVOIR, VA 22060		12. REPORT DATE Nov 1974
14. MONITORING AGENCY NAME & ADDRESS (if different from Controlling Office)		13. NUMBER OF PAGES VOL. I - 133 VOL. II - 534
		15. SECURITY CLASS. (of this report) UNCLASSIFIED
		15a. DECLASSIFICATION/DOWNGRADING SCHEDULE
16. DISTRIBUTION STATEMENT (of this Report) APPROVED FOR PUBLIC RELEASE; DISTRIBUTION UNLIMITED		
17. DISTRIBUTION STATEMENT (of the abstract entered in Block 20, if different from Report)		
18. SUPPLEMENTARY NOTES		
19. KEY WORDS (Continue on reverse side if necessary and identify by block number) Coastal Engineering Dean's Stream-Function Wave Theory Water-Wave Theories Wave Tables		
20. ABSTRACT (Continue on reverse side if necessary and identify by block number) Volume I of this report presents the results of a research program to evaluate and develop water-wave theories for engineering application. Volume II presents wave tables developed for preliminary design in offshore problems. ✓ Volume I describes: (1) an evaluation of the degree to which various available wave theories satisfy the nonlinear water-wave mathematical formulation and (2) a comparison of water particle velocities measured in the laboratory with those predicted by a number of available wave theories. The results indicated that Dean's Stream-Function Wave Theory provided generally better agreement with both the mathematical formulation and (Continued)		

DDC
JAN 19 1978
RECEIVED

DD FORM 1 JAN 73 1473 EDITION OF 1 NOV 65 IS OBSOLETE

UNCLASSIFIED

SECURITY CLASSIFICATION OF THIS PAGE (When Data Entered)

408 006

over

UNCLASSIFIED

SECURITY CLASSIFICATION OF THIS PAGE(When Data Entered)

the laboratory data. Volume I also includes a number of examples illustrating the application of the wave tables (described below) to offshore design problems.

✓ Based on the evaluation phase described above, a set of wave tables was developed and is presented as Volume II. The tables consist of dimensionless quantities which describe the kinematic and dynamic fields of a two-dimensional progressive water wave. In addition, quantities are included which are directly applicable to frequently required design calculations and also parameters which should be of interest to the researcher and scientist. ←

ACCESSION for		
NTIS	White Section <input checked="" type="checkbox"/>	
DDC	Buff Section <input type="checkbox"/>	
UNANNOUNCED	<input type="checkbox"/>	
JUSTIFICATION		
BY		
DISTRIBUTION/AVAILABILITY NOTES		
Dist.	Avail.	Dist.
A		

UNCLASSIFIED

SECURITY CLASSIFICATION OF THIS PAGE(When Data Entered)

PREFACE

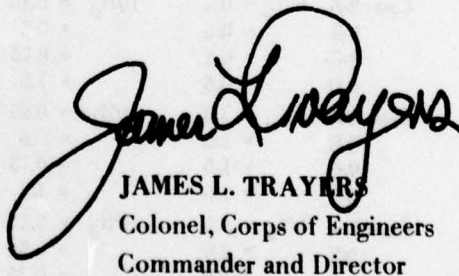
The U.S. Army Coastal Engineering Research Center (CERC) is publishing this report and collection of Stream-function tables to assist coastal engineers in the design of structures vulnerable to wave forces. The report was prepared by R. G. Dean, College of Engineering, University of Florida.

The author acknowledges the help of other people in the preparation of this report. E. Olsen and B. Beechley made many of the computer calculations and organized the results. R. A. Dalrymple assisted in the later phases by applying some of the Stream-function computer techniques which he has developed. M. P. O'Brien, senior civilian member of the Coastal Engineering Research Board offered constructive suggestions and discussions. J. Richard Weggel, Special Assistant to the Commander and Director, CERC, made several useful suggestions which simplified the application of the tables to design problems. D. Lee Harris, the contract monitor for CERC, provided encouragement and useful comments regarding the format of the tables. Reviews of an early draft by persons actively involved in offshore design or wave theory studies assisted in preparation of the report. The constructive comments and suggestions from these reviews are greatly appreciated.

This report was prepared for the Coastal Engineering Research Center under Contract DACW 72-67-C-0009 with the University of Florida.

NOTE: Comments on this publication are invited.

Approved for publication in accordance with Public Law 166, 79th Congress approved 31 July 1949, as supplemented by Public Law 172, 88th Congress, approved 7 November 1963.



JAMES L. TRAYERS
Colonel, Corps of Engineers
Commander and Director

TABLE OF CONTENTS

VOLUME II

CHAPTER		Page
I	INTRODUCTION TO TABLES	1
II	STREAM-FUNCTION THEORY TABULATIONS IN DIMENSIONLESS FORM FOR 40 SETS OF WAVE CHARACTERISTICS	13
Case	1-A $h/L_0 = 0.002$ $H/H_B = 0.25$	15
	1-B $= 0.002$ $= 0.5$	28
	1-C $= 0.002$ $= 0.75$	41
	1-D $= 0.002$ $= 1.0$	54
Case	2-A $h/L_0 = 0.005$ $H/H_B = 0.25$	67
	2-B $= 0.005$ $= 0.5$	80
	2-C $= 0.005$ $= 0.75$	93
	2-D $= 0.005$ $= 1.0$	106
Case	3-A $h/L_0 = 0.01$ $H/H_B = 0.25$	119
	3-B $= 0.01$ $= 0.5$	132
	3-C $= 0.01$ $= 0.75$	145
	3-D $= 0.01$ $= 1.0$	158
Case	4-A $h/L_0 = 0.02$ $H/H_B = 0.25$	171
	4-B $= 0.02$ $= 0.5$	184
	4-C $= 0.02$ $= 0.75$	197
	4-D $= 0.02$ $= 1.0$	210
Case	5-A $h/L_0 = 0.05$ $H/H_B = 0.25$	223
	5-B $= 0.05$ $= 0.5$	236
	5-C $= 0.05$ $= 0.75$	249
	5-D $= 0.05$ $= 1.0$	262
Case	6-A $h/L_0 = 0.1$ $H/H_B = 0.25$	275
	6-B $= 0.1$ $= 0.5$	288
	6-C $= 0.1$ $= 0.75$	301
	6-D $= 0.1$ $= 1.0$	314
Case	7-A $h/L_0 = 0.2$ $H/H_B = 0.25$	327
	7-B $= 0.2$ $= 0.5$	340
	7-C $= 0.2$ $= 0.75$	353
	7-D $= 0.2$ $= 1.0$	366
Case	8-A $h/L_0 = 0.5$ $H/H_B = 0.25$	379
	8-B $= 0.5$ $= 0.5$	392
	8-C $= 0.5$ $= 0.75$	405
	8-D $= 0.5$ $= 1.0$	418
Case	9-A $h/L_0 = 1.0$ $H/H_B = 0.25$	431
	9-B $= 1.0$ $= 0.5$	444
	9-C $= 1.0$ $= 0.75$	457
	9-D $= 1.0$ $= 1.0$	470
Case	10-A $h/L_0 = 2.0$ $H/H_B = 0.25$	483
	10-B $= 2.0$ $= 0.5$	496
	10-C $= 2.0$ $= 0.75$	509
	10-D $= 2.0$ $= 1.0$	522

TABLE OF CONTENTS

VOLUME I

	Page
ABSTRACT	ii
PREFACE	iii
LIST OF TABLES	vii
LIST OF FIGURES	viii
LIST OF SYMBOLS	xi
CHAPTER	
I INTRODUCTION	1
II STREAM FUNCTION WAVE THEORY	2
Introduction	2
Formulation	3
Differential Equation	3
Boundary Conditions	4
Bottom Boundary Condition (BBC)	4
Kinematic Free Surface Boundary Condition (KFSBC)	4
Dynamic Free Surface Boundary Condition (DFSBC)	4
The Stream-function Solution	6
III EVALUATION OF VALIDITIES OF WAVE THEORIES	6
Introduction	6
Discussion of Differences Between Stream-function and	
Other Wave Theories	6
Analytical Validity	8
Definition of Boundary Condition Errors	8
Results of Analytical Validity Comparison	10
Comparison with Stream-function Theory Developed by	
Von Schwind and Reid	18
Conclusions Resulting from the Analytical Validity Study	18
Experimental Validity	22
Conclusions Resulting from the Experimental Validity Study	25

TABLE OF CONTENTS—Continued

CHAPTER		Page
IV	DESCRIPTION OF TABLES	38
	Introduction	38
	Variables Presented in Tabular Form	38
	Internal Field Variables Depending on θ and S	45
	Horizontal Water Particle Velocity Component, $u(\theta, S)$	45
	Vertical Water Particle Velocity Component, $w(\theta, S)$	47
	Horizontal Water Particle Acceleration, Du/Dt	47
	Vertical Water Particle Acceleration, Dw/Dt	47
	Drag Force Component, $F_D(\theta, S)$	47
	Inertia Force Component, $F_I(\theta, S)$	47
	Drag Moment Component, $M_D(\theta, S)$	47
	Inertia Moment Component, $M_I(\theta, S)$	47
	Dynamic Pressure Component, $p_D(\theta, S)$	47
	Variables Depending on θ Only	47
	Water Surface Displacement, $\eta(\theta)$	47
	Total Drag Force Component, $F_D(\theta)$	47
	Total Inertia Force Component, $F_I(\theta)$	49
	Total Drag Moment Component, $M_D(\theta)$	49
	Total Inertia Moment Component, $M_I(\theta)$	49
	Kinematic Free Surface Boundary Condition Error, $\epsilon_1(\theta)$	49
	Dynamic Free Surface Boundary Condition Error, $\epsilon_2(\theta)$	49
	Overall Variables (do not depend on θ or S)	50
	Wavelength, L	50
	Average Potential Energy, PE	50
	Average Kinetic Energy, KE	50
	Average Total Energy, TE	50
	Average Total Energy Flux, F_{TE}	51
	Group Velocity, C_G	51
	Average Momentum, M	51
	Average Momentum Flux in Wave Direction, F_{m_x}	51
	Average Momentum Flux Transverse to Wave Direction, F_{m_y}	51
	Kinematic Free Surface Boundary Condition Errors, ϵ_1	52
	Dynamic Free Surface Boundary Condition Errors, ϵ_2	52
	Kinematic Free Surface Breaking Parameter, β_1	52
	Dynamic Free Surface Breaking Parameter, β_2	52
	Variables Presented in Graphical Form—Combined Effect of Shoaling and Refraction	52

TABLE OF CONTENTS—Continued

CHAPTER	Page
V EXAMPLES ILLUSTRATING USE OF WAVE TABLES	58
Introduction	58
Example 1—Deck Elevation and Wave Forces and Moments on an Offshore Platform	58
Deck Elevation	60
Forces on Member "a"	60
Forces on Member "b"	61
Forces on Member "c"	63
Moments on Member "a"	65
Moments on Member "b"	69
Moments on Member "c"	69
Example 2—Wave Characteristics, Kinematics and Pressure Fields . .	74
Wavelength	74
Wave Profile	74
Water Particle Kinematics	75
Dynamic Pressure	78
Example 3—Free Surface Boundary Condition Errors	78
Distributed Boundary Condition Errors	78
Overall Kinematic Free Surface Boundary Condition Errors . . .	78
Overall Dynamic Free Surface Boundary Condition Errors	81
Example 4—Calculation of Energy, Momentum, and Energy and Momentum Fluxes	82
Average Potential Energy	82
Average Kinetic Energy	82
Total Energy	82
Energy Flux	82
Group Velocity	82
Average Momentum	83
Average Momentum Flux in Wave Direction	83
Average Momentum Flux Transverse to Wave Direction	83
Example 5—Free Surface Breaking Parameters	83
Example 6—Combined Shoaling-refraction	84
Example 6-a	84
Example 6-b	85

TABLE OF CONTENTS—Continued

CHAPTER	Page
Example 7—Use of Tables for Nontabulated Wave Conditions	86
Method	88
Example 7-a—Numerical Illustration of Interpolation Procedure .	90
Example 7-b—Assessment of the Interpolation Method	93
VI SUMMARY	96
VII REFERENCES	97
APPENDIX	
I NUMERICAL SOLUTION OF STREAM-FUNCTION PARAMETERS .	99
Introduction	99
Review of Problem Formulation	99
Stream-function Solution	100
II DEVELOPMENT OF COMBINED SHOALING-REFRACTION COEFFICIENTS	103
Introduction	103
Background	103
Method	103
Solution	105
III SAMPLE SET OF WAVE TABLES FOR CASE 4-D	108

TABLES

Table

A Water-wave Theories Included in Evaluation Presented by Dean (1968a) . .	9
B Experimental Waves; Characteristics and Variables Measured	26
C Standard Deviation of Differences Between Horizontal Velocities:	
Measured vs. Predicted	37
D Internal Field Variables (Functions of θ and S)	40
E Variables Depending on θ Only	42
F Overall Variables (Do Not Depend on θ or S)	43
G Horizontal Wave Forces on Member "a"	61

TABLES—Continued

Table	Page
H Horizontal Wave Forces on Member "b"	63
I Horizontal Wave Forces on Member "c"	66
J Summary of Maximum Wave Forces on Several Platform Components . . .	68
K Wave Moments (About Mudline) on Member "a"	69
L Wave Moments (About Mudline) on Member "b"	71
M Wave Moments (About Mudline) on Member "c"	71
N Summary of Maximum Wave Forces and Moments	74
O Calculated Wave Profile, Kinematics, and Dynamic Pressure	76
P Free Surface Boundary Condition Errors	79
Q Summary of $F'_D(0^\circ, \text{Surf.})$ Required for Example 7-a	91
R Wave Characteristics Selected for Accuracy Evaluation of Interpolation Method	93
S Summary of Percentage Differences Between Values Determined by Stream-function Solutions and by Interpolation	94

FIGURES

Figure		Page
1	Definition sketch, progressive wave system	3
2	Wave characteristics selected for evaluation	11
3	Dimensionless error, $\sqrt{\epsilon_1^2}$, in kinematic free surface boundary condition, $H/H_B = 0.25$; all wave theories	12
4	Dimensionless error, $\sqrt{\epsilon_1^2}$, in kinematic free surface boundary condition, $H/H_B = 1.0$; all wave theories	13
5	Dimensionless error, $\sqrt{\epsilon_2^2}/H$, in dynamic free surface boundary condition, $H/H_B = 0.25$; all wave theories	14
6	Dimensionless error, $\sqrt{\epsilon_2^2}/H$, in dynamic free surface boundary condition, $H/H_B = 1.0$; all wave theories	15
7	Periodic wave theories providing best fit to dynamic free surface boundary condition (Analytical theories only)	16
8	Periodic wave theories providing best fit to dynamic free surface boundary condition (Analytical and Stream-function V theories)	18
9	Comparison of errors in dynamic free surface boundary condition for three numerical wave theories, Wave no. 1	19
10	Comparison of errors in dynamic free surface boundary condition for three numerical wave theories, Wave no. 2	20

FIGURES—Continued

Figure		Page
11	Comparison of errors in dynamic free surface boundary condition for three numerical wave theories, Wave no. 3	21
12	Experimental wave characteristics	24
13	Horizontal water particle velocity under the crest, Case 1	27
14	Horizontal water particle velocity under the crest, Case 2	28
15	Horizontal water particle velocity under the crest, Case 3	29
16	Horizontal water particle velocity under the crest, Case 4	30
17	Horizontal water particle velocity under the crest, Case 5	31
18	Horizontal water particle velocity under the crest, Case 6	32
19	Horizontal water particle velocity under the crest, Case 7	33
20	Horizontal water particle velocity under the crest, Case 8	34
21	Vertical water particle velocity, Case 9	35
22	Free surface elevation, Case 10	36
23	Wave characteristics selected for tabulation	39
24	Example output for dimensionless horizontal velocity component field . . .	46
25	Combined shoaling-refraction for a deepwater wave direction, $\alpha_o = 0^\circ$. . .	53
26	Combined shoaling-refraction for a deepwater wave direction, $\alpha_o = 10^\circ$. . .	54
27	Combined shoaling-refraction for a deepwater wave direction, $\alpha_o = 20^\circ$. . .	55
28	Combined shoaling-refraction for a deepwater wave direction, $\alpha_o = 40^\circ$. . .	56
29	Combined shoaling-refraction for a deepwater wave direction, $\alpha_o = 60^\circ$. . .	57
30	Definition sketch, wave approaching platform	59
31	Horizontal wave forces on member "a"	62
32	Horizontal wave forces on member "b"	64
33	Horizontal wave forces on member "c"	67
34	Wave moments on member "a"	70
35	Wave moments on member "b"	72
36	Wave moments on member "c"	73
37	Example calculations of wave profile, kinematics and dynamic pressure . . .	77
38	Free surface boundary condition errors	80
39	Example 6-b, shoaling-refraction for $\alpha_o = 10^\circ$. Interpolation from $h/L_o = 0.0814$ and $H/L_o = 0.0271$ to $h/L_o = 0.0542$	87
40	Interpolation aid	89
41	Auxiliary plot of F'_D for example 7a	92
II-1	Definition sketch for shoaling-refraction considerations	104
II-2	Variation of F'_{TE} and L' for $h/L_o = 0.02$	106

SYMBOLS

Symbol	Description
BBC	Bottom boundary condition, defined by Equation (10)
C	Wave celerity
C_D	Drag coefficient
C_G	Group velocity
C'_G	Dimensionless group velocity, defined by Equation (42)
C_M	Inertia coefficient
D	File diameter
DFSBC	Dynamic free surface boundary condition, defined in Equation (12)
DFSBP	Dynamic free surface breaking parameter defined in Equation (49)
\bar{D}	Subscript "D" denoting "design" value, also drag component of force and moment
e_2	Dynamic free surface boundary condition error, utilized by Chappelear and Von Schwind and Reid defined in Equation (17a)
E_1	Root mean square error in kinematic free surface boundary condition
E_2	Root mean square error in dynamic free surface boundary condition
E	Mean square error in dynamic free surface boundary condition
F_D	Drag force component
F'_D	Dimensionless drag force component, defined by Equation (25)
F_I	Inertia force component
F'_I	Dimensionless inertia force component, defined by Equation (26)
F_{TE}	Total energy flux in direction of wave propagation, per unit width
F'_{TE}	Dimensionless form of F_{TE} , defined by Equation (41)
F_{m_x}	Momentum flux in direction of wave propagation
F'_{m_x}	Dimensionless form of F_{m_x} , defined by Equation (44)
F_{m_y}	Momentum flux transverse to direction of wave propagation
F'_{m_y}	Dimensionless form of F_{m_y} , defined by Equation (45)
g	Gravitational constant
h	Water depth
h'	Freeboard used in establishing deck elevation
h_B	Breaking water depth

SYMBOLS—Continued

Symbol	Description
H	Wave height
H_B	Breaking wave height
H_o	Deepwater wave height
j	Index used in summation
J	Maximum value of j in summation
KE	Kinetic energy of waves
KE'	Dimensionless form of KE , defined by Equation (39)
$KFSBC$	Kinematic free surface boundary condition, defined in Equation (11)
$KFSBP$	Kinematic free surface breaking parameter, defined by Equation (48)
L	Wavelength
L'	Dimensionless form of L , defined by Equation (37)
L_o	Small-amplitude deepwater wave length = $gT^2/(2\pi)$
\bar{L}	Subscript "L" denoting "lower"
M_D	Drag moment component
M'_D	Dimensionless form of M_D , defined in Equation (27)
M_I	Inertia moment component
M'_I	Dimensionless form of M_I , defined in Equation (28)
n	Index used in summation
NN	Order of wave theory
p	Pressure
p_a	Atmospheric pressure
p_D	Dynamic component of wave pressure
p'_D	Dimensionless form of p_D , defined in Equation (29)
Q	Bernoulli term, defined in Equation (8)
\bar{Q}	Average value of Q
S	Vertical coordinate, referenced to bottom, positive upwards
t	Time coordinate
T	Wave period

SYMBOLS—Continued

Symbol	Description
u	Horizontal component of water particle velocity
u'	Dimensionless form of u , defined in Equation (21)
u_M	Measured horizontal component of water particle velocity
u_T	Theoretical horizontal component of water particle velocity
\overline{U}	Subscript "U" denoting upper value
w	Vertical component of water particle velocity
w'	Dimensionless form of w , defined in Equation (22)
$W_{L,U}$	Weighting coefficients, defined by Equation (50)
x	Horizontal coordinate
X	Stream-function coefficients
z	Vertical coordinate, referenced to still water level, positive upwards
α	Wave crest alignment relative to bottom contours
α_o	Deepwater value of
α_B	Wave crest alignment at breaking conditions
β_1	Kinematic free surface breaking parameter, defined by Equation (48)
β_2	Dynamic free surface breaking parameter, defined by Equation (49)
γ	Specific weight of water
ϵ_1	Distributed error in kinematic free surface boundary condition
ϵ_2	Distributed error in dynamic free surface boundary condition
ϵ'_2	Dimensionless form of ϵ_2 , defined by Equation (36)
η	Water surface displacement
η'	Dimensionless form of η , defined by Equation (30)
θ	Phase angle
π	Numerical constant, 3.14159
ρ	Mass density of water
σ	Standard deviation
ϕ	Velocity potential
ψ	Stream function
ψ_η	Stream-function value evaluated on free surface of an "arrested" wave

EVALUATION AND DEVELOPMENT OF WATER WAVE THEORIES FOR ENGINEERING APPLICATION

by
R. G. Dean

I. INTRODUCTION

The following were the primary goals of the research reported: (1) for given wave conditions, to establish a rational basis for selection of one of the numerous available progressive-water-wave theories and (2) to tabulate the most appropriate wave theory or theories in a form convenient for preliminary design use. The main emphasis has been an attempt to assist the engineer in his selection and application of wave theories in marine design problems. The research has proceeded in several distinct phases which are described briefly below.

An early phase of the research was related to evaluating the *analytical* validity of water-wave theories; that is, the degree to which the various available theories satisfy the equations constituting the mathematical formulation. The results of this phase, first published in September, 1968 (Dean, 1968a), established that, of the eight theories included in the study, the Stream-function fifth-order provided the best fit over a wide range of wave conditions. For very shallow water waves, the Airy and first-order Cnoidal theories provided the best fit. However, because the Stream-function theory can be extended to quite high orders, it was expected that it would provide the best fit, even for most shallow water wave conditions. Based on the results of this phase, the following phases concentrated on further exploration and development of the Stream-function theory for engineering application.

The second phase represented an examination of near-breaking wave conditions using the Stream-function theory (Dean, 1968b). This problem is complicated because breaking conditions represent a mathematical as well as a hydrodynamic instability, and therefore the computational aspects are not straightforward. The results of this study indicated that of the two stability criteria, the kinematic criterion rather than the dynamic criterion governs at breaking. It was also found that near breaking the pressure distribution was hydrostatic rather than characterized by a zero pressure gradient as predicted by some other studies. The complexities of the numerical computations led to an attempt to establish the breaking index for only three relative water depths (shallow, transitional zone and deep). It was found that for shallow and deepwater waves, the breaking heights established from the Stream-function wave theory were up to 28 percent higher than those established earlier by other investigations. For transitional depth conditions, however, the breaking heights determined in the study agreed well with those of earlier investigations.

The third phase of the investigation (Dean and LeMehaute, 1970) was related to the "experimental validity of water wave theories" as compared to "analytical validity." The motivation of this phase was the recent publication of a fairly comprehensive set of measurements of water particle velocities for shallow water waves and comparison with a number of wave theories by LeMehaute, Divoky, and Lin (1968); a comparison with the

Stream-function theory was therefore conducted as a part of the present study. On an overall basis, the Stream-function theory provided a significantly better fit to the measured water particle velocities than the other theories. The standard deviation between the measured and Stream-function representations was 0.17 foot/second as compared to 0.24 foot/second for the theory providing the next best fit. The primary significance of this phase of the study is that the wave conditions are in the shallow-water region where theories other than the Stream-function would be expected to provide better comparisons with measurements. Although this favorable comparison is not taken as demonstration of the superiority of the Stream-function for all wave conditions, the results were very encouraging and, to some extent, surprising.

The final phase of the investigation has been the development of a computer program to tabulate wave quantities that would be of value to engineers in design, and that would also be valuable to persons concerned with the further development and improvement of water-wave theories. During the development of the tables, it has been found that more meaningful information than originally anticipated could be presented.

In the early phases of this study, dimensional variables [i.e., water depth/(wave period) and wave height/(wave period)] were used to characterize the wave conditions (Dean, 1968b). This feature will be evident in the description of some of the results. In the latter phases of the study, it was decided to characterize the wave conditions by the following dimensionless quantities: h/L_o and H/L_o , where h , H and L_o represent the water depth, wave height, and small-amplitude deepwater wavelength, respectively. The tables are developed for 40 cases of $(h/L_o, H/L_o)$.

The results of the research are presented in two volumes. The present report (Volume I) documents the research results and describes the wave tables and their application. Volume II presents the wave tables that have been developed for 40 cases encompassing most conditions encountered in engineering design.

It should be noted that all of the available wave theories have not been included in the comparisons described earlier. Some of the theories omitted were developed during the period of this research; some have been available, but were not compared, usually because they are not employed extensively for engineering purposes.

II. STREAM FUNCTION WAVE THEORY

Introduction

At an early stage of the research, the study indicated that the Stream-function theory generally provided a better fit to the boundary conditions and also to available laboratory measurements. The study therefore developed into an effort to explore and develop the Stream-function theory for engineering application. Before presenting this work, the basis for the Stream-function theory will be described in some detail in an attempt to define the similarities with and differences from other theories. It should be noted that there are two representations of the Stream-function theory: (1) for a given wave height, H , water

depth, h , and wave period, T , a (symmetrical) representation can be developed to describe the kinematics and dynamics of the motion and (2) for a given *measured* water surface displacement, $\eta(t)$ representing a single oscillation (e.g., trough-to-trough), a representation can be determined which completely defines the kinematics and dynamics of the wave motion. The first case is, of course, of more interest to designers; in another application, the second case has been employed for the analysis of hurricane-generated wave and wave-force data. Only the first mode has been explored under the present study.

Formulation

The water-wave phenomenon of interest here can be idealized as a two-dimensional boundary value problem of ideal flow. The assumption of ideal flow is essential to a mathematical formulation that can be readily solved by known techniques. Figure 1 defines terms employed in the formulation.

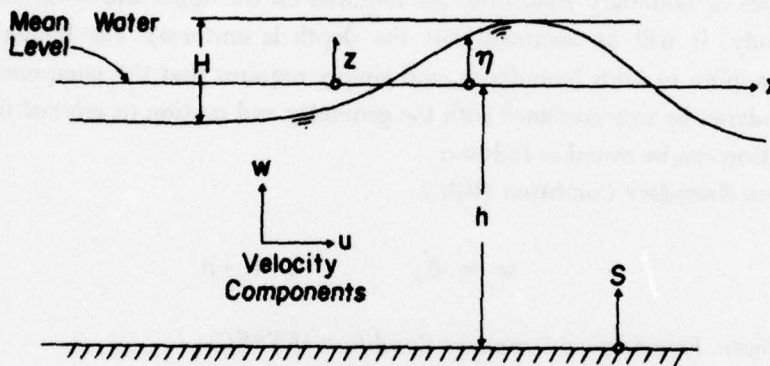


Figure 1. Definition sketch, progressive wave system

Differential Equation

Ideal flow incorporates the assumptions of an incompressible fluid and irrotational motion. For pressures normally experienced in progressive water-wave motions, the incompressibility assumption can be shown to be valid. Shock pressures due to a wave breaking against a seawall may be an important exception; however these are not encompassed by the results of this research. The assumption of irrotational flow may be questioned. Probably the best reason for this assumption, at this stage, is that it allows formulation of a boundary-value problem that can be solved in an approximate manner. The solutions can then be compared with measurements to determine the apparent need for the refinement to include a nonzero rotation.

The differential equation (DE) for two-dimensional ideal flow, the Laplace equation, can be presented in terms of either the velocity potential, ϕ or stream function, ψ ,

$$\nabla^2 \phi = 0 \quad (1)$$

$$\nabla^2 \psi = 0 \quad (2)$$

where, in two dimensions

$$\nabla^2 \equiv \frac{\partial^2}{\partial x^2} + \frac{\partial^2}{\partial z^2} \quad (3)$$

and ϕ and ψ are defined in terms of the velocity components u and w (see Figure 1) as:

$$u = -\frac{\partial \phi}{\partial x} = -\frac{\partial \psi}{\partial z} \quad (4)$$

$$w = -\frac{\partial \phi}{\partial z} = +\frac{\partial \psi}{\partial x}$$

Boundary Conditions

Two types of boundary conditions are required on the upper and lower surfaces (for the present study, it will be assumed that the depth is uniform). The kinematic boundary condition applies to both boundaries, and simply requires that the components of flow at these boundaries be in accordance with the geometry and motion (if any) of the boundaries. This condition can be stated as follows:

Bottom Boundary Condition (BBC)

$$w = 0, \quad z = -h \quad (5)$$

Kinematic Free Surface Boundary Condition (KFSBC)

$$\frac{\partial \eta}{\partial t} + u \frac{\partial \eta}{\partial x} = w, \quad z = \eta(x, t) \quad (6)$$

Dynamic Free Surface Boundary Condition (DFSBC)

The remaining free surface boundary condition, the so-called dynamic free surface boundary condition (DFSBC), requires that the pressure immediately below the free surface be uniform and equal to the atmospheric pressure, p_a .

$$\eta + \frac{p_a}{\rho g} + \frac{1}{2g} (u^2 + w^2) - \frac{1}{g} \frac{\partial \phi}{\partial t} = \text{constant} \equiv Q', \quad z = \eta(x, t) \quad (7)$$

In the above formulation, it is tacitly assumed that surface tension effects are negligible. It is customary to incorporate the atmospheric pressure term into the constant, Q' , to yield a new constant, Q

$$\eta + \frac{1}{2g} (u^2 + w^2) - \frac{1}{g} \frac{\partial \phi}{\partial t} = Q \quad (8)$$

In the formulation presented, no requirements have been placed on the *permanence of wave form*; that is, the wave could change form as it propagates due to the relative motion and interference of components propagating with various phase speeds. The treatment of this general problem including the nonlinearities is complex, and was not the subject of this research. Rather, in the present investigation, it is assumed that the wave propagates with constant speed, C , and without change of form. It is then possible to choose a coordinate system propagating with the speed of and in the same direction as the wave, and relative to this coordinate system the motion does not change, and is therefore steady. The time dependency in the formulation vanishes, the horizontal velocity component with respect to the moving coordinate system is $u-C$; and the formulation may be summarized as:

$$\left\{ \begin{array}{ll} \text{DE:} & \nabla^2 \phi = \nabla^2 \psi = 0 \quad (9) \\ \text{BBC:} & w = 0, \quad z = -h \quad (10) \\ \text{Boundary} & \text{KFSBC: } \frac{\partial \eta}{\partial x} = \frac{w}{u - C}, \quad z = \eta(x) \quad (11) \\ \text{Conditions} & \text{DFSBC: } \eta + \frac{1}{2g} \left[(u - C)^2 + w^2 \right] - \frac{C^2}{2g} = Q, \quad z = \eta(x) \quad (12) \\ & \text{Motion is periodic in } x \text{ with spatial periodicity of the wavelength, } L. \quad (13) \end{array} \right.$$

To avoid misimpressions about the assumptions and formulation presented here and those employed in other investigations of nonlinear waves, it is noted that the formulation incorporating the assumption of propagation without change of form is common to the development of all the following nonlinear water wave theories:

Stokes 2nd, and higher order wave theories

Cnoidal 1st and 2nd order theories by e.g., Keulegan and Patterson (1940),
and Laitone (1960)

Solitary wave theory, 1st order by Boussinesq (Munk, 1949)

Solitary wave theory, 2nd order by McCowan (Munk, 1949)

Stream-function wave theory by Von Schwind and Reid (1972)

To reiterate, *analytical validity* will be based on the degree to which a theory satisfies the boundary-value problem formulation, Equations (9) through (13). If a theory could be found that provided exact agreement to the formulations, then the analytical validity would be perfect. There is no guarantee that good analytical validity ensures that a theory will provide a good representation of the natural phenomenon, because implicit in the formulation are the assumptions that capillary and rotation forces and other effects are negligible. *Experimental validity* will be based on the agreement between wave theories and measured data.

The Stream-function Solution

For the formulation expressed in Equations (9) through (13), a Stream-function solution may be expressed as:

$$\psi(x, z) = \frac{L}{T} z + \sum_{n=1}^{NN} X(n) \sinh \left(\frac{2\pi n}{L} (h + z) \right) \cos \left(\frac{2\pi n}{L} x \right) \quad (14)$$

Evaluating this expression on the free surface, i.e., setting $z = \eta$, we find

$$\eta = \frac{T}{L} \psi_{\eta} - \frac{T}{L} \sum_{n=1}^{NN} X(n) \sinh \left(\frac{2\pi n}{L} (h + \eta) \right) \cos \left(\frac{2\pi n}{L} x \right) \quad (15)$$

where NN represents the order of the representation, i.e., the number of terms contributing to the series expression, ψ_{η} represents the (constant) value of the Stream-function on the free surface, L is the (undetermined) wavelength, and the X(n) represent, at this stage, undetermined coefficients.

For particular wave conditions, it is regarded that the wave height, period, and water depth are specified. Equation (14) exactly satisfies the governing differential equation and the bottom and free surface kinematic boundary conditions for arbitrary values of L, ψ_{η} and the X(n) coefficients. The Stream-function expression is also periodic in x with wavelength, L. The only remaining boundary condition is the dynamic free-surface boundary condition; the parameters L and the X(n)'s are to be chosen such that this boundary condition is best satisfied for a specified wave height.

The procedure for determining the unknown parameters, which can be considered as a nonlinear numerical perturbation procedure, is presented in Appendix I.

III. EVALUATION OF VALIDITIES OF WAVE THEORIES

Introduction

As discussed earlier, there are two types of validity that were examined. "Analytical validity" is based on the degree to which a theory satisfies the governing equations (of the boundary value problem formulation). Good analytical validity, however, does not necessarily imply good representation of the natural phenomenon. Experimental validity is based on the agreement between a theory and measurements. To date, some reasonably good laboratory data are available, and at least two field measurements of water particle velocities are reportedly underway (as of 1972) in the petroleum industry, and hopefully, will be available within the next few years.

Discussion of Differences Between Stream-function and Other Wave Theories

Later in this section, it will be shown that the Stream-function theory provides a better fit than other theories to the boundary conditions and also provides a better fit to

laboratory measurements of water particle velocities. It is therefore worthwhile to compare some of the inherent features of the Stream-function and other theories. Although it is difficult to discuss all other theories in general statements, an attempt will be made to present the more significant representative differences.

Consider, as an example, the Stokes higher order wave theories. The general form of the solution exactly satisfies the differential equation, the bottom boundary condition, and, is properly periodic in the x-direction. The solution does not provide exact fits to either the kinematic or dynamic free surface boundary conditions. Suppose that the $(n-1)^{th}$ order solution is known and that the n^{th} order theory is to be developed. The n^{th} coefficients are determined such that they minimize the errors in the two free surface boundary conditions at the $(n-1)^{th}$ order. A significant problem is that the configuration of the n^{th} order water surface is not known, a priori; it is therefore necessary to best satisfy the boundary conditions on an approximate expansion of the n^{th} order water surface. The apparent effect of minimizing the errors present on the approximate n^{th} order water surface is that the resulting theory of a given order, if convergent, may not provide the best fit possible for the number of terms (order) included.

As a comparison with the preceding discussion of the Stokes' theory, consider the corresponding features of a Stream-function theory solution. The general form of the solution exactly satisfies all of the boundary value problem requirements except the DFSBC.

At this stage, one inherent advantage of the Stream-function theory is evident—all of the "free" parameters can be chosen to provide a best fit to the DFSBC. A second and important inherent advantage is that for a given n^{th} order wave theory, *all* of the coefficients are chosen such that they best satisfy the boundary condition on the n^{th} order water surface. The distinction is that because a numerical iteration approach is used, the n^{th} order wave form is known (through iteration) at that order of solution. Other advantages of the Stream-function theory are that a solution can readily be obtained to any reasonable order, and that a measure of the fit to the one remaining boundary condition is more or less automatically obtained in the course of the solution. Also, the form of the terms in the solution is inherently better for representing nonlinear waves, due to the η term appearing in the argument of the hyperbolic sine term [cf. Equation (15)].

The disadvantage of the Stream-function theory is that, unless tabulated parameters are available, it does require the use of a digital computer with a reasonably large memory. The complexity of other nonlinear theories, however, generally also requires the use of a high-speed computer.

It is noted that a similar but different Stream-function theory has been developed and reported by Von Schwind and Reid (1972) subsequent to the analytical validity study reported here, and employs a definition of the DFSBC error which differs from that in the present study. The paper by Von Schwind and Reid presents boundary condition errors for three wave cases. A comparison between their errors and those resulting from the Stream-function theory will be presented.

Analytical Validity

The analytical validity of a particular wave theory has been previously defined as the degree to which the theory satisfies the defining equations, i.e., Equations (9) through (13). Again, for emphasis, it is noted that a theory providing an exact fit to the boundary conditions would have a perfect analytical validity. However, due to assumptions of ideal flow, etc., in the formulation of the problem, a perfect analytical validity does not ensure that the theory would provide a good representation of laboratory or field phenomenon.

The reason for viewing the problem in two steps, i.e., analytical and experimental validity, is that the results of the analytical validity test would at least tend to indicate the relative applicability of the available wave theories for particular wave conditions. Also, the results would provide guidance about whether the most fruitful approach would be directed toward a more representative formulation of water-wave theories or toward the improvement of the solutions of existing formulations.

Definition of Boundary Condition Errors

Most wave theories exactly satisfy the governing differential equation and bottom boundary condition, although some of the solutions only approximately satisfy the differential equation. Table A lists a number of the theories available for design use and also indicates the conditions of the formulation which are satisfied exactly by each of the theories. Inspection of Table A shows that the two nonlinear (free surface) boundary conditions provide the best basis for assessing the analytical validity, because no theory exactly satisfies both of these conditions.

Errors based on the dynamic and kinematic free surface boundary conditions, are defined as functions of phase angle (θ) as follows:

$$\epsilon_1(\theta) \equiv \frac{\partial \eta}{\partial x} - \frac{w}{u - c} \quad (16)$$

$$\epsilon_2(\theta) \equiv \eta + \frac{1}{2g} [(u - c)^2 + w^2] - \frac{c^2}{2g} - \bar{Q} \quad (17)$$

where \bar{Q} represents the mean value of the quantity Q (Bernoulli constant) defined in Equation (12). Overall errors are defined as the root mean squares of the distributed errors,

$$E_1 \equiv \sqrt{\frac{1}{J} \sum_{j=1}^J \epsilon_{1j}^2} \equiv \sqrt{\epsilon_1^2} \quad (18)$$

$$E_2 \equiv \sqrt{\frac{1}{J} \sum_{j=1}^J \epsilon_{2j}^2} \equiv \sqrt{\epsilon_2^2} \quad (19)$$

where j represents sampling at various (evenly spaced) phase angles.

TABLE A

Water Wave Theories Included in Evaluation Presented by Dean (1968a)

Theory	Exactly Satisfies			
	DE	BBC	KFSBC	DFSBC
Linear Wave Theory—Airy (Ippen, 1966)	X	X	---	---
Third Order Stokes (Skjelbreia and Hendrickson, 1961, as summarized by Le Mehaute and Webb, 1964)	X	X	---	---
Fifth Order Stokes (Skjelbreia and Hendrickson, 1961)	X	X	---	---
First Order Cnoidal (Laitone, 1960)	---	X	---	---
Second Order Cnoidal (Laitone, 1960)	---	X	---	---
First Order Solitary (Boussinesq, as summarized by Munk, 1949)	X	X	---	---
Second Order Solitary (McCowan, as summarized by Munk, 1949)	X	X	X	---
Stream-Function Numerical Wave Theory—Fifth Order (Dean, 1968a)	X	X	X	---

Results of Analytical Validity Comparison

Most of the results of the study of analytical validity carried out under this project have been published elsewhere (Dean, 1968a), and therefore will be reviewed only briefly here.

The study included 40 wave cases as shown in Figure 2. For each of these cases, the overall errors, E_1 and E_2 were calculated for the wave theories shown in Table A. The overall dynamic free surface boundary condition errors were made dimensionless by dividing by the wave height, H , i.e.,

$$E_2' = E_2/H \quad (20)$$

The overall kinematic free surface boundary condition error is dimensionless as defined in Equation (18).

Plots of the dimensionless kinematic and dynamic free surface boundary condition errors are presented in Figures 3, 4, 5, and 6 for $H/H_B = 0.25$ and 1.0 (H_B = breaking wave height). The KFSBC error is identically zero for the Stream-function and McCowan theories.

As stated previously, it is difficult to select a single index that would clearly be representative of the overall validity of all wave theories. However, an index was chosen that provided a severe test for the Stream-function theory, and yet this theory provided the best general analytical validity.

The following evaluation plan was adopted, the results of which would be somewhat biased against the Stream-function theory. Most of the wave theories do not satisfy exactly either the DFSBC or KFSBC; however, the Stream-function theory does satisfy exactly the KFSBC. It therefore seems reasonable that if the Stream-function theory can be shown to compare favorably against other theories on the basis of only the DFSBC, then it should provide an even better analytical validity than the comparison shows.

In the analytical validity investigation, the eight wave theories in Table A were examined. Because the fifth order was the highest of the Stokes theories available, it was arbitrarily decided to include the Stream-function theory only to the fifth order.

The evaluation was then based on comparisons presented in Figures 3, 4, 5, and 6 and also on the corresponding figures for $H/H_B = 0.50$ and 0.75 , which are not presented here. The results of this study are shown in Figures 7 and 8.

Figure 7 presents the results for all theories excluding the Stream-function theory. It is seen that the Stokes V theory provides the best fit for deep water, the Airy theory provides the best fit in a part of the transitional and shallow-water ranges, and the first-order Cnoidal wave theory generally provides the best fit in the shallow-water range.

Figure 8 presents the same type of information. Only the fifth-order Stream-function theory is included and provides the best fit over a wide range including *all* of the transitional and deepwater wave regions and also a significant part of the shallow-water range included in the comparison. The Airy wave theory provides the best fit for a small part of the shallow-water, near-breaking waves and the first-order Cnoidal wave theory provides the best fit for the remainder of the shallow-water region.

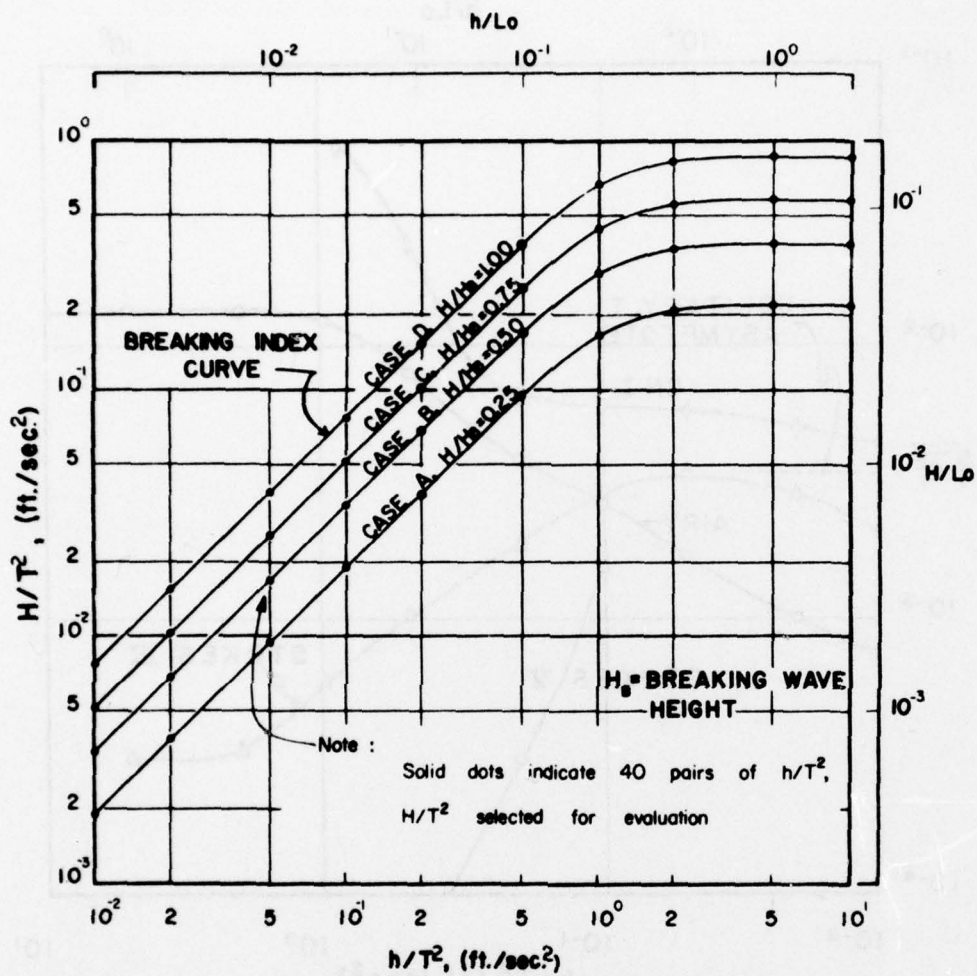


Figure 2. Wave characteristics selected for evaluation

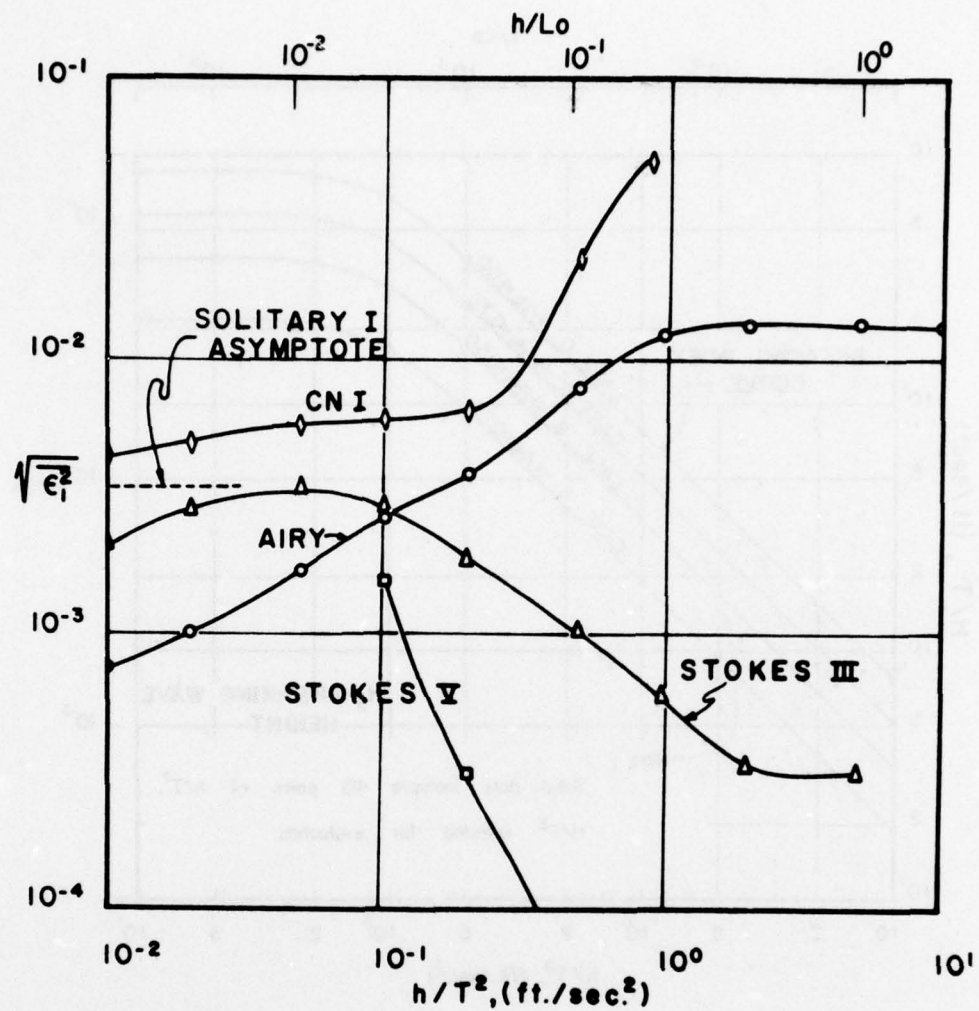


Figure 3. Dimensionless error, $\sqrt{\epsilon_1^2}$, in kinematic free surface boundary condition, $H/H_B = 0.25$; all wave theories

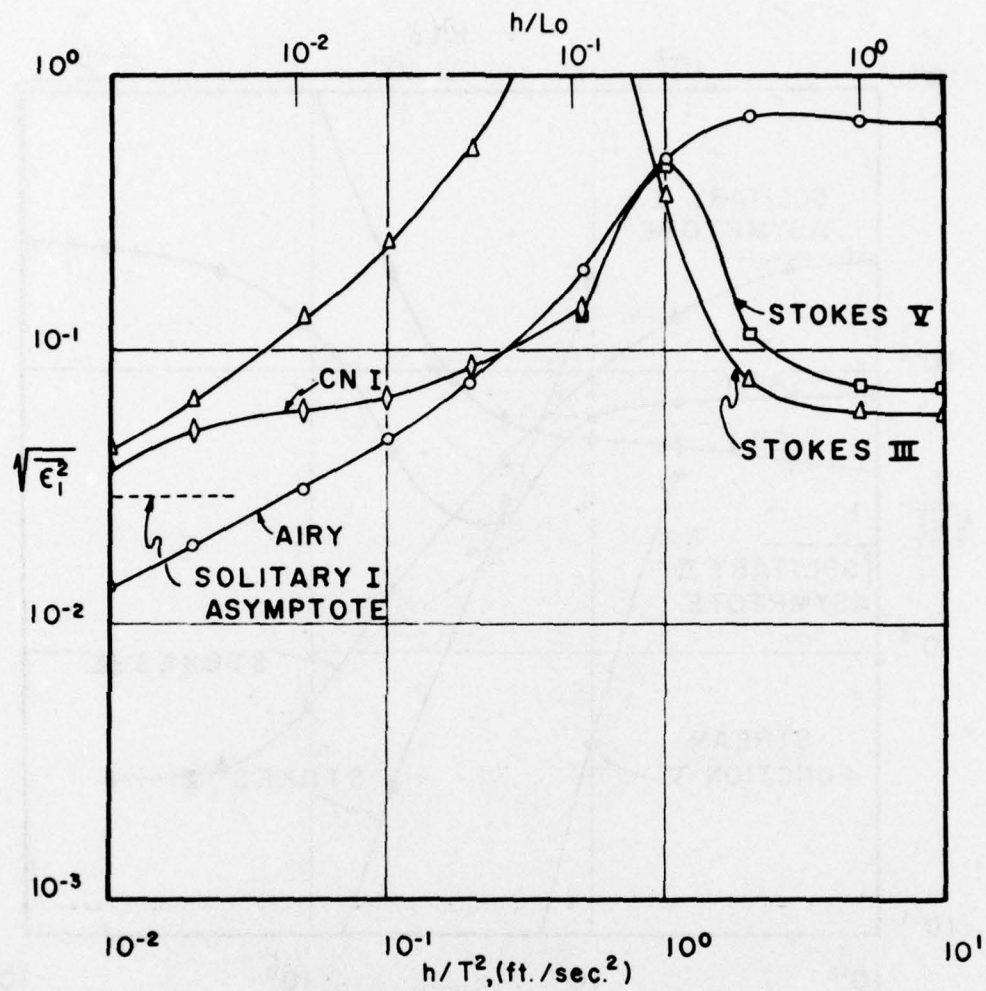


Figure 4. Dimensionless error, $\sqrt{\epsilon_1^2}$, in kinematic free surface boundary condition, $H/H_B = 1.0$; all wave theories

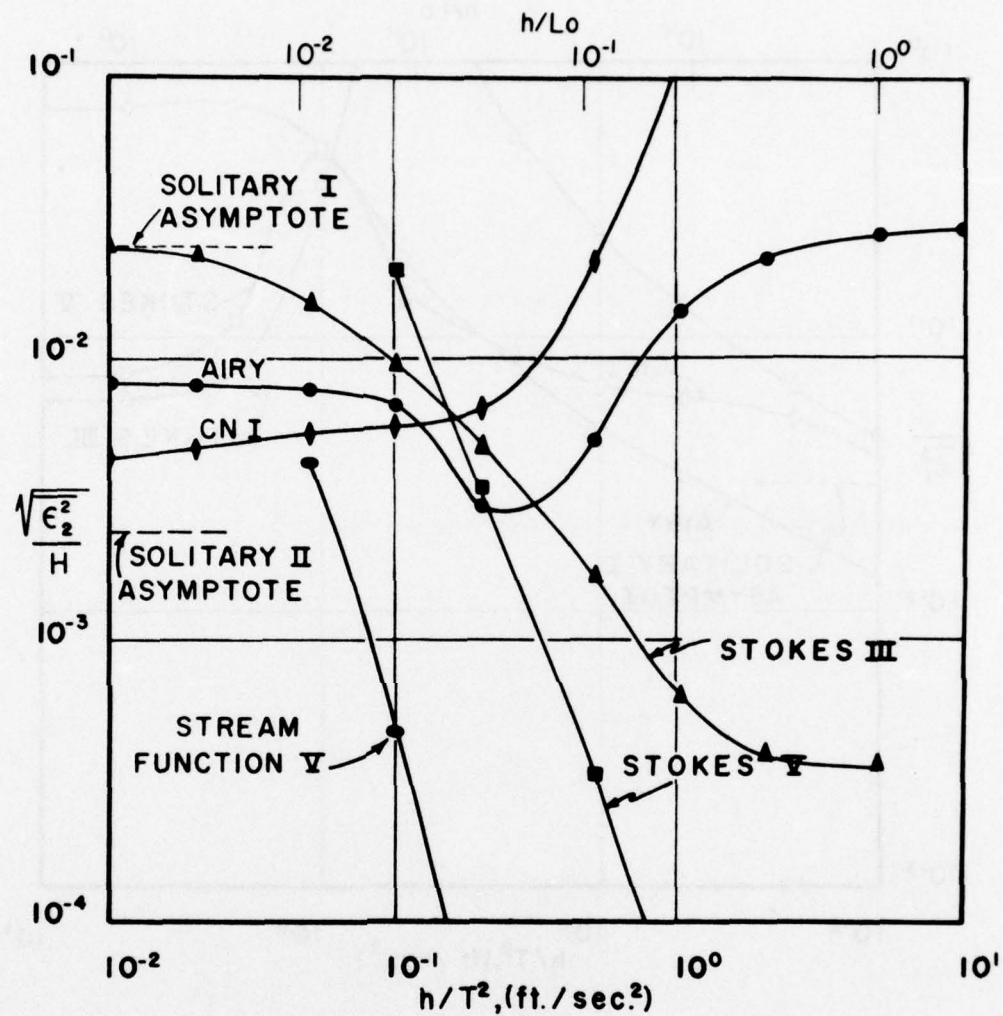


Figure 5. Dimensionless error, $\sqrt{\epsilon_2^2}/H$, in dynamic free surface boundary condition, $H/H_B = 0.25$, all wave theories

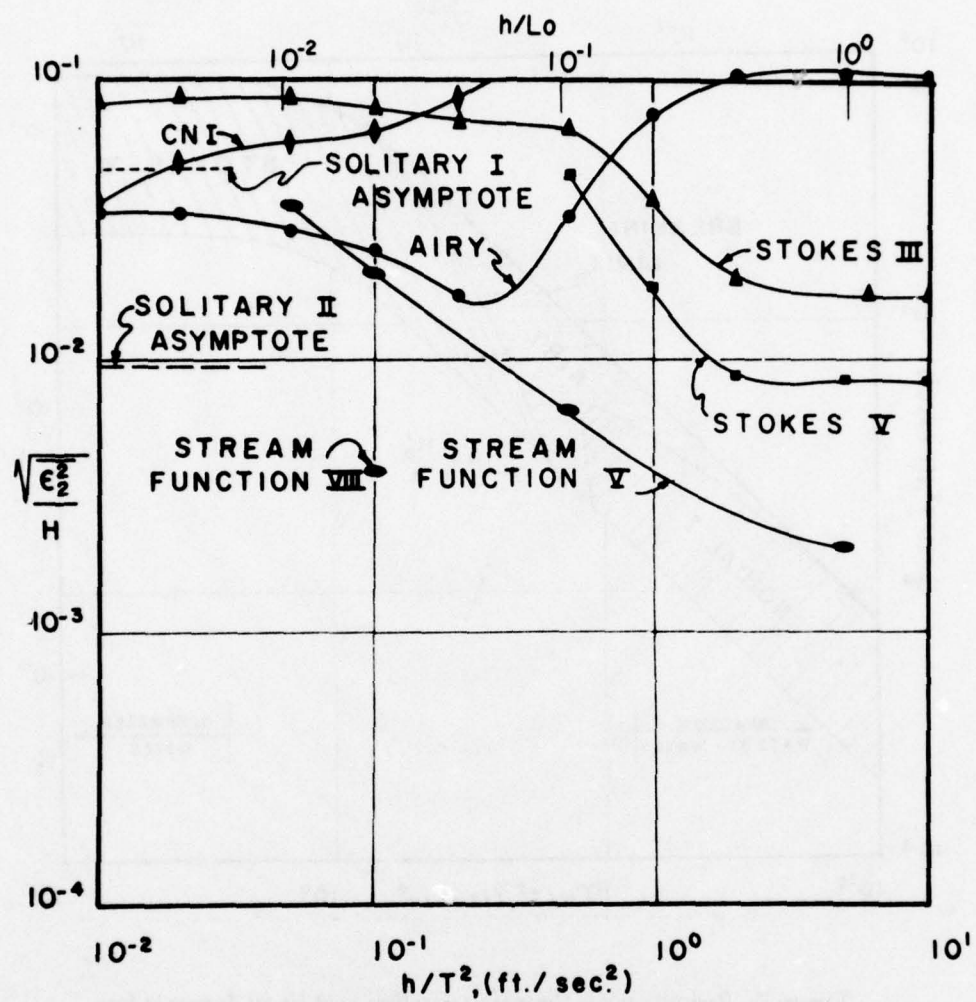


Figure 6. Dimensionless error, $\sqrt{\epsilon_2^2}/H$, in dynamic free surface boundary condition, $H/H_B = 1.0$; all wave theories

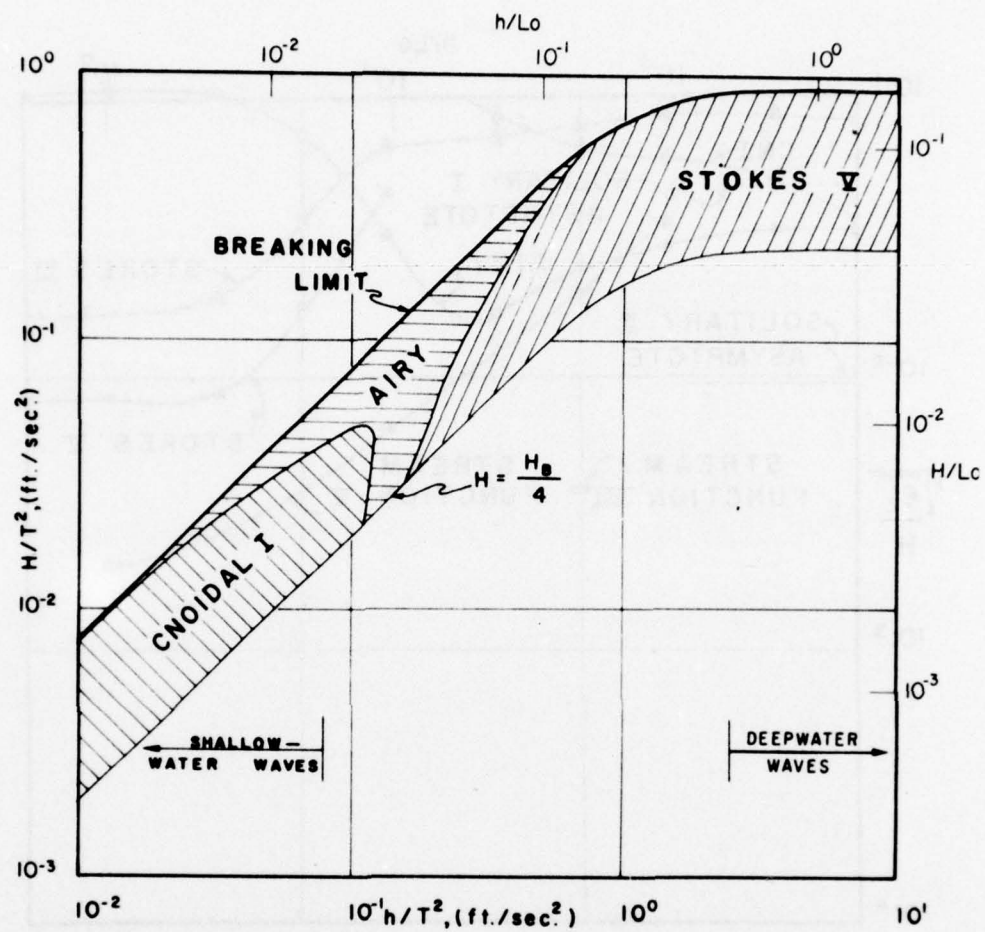


Figure 7. Periodic wave theories providing best fit to dynamic free surface boundary condition (Analytical theories only)

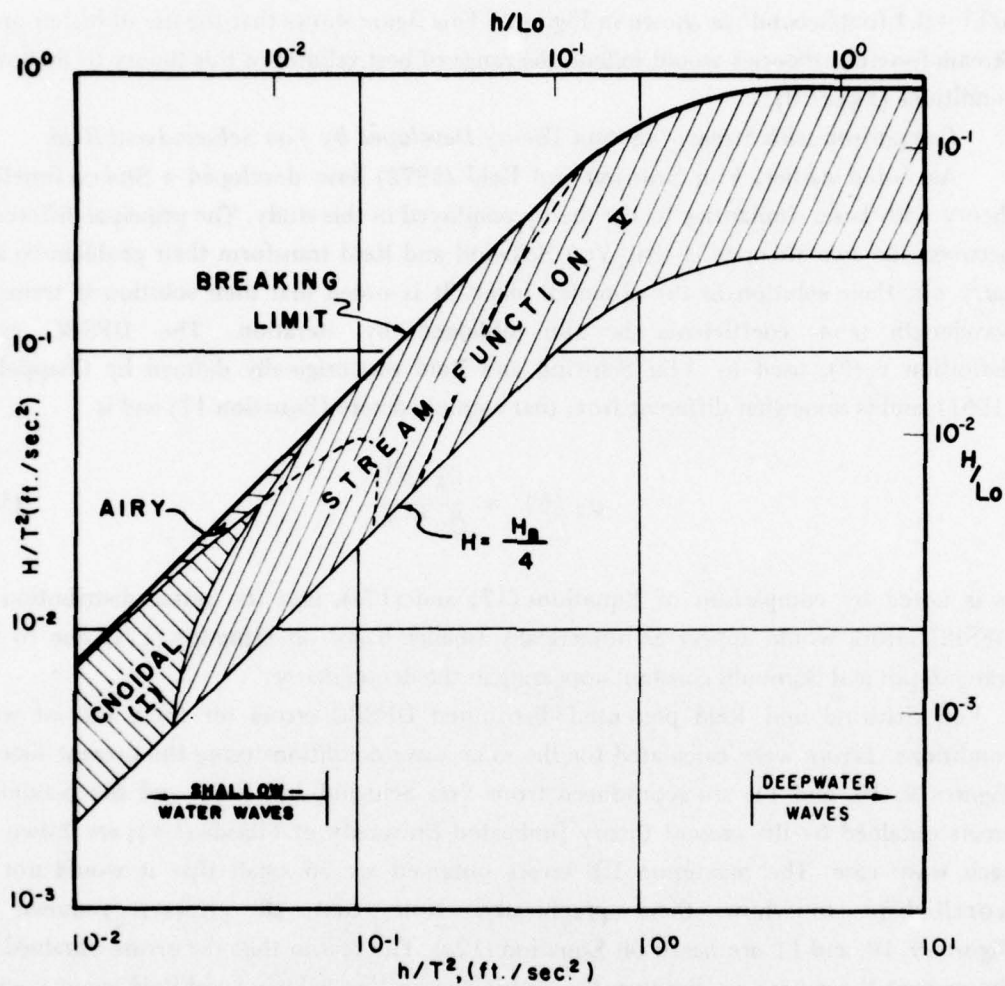


Figure 8. Periodic wave theories providing best fit to dynamic free surface boundary condition (Analytical and Stream Function V theories)

In evaluating the results obtained in the shallow-water region, it is noted that one eighth-order Stream-function theory was calculated for breaking wave conditions and $h/T^2 = 0.1$ foot/second² as shown in Figure 6. This figure shows that the use of higher order Stream-function theories would extend the range of best validity of this theory to shallower conditions (Figure 8).

Comparison with Stream-function Theory Developed by Von Schwind and Reid

As noted earlier, Von Schwind and Reid (1972) have developed a Stream-function theory with basic similarities to the theory employed in this study. The principal difference between the two theories is that Von Schwind and Reid transform their problem to and carry out their solution in the complex plane. It is noted that their solution in terms of wavelength and coefficients is also obtained by iteration. The DFSBC error definition $e_2(\theta)$, used by Von Schwind and Reid was originally defined by Chappellear (1961), and is somewhat different from that employed here (Equation 17) and is

$$e_2(\theta) = \frac{\epsilon_2(\theta)}{\bar{Q} + h} \quad (17a)$$

It is noted by comparison of Equations (17) and (17a), that the actual distribution of DFSBC errors would appear as numerically smaller based on Equation (17a) due to the water depth and Bernoulli constant appearing in the denominator.

Von Schwind and Reid presented distributed DFSBC errors for three sets of wave conditions. Errors were calculated for the same wave conditions using the present theory. Figures 9, 10, and 11, are reproduced from Von Schwind and Reid, and the maximum errors obtained by the present theory [indicated University of Florida (UF)] are shown for each wave case. The maximum UF errors obtained are so small that it would not be worthwhile to show them graphically. Note that all errors (e_2) shown in Figures 9, 10, and 11 are based on Equation (17a). The reason that the errors obtained by the present theory are smaller than those obtained by Von Schwind and Reid is not known. With a numerical solution, it is possible to obtain a low error (down to some limit) by increasing the order of the theory or by increasing the number of iterations used to obtain the solution. For the three cases shown in Figures 9 through 11, the UF waves were seventh-order and each solution was obtained by 15 iterations; the corresponding values for the Von Schwind-Reid waves are not known.

Conclusions Resulting from the Analytical Validity Study

The analytical validity evaluation is based on the degree to which the various theories satisfy the governing equations in the boundary value problem formulation. It is stressed again that there is no guarantee that a theory providing a good analytical validity will necessarily represent well the features of the natural wave phenomenon. The reason is that there are assumptions (negligible viscosity and capillary effects) introduced into the

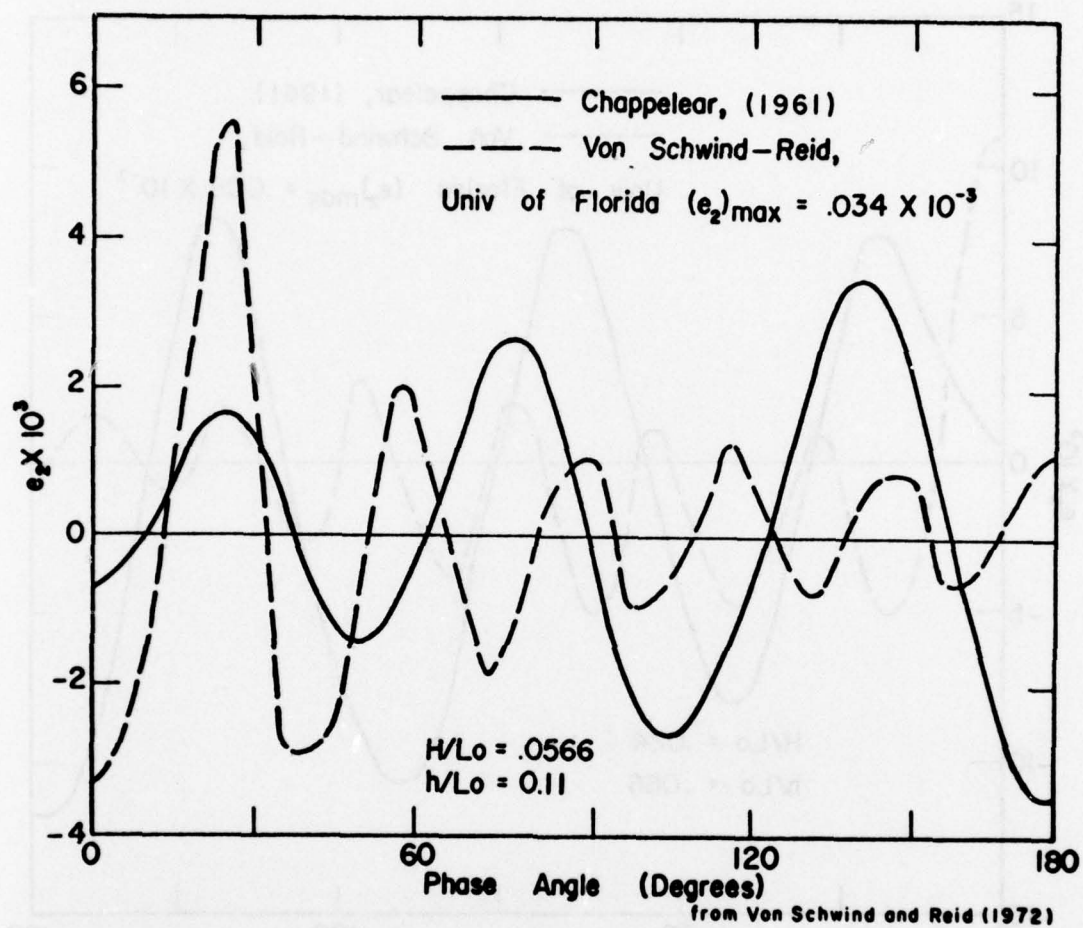


Figure 9. Comparison of errors in dynamic free surface boundary condition for three numerical wave theories, wave no. 1

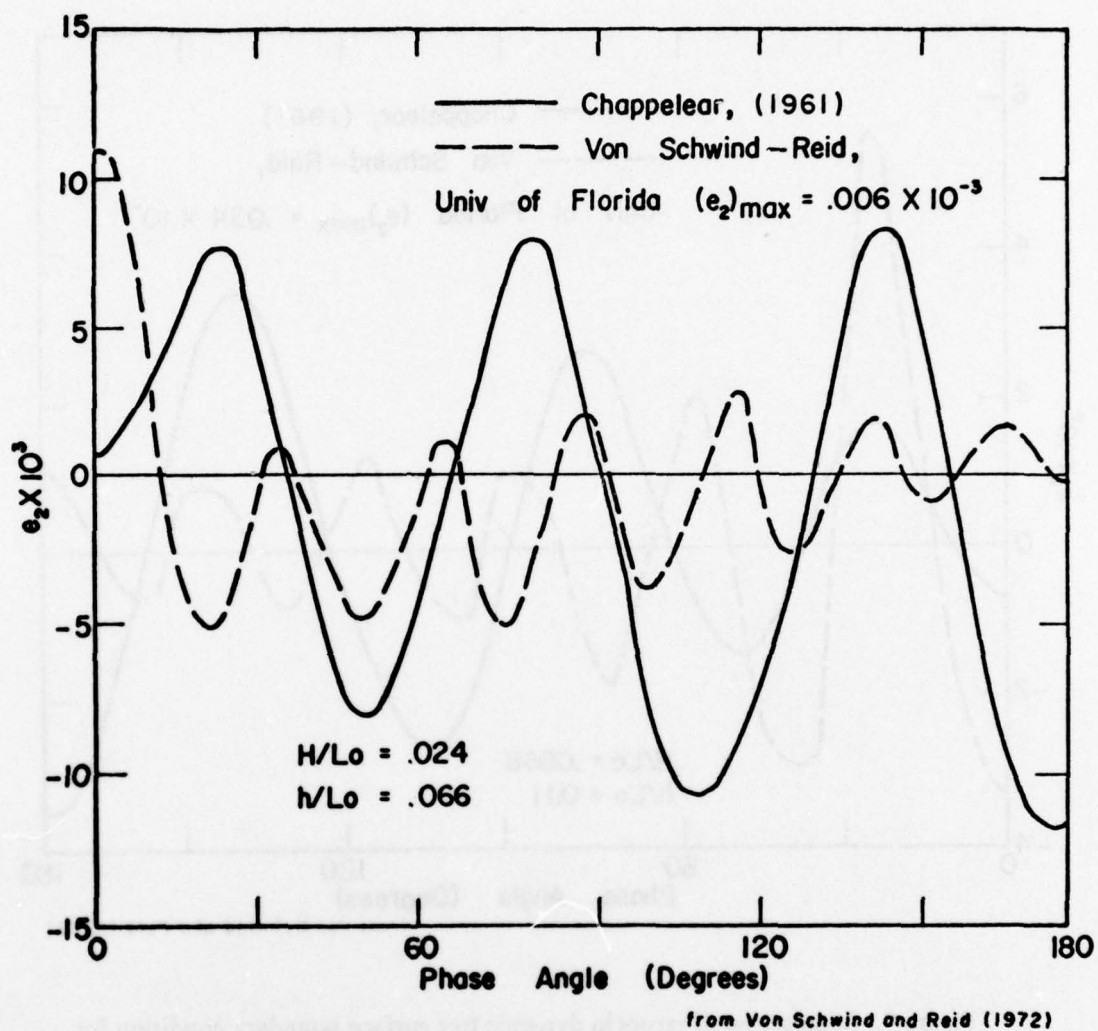


Figure 10. Comparison of errors in dynamic free surface boundary condition for three numerical wave theories, wave no. 2

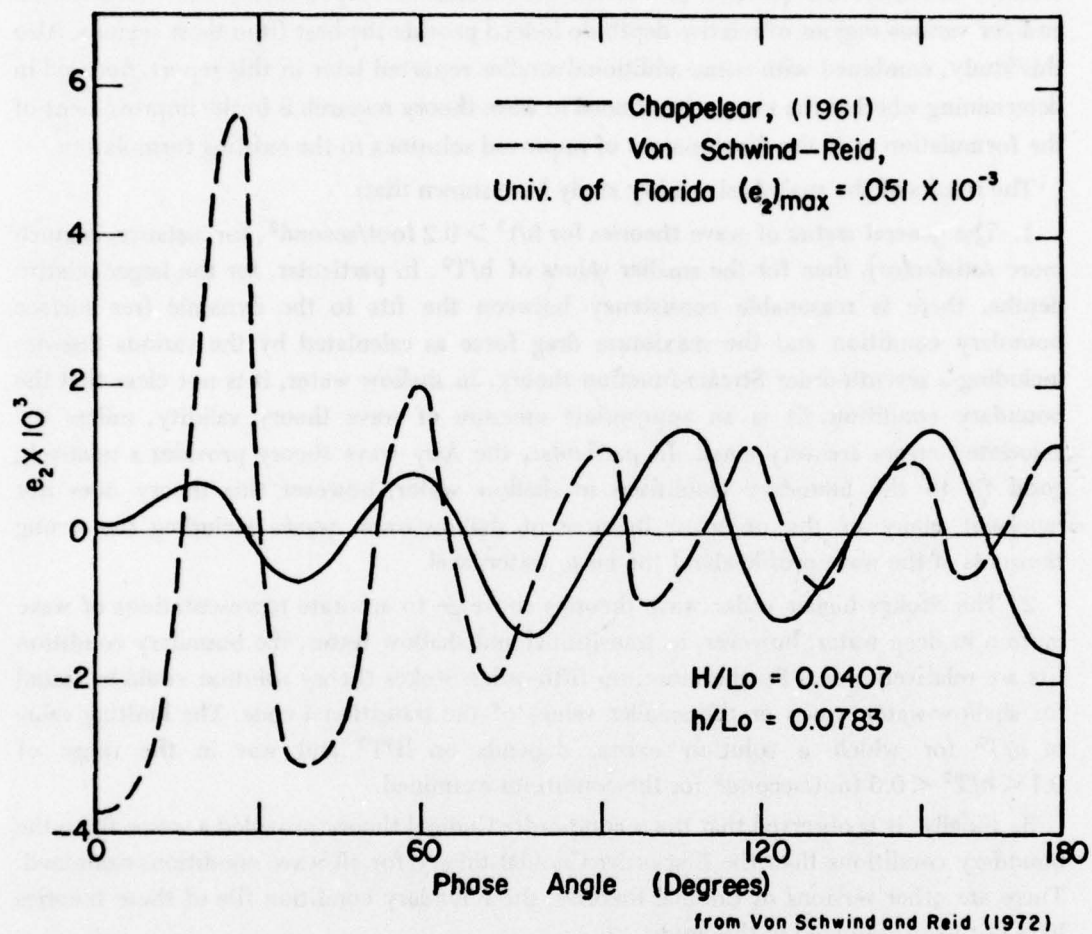


Figure 11. Comparison of errors in dynamic free surface boundary condition for three numerical wave theories, wave no. 3

governing equations which may adversely affect the degree to which the formulation represents real wave motion. The purpose of the analytical validity study, rather, was to attempt to resolve the question of whether the theories developed for the same formulation and for various regions of relative depth do indeed provide the best fit in these regions. Also this study, combined with some additional studies reported later in this report, does aid in determining whether the most critical need in wave theory research is in the improvement of the formulation or in the development of improved solutions to the existing formulation.

The results of the analytical validity study have shown that:

1. The general status of wave theories for $h/t^2 > 0.2$ foot/second², for instance, is much more satisfactory than for the smaller values of h/T^2 . In particular, for the larger relative depths, there is reasonable consistency between the fits to the dynamic free surface boundary condition and the maximum drag force as calculated by the various theories including a seventh-order Stream-function theory. In shallow water, it is not clear that the boundary condition fit is an appropriate measure of wave theory validity, unless the associated errors are very small. In particular, the Airy wave theory provides a relatively good fit to the boundary conditions in shallow water; however this theory does not represent many of the observed features of shallow-water waves including the strong skewness of the wave profile about the mean water level.
2. The Stokes higher order wave theories converge to accurate representations of wave motion in deep water; however, in transitional and shallow water, the boundary condition fits are relatively poor. Furthermore, no fifth-order Stokes theory solution could be found for shallow-water waves or the smaller values of the transitional zone. The limiting value of h/T^2 for which a solution exists, depends on H/T^2 and was in the range of $0.1 < h/T^2 < 0.5$ foot/second² for the conditions examined.
3. Finally, it is observed that the second-order Cnoidal theory provided a worse fit to the boundary conditions than the first-order Cnoidal theory for all wave conditions examined. There are other versions of Cnoidal theories; the boundary condition fits of these theories have not been evaluated in this study.
4. The Stream-function theory described in this report provides good analytical validity over a wide range of wave conditions.

The reader is referred to Dean, (1968a) for reinforcement of statements presented.

Experimental Validity

As previously described, experimental validity is based on the comparison of theoretical predictions and measured wave phenomena. If it could be generally shown that the theory providing the best analytical validity also provides the best experimental validity, then it could be concluded that the formulation is valid and that the errors in the boundary conditions are also good indicators of experimental validity. If the differences between the theory and experiments were of the same order as the estimated experimental error, and if this could be shown to be the situation generally, then the most productive direction in

water-wave research on this problem would be improved measurements. If however, the disagreement between theory and experiment is much larger than can be attributed to experimental error, and especially if this difference were of engineering significance, then additional efforts on the formulation and solution of water wave theories would be indicated.

The availability of data is inadequate to carry out a comprehensive evaluation of experimental validity over all ranges of relative depth and heights of engineering importance. Le Mehaute, Divorky, and Lin (1968) have carried out a measurement program in which distributions over depth of horizontal water particle velocities were measured under the crest phase position of fairly high waves in the shallow and transitional depth ranges. The results included measured horizontal water particle velocity distributions for eight cases, and also a vertical water particle velocity distribution for one case, and one measured wave profile. Le Mehaute, Divorky, and Lin compared a number of wave theories with their data; however the Stream-function theory was not included. The experimental validity reported in this study was based on a comparison of the Stream-function theory with the data described earlier.

It should be emphasized that the only addition to the paper by Le Mehaute, Divorky, and Lin (1968) is (1) comparison of the Stream-function theory with the data and (2) calculations which represent the overall agreement between the data and several of the theories. In the Stream-function horizontal velocity component profiles presented, a uniform mass transport velocity has been subtracted out, whereas due to time limitations, the other theoretical velocity distributions were simply plotted from Le Mehaute, Divorky, and Lin. It is not clear whether or not the mass transport term should be subtracted out. Although the experiments were conducted in a closed tank, the data were taken before waves reflected from the beach had propagated back to the tank test section, and the zero net flow over depth had probably not been established completely.

In all, data for 10 different wave conditions are available. These waves are in the shallow and transitional depth regions, and according to the conventional breaking criteria, the wave heights range from 0.43 to 0.70 of the breaking height. The wave conditions are shown as points in Figure 12 where isolines representing various ratios of wave height to breaking wave height are also presented. It is emphasized that the breaking wave height in Figure 12 is the conventional breaking height: i.e., $H/h = 0.78$ in shallow water (McCowan reviewed by Munk, 1949); $H/L = 0.142$ in deep water (Michell, 1893); in the transitional range, the breaking limit was first established by Reid and Bretschneider (1953) by interpolating on the basis of measured data and is presented in several more available references, e.g. (Ippen, 1966) and (Bretschneider, 1960). A recent paper by Divorky, Le Mehaute, and Lin (1970) reports an experimentally determined shallow-water breaking limit of approximately $H_B/h = 0.60$ to 0.66 as compared to the conventional value of 0.78 . The recent experiments resulting in the lower value were obtained with a laterally converging wave channel. Certainly it is apparent that more work is needed to better resolve wave breaking limits.

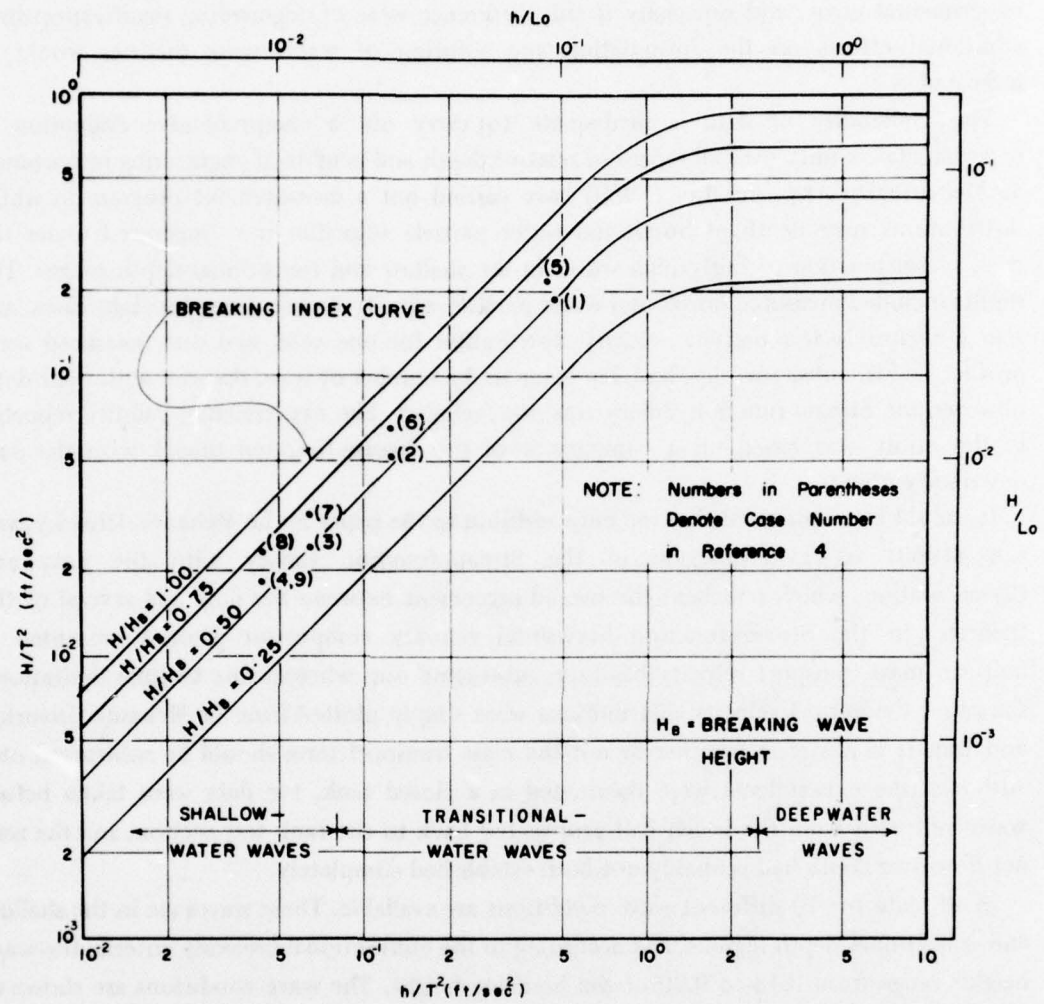


Figure 12. Experimental wave characteristics

Table B presents the comparison results included in the experimental validity evaluation. The eight comparisons of horizontal water particle velocity are presented in Figures 13 through 20; the vertical velocity comparison is presented in Figure 21; and the wave profile is presented in Figure 22.

Figures 13 through 20 indicate that the Stream-function theory is in reasonable agreement with the data. It is noteworthy that the shallow-water wave theories which should provide good fits to the data are so poor. Another interesting feature of the comparison is that the linear (Airy) wave theory agrees better with the data than would be expected.

Of the 12 theories included in the comparison, the better agreements with data were provided by the following five theories: Airy, Keulegan and Patterson Cnoidal wave theory, Goda, Long-Wave, and Stream-function. These five theories were then selected for further examination of their agreement with the data. The standard deviations between each of these theories and the data were calculated, and are presented in Table C where it is seen that the Stream-function theory provided the best fit to the data, followed, in order, by the Goda, Keulegan and Patterson Cnoidal, Airy, and the Long-Wave Theories.

The Goda "theory" is actually a series representation in which the analytical forms of the terms comprising the series are the same as the hyperbolic and trigonometric functions in the Stokes theories. However, the coefficients modifying these terms were determined empirically by wave tank experiments.

Additional calculations not presented here showed that, assuming the data were valid, the Stream-function wave theory would on the average overpredict the maximum total drag force on a vertical cylinder by 21 percent.

Data representing the vertical velocity distribution with depth are available for only one set of wave conditions. (see Figure 21). The McCowan theory provides the best fit to the data; the next best fit is associated with the Stream-function theory. Differences between the McCowan and Stream-function theories, however, are quite small and it is probably not justified to draw conclusions from only one set of data. Interpreted in terms of vertical drag forces on a horizontal cylinder, the Stream-function would underpredict the forces by 30 percent.

The one set of wave profile data are compared with the various theories in Figure 22. Although no detailed comparisons were made, it appears that the Stream-function theory is in as good or better agreement than any of the other theories shown.

Conclusions Resulting from the Experimental Validity Study

Comparisons of Stream-function theory predictions with measurements of velocity components and one wave form representing transitional and shallow-water waves indicate reasonably good agreement. Interpreted on the basis of maximum horizontal drag force components, the Stream-function theory would over predict by an average of 21 percent. Recognizing that the experimental accuracy is approximately 5 percent these results are considered reasonable for engineering applications. The predicted maximum vertical drag

TABLE B
Experimental Waves; Characteristics and Variables Measured

Case No.	Wave Characteristics			Ratio of Wave Height to Breaking Height	Variable Measured	Compared in Figure No.
	H (ft)	T (sec)	h (ft)			
1	0.255	1.16	0.587	0.56	Horizontal Water Particle Velocity Component at Crest	13
2	0.260	2.2	0.619	0.54	Horizontal Water Particle Velocity Component at Crest	14
3	0.232	3.06	0.596	0.50	Horizontal Water Particle Velocity Component at Crest	15
4	0.241	3.58	0.556	0.56	Horizontal Water Particle Velocity Component at Crest	16
5	0.293	1.16	0.587	0.64	Horizontal Water Particle Velocity Component at Crest	17
6	0.323	2.2	0.619	0.67	Horizontal Water Particle Velocity Component at Crest	18
7	0.293	3.06	0.595	0.64	Horizontal Water Particle Velocity Component at Crest	19
8	0.304	3.58	0.555	0.70	Horizontal Water Particle Velocity Component at Crest	20
9	0.241	3.58	0.556	0.43	Vertical Water Particle Velocity Component*	21
10	0.271	1.6	0.586	0.60	Wave Profile	22

*Maximum velocity, regardless of phase angle.

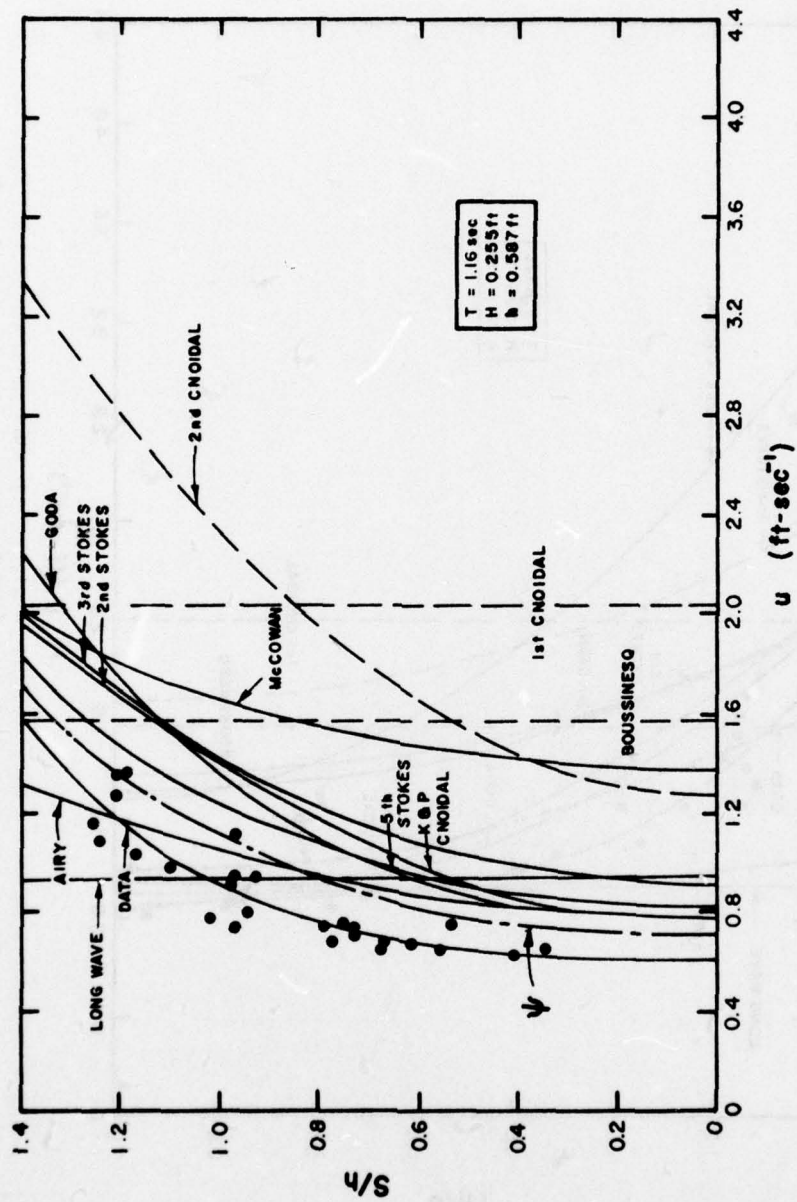


Figure 13. Horizontal water particle velocity under the crest, Case 1

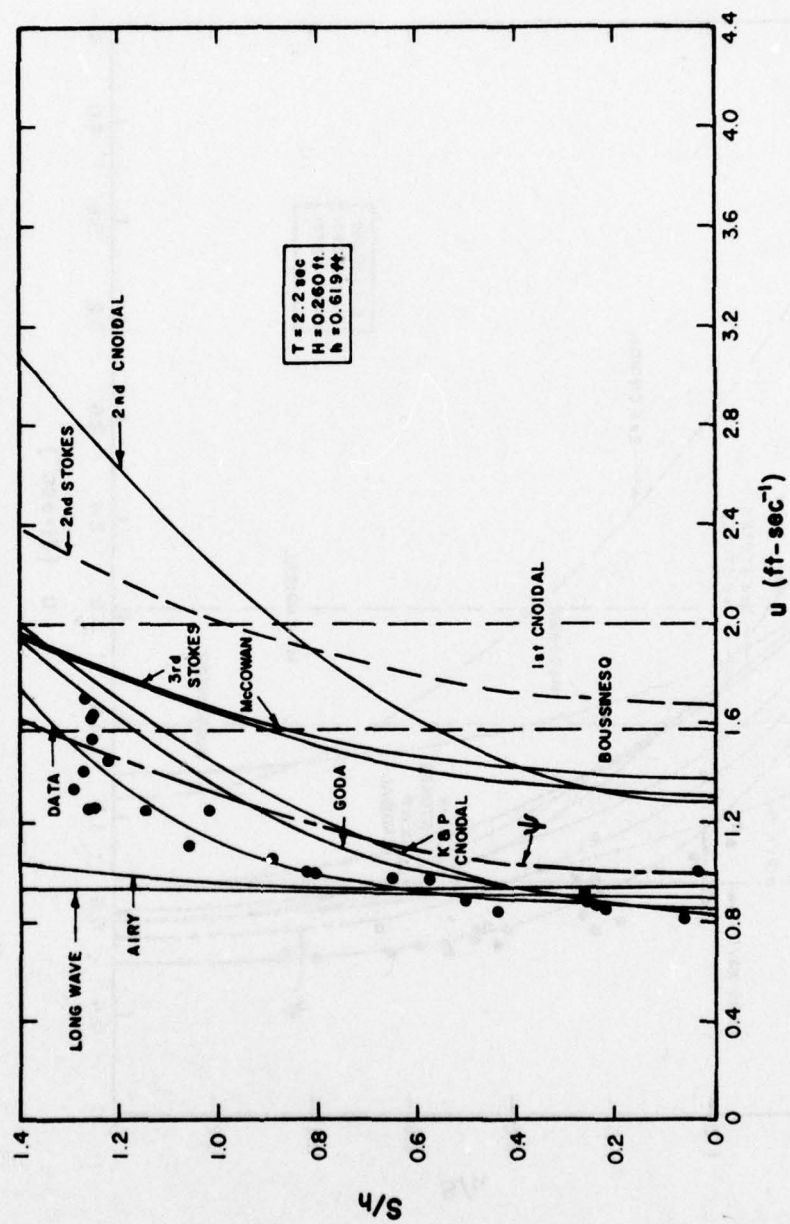


Figure 14. Horizontal water particle velocity under the crest, Case 2

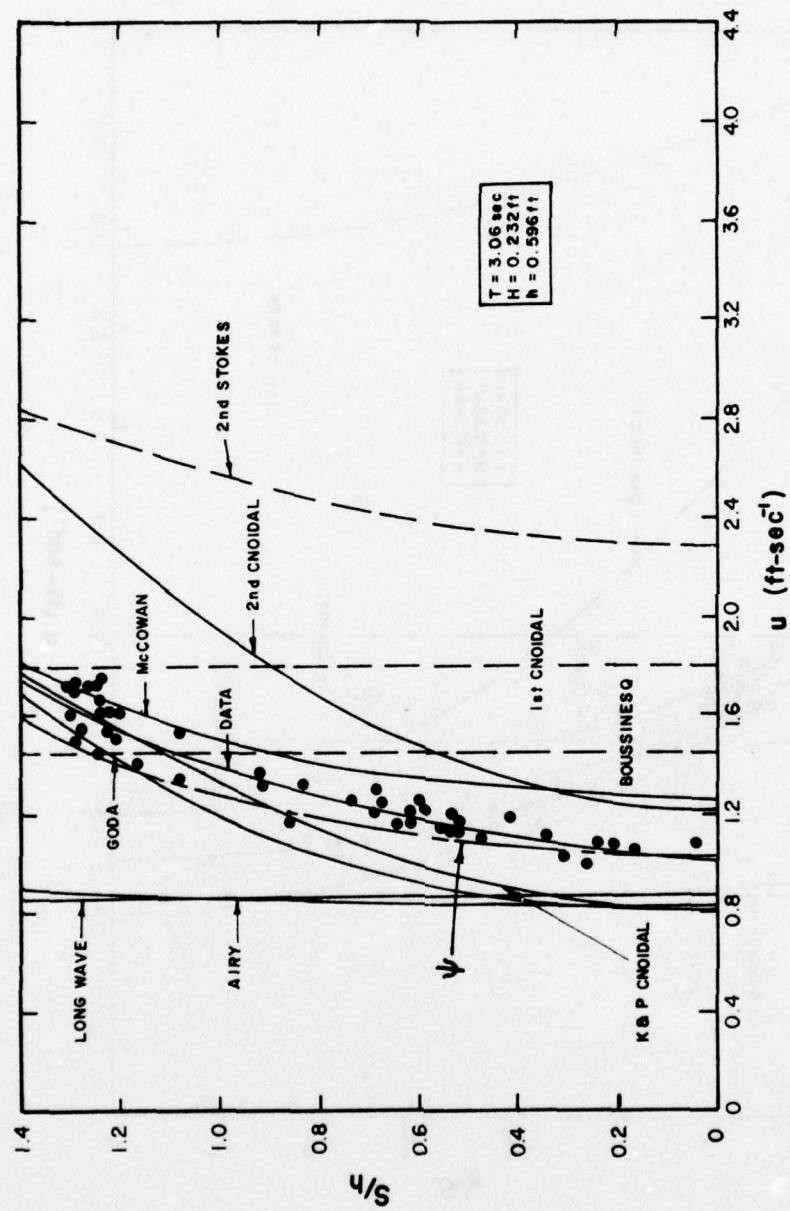


Figure 15. Horizontal water particle velocity under the crest, Case 3

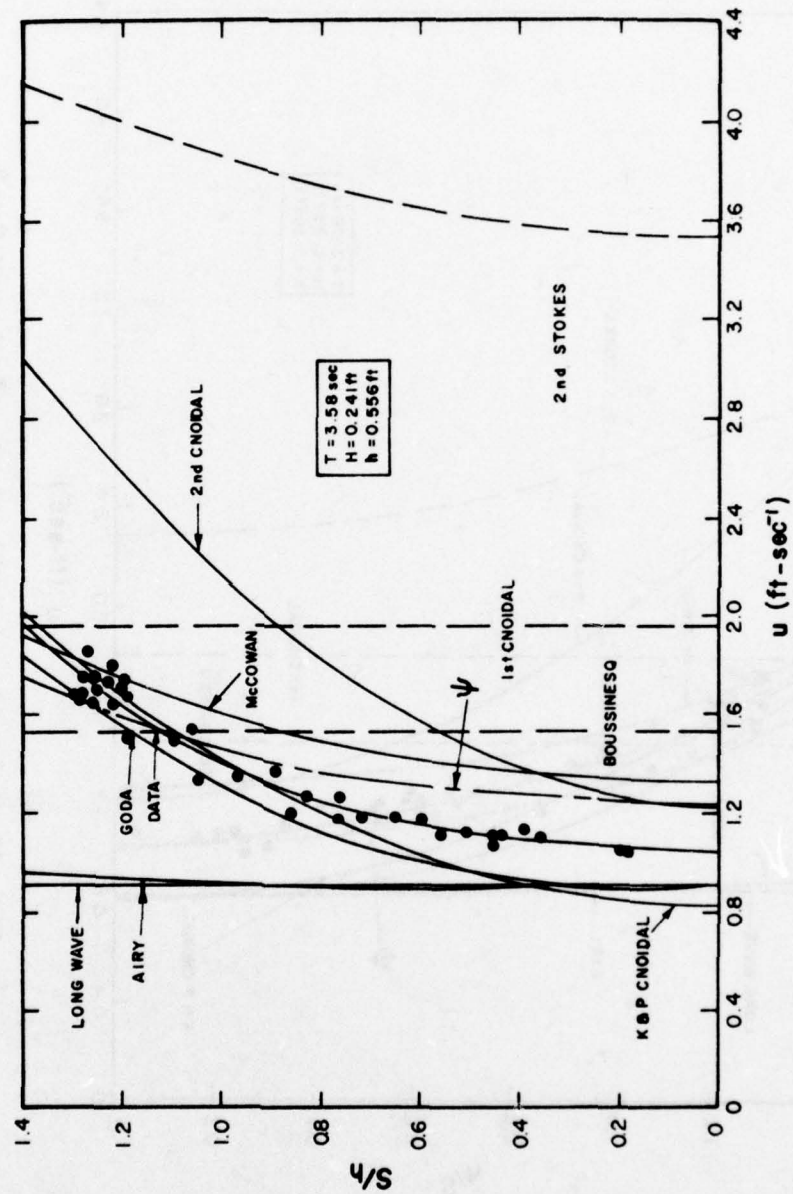


Figure 16. Horizontal water particle velocity under the crest, Case 4

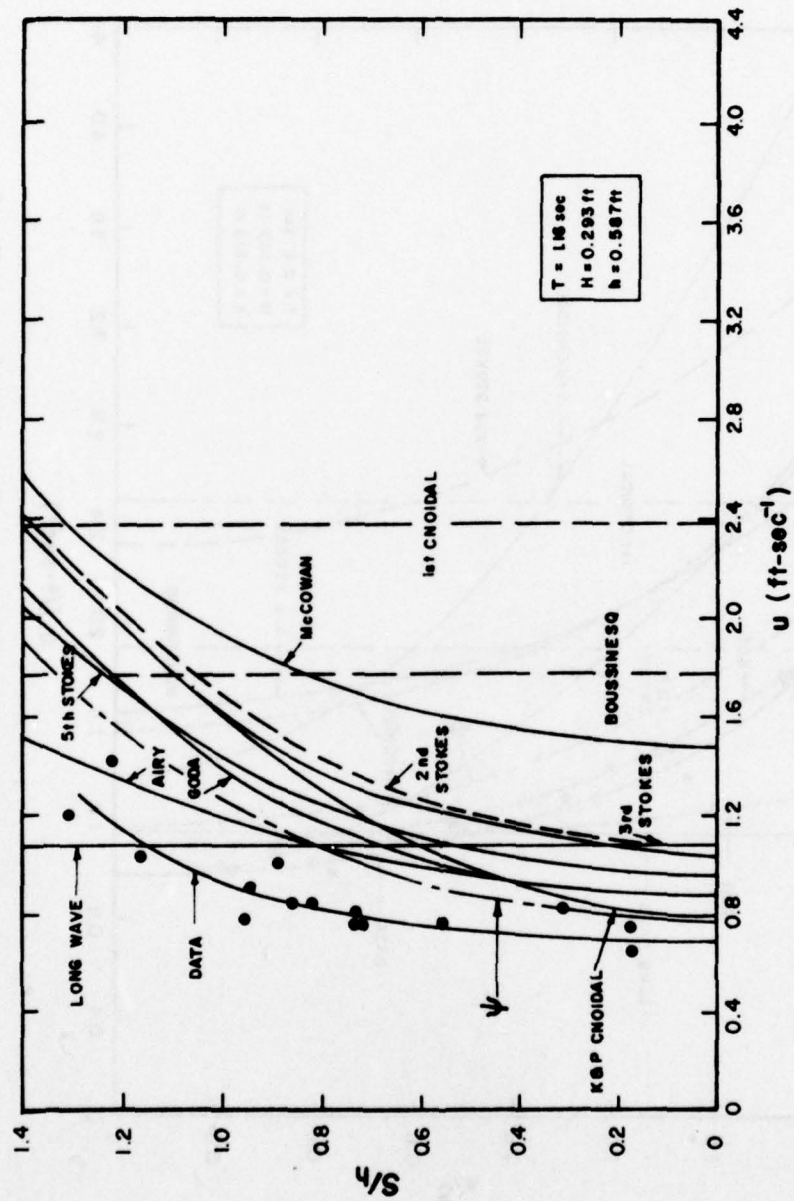


Figure 17. Horizontal water particle velocity under the crest, Case 5

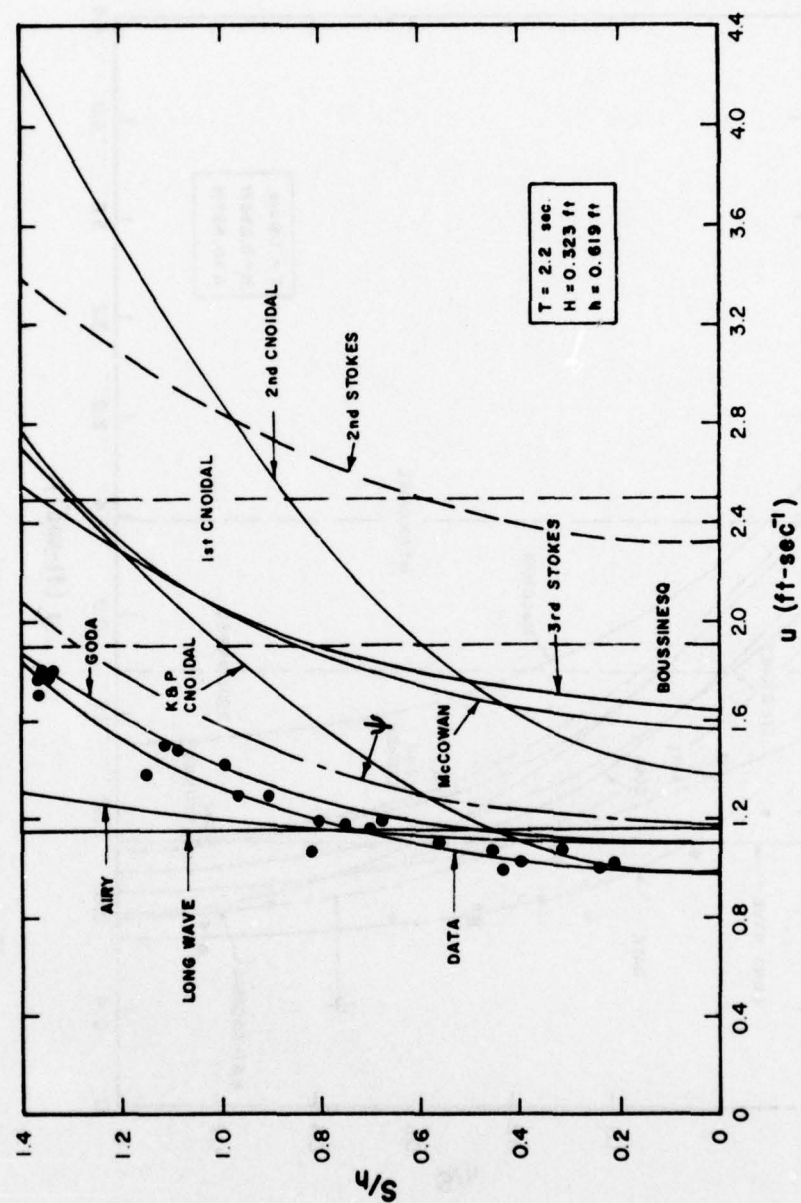


Figure 18. Horizontal water particle velocity under the crest, Case 6

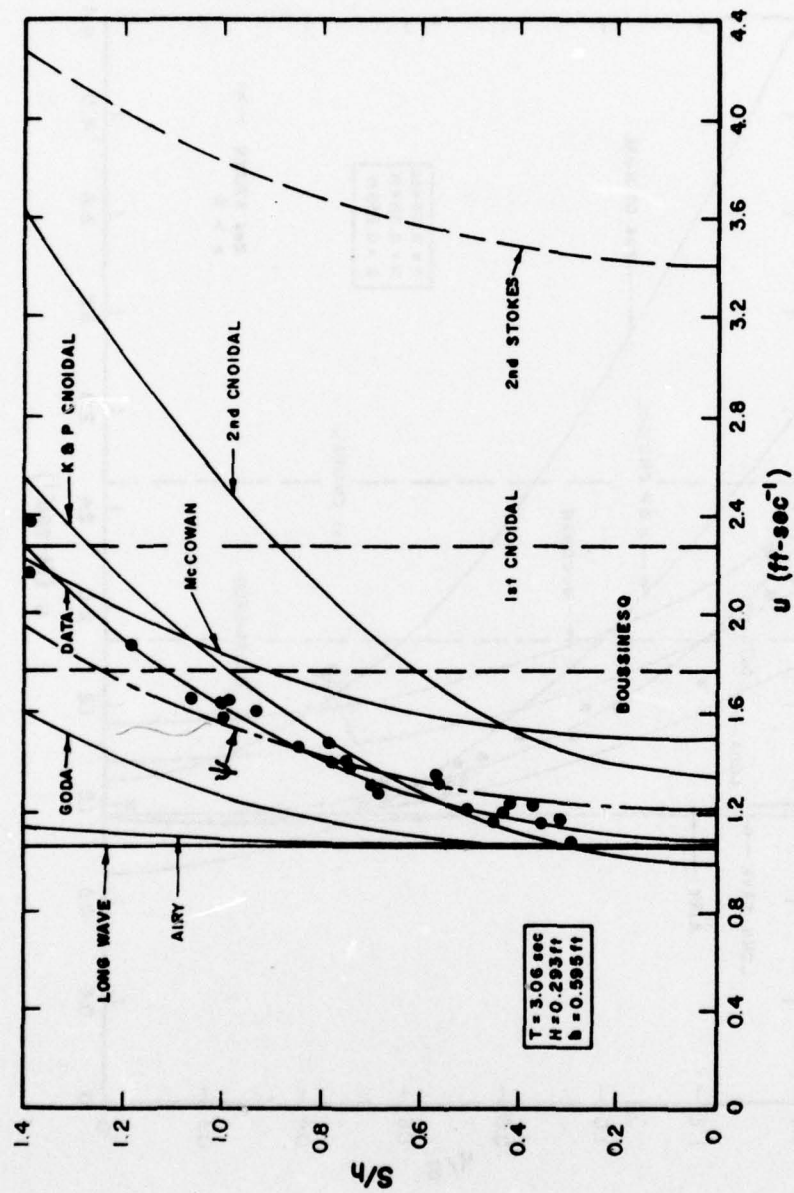


Figure 19. Horizontal water particle velocity under the crest, Case 7

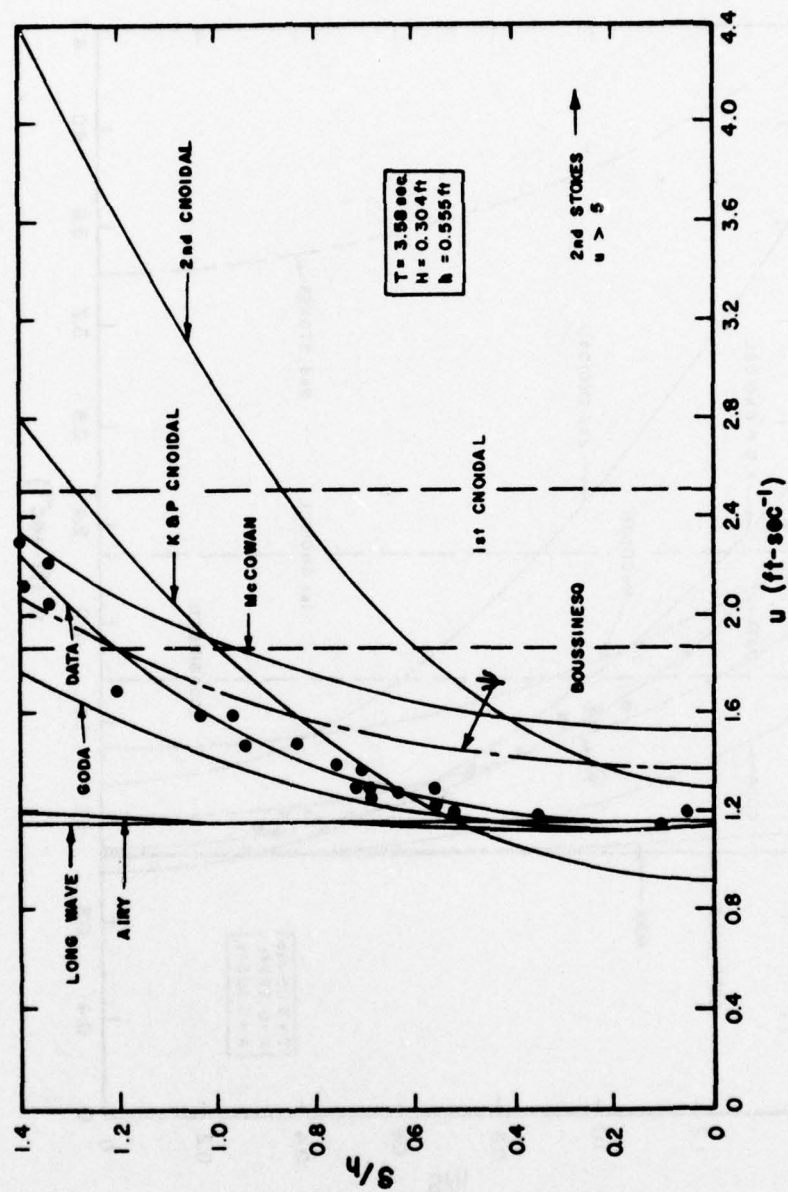


Figure 20. Horizontal water particle velocity under the crest, Case 8

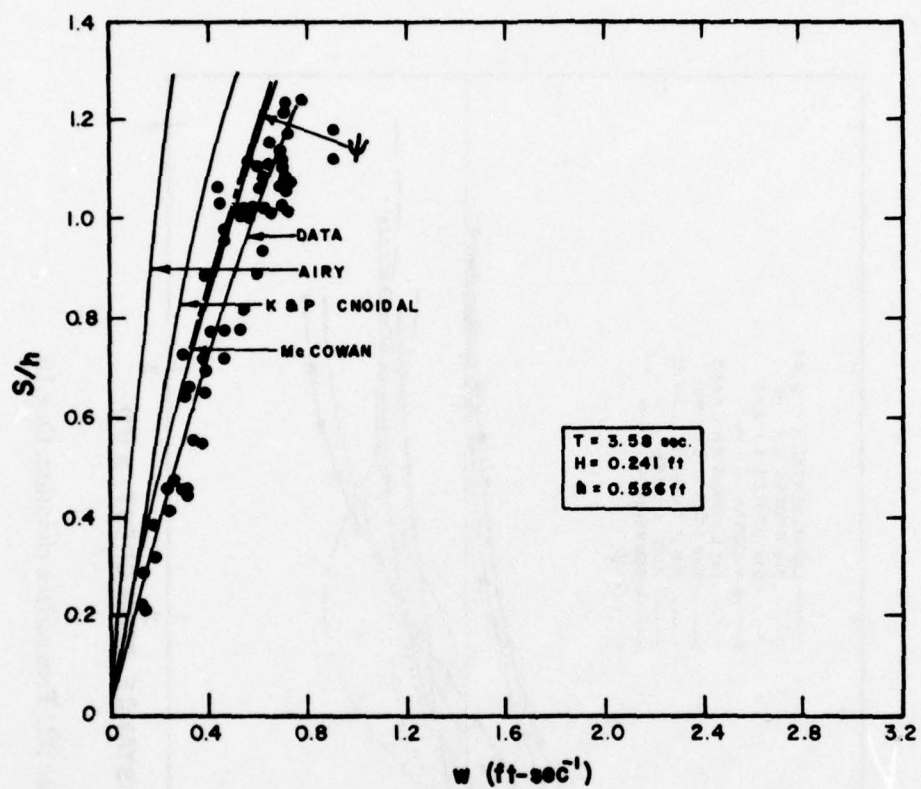


Figure 21. Vertical water particle velocity, Case 9

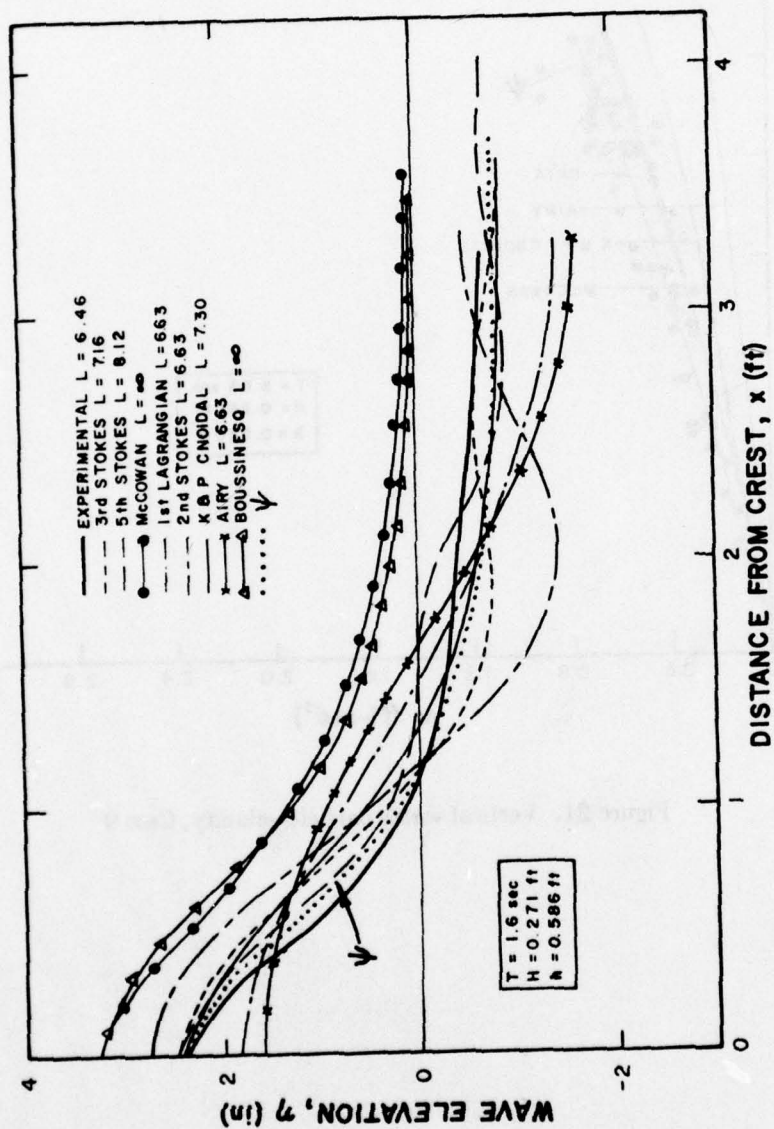


Figure 22. Free surface elevation, Case 10

TABLE C

Standard Deviation of Differences Between Horizontal
Velocities: Measured vs. Predicted

Case No.	Standard Deviation, σ (ft/sec)				
	Theory				
	ψ	Airy	Long Wave	Goda	K & P Cnoidal
1	0.229	0.232	0.328	0.413	0.396
2	0.139	0.234	0.297	0.146	0.211
3	0.096	0.470	0.468	0.206	0.155
4	0.126	0.442	0.453	0.134	0.136
5	0.245	0.225	0.291	0.357	0.487
6	0.216	0.181	0.244	0.095	0.469
7	0.123	0.493	0.513	0.316	0.188
8	0.183	0.418	0.434	0.215	0.272
Average	0.170	0.337	0.379	0.235	0.289

$$\sigma \equiv \sqrt{\frac{1}{J} \sum_{j=1}^J (u_M - u_T)^2}$$

u_M = measured velocity component

u_T = theoretical velocity component

J = number of levels considered for each case (14 to 15)

forces on a horizontal cylinder would be too small by 30 percent; however, this statement is based on a comparison with only one set of data. Good qualitative agreement was found between measured and predicted wave profiles.

Finally, based on the results of both the analytical and experimental validity studies, it is concluded that the Stream-function theory is best suited for engineering design purposes. It was decided to tabulate variables that would be of use in engineering design as calculated from the Stream-function theory. The next section describes the variables included in the tables.

IV. DESCRIPTION OF TABLES

Introduction

An attempt has been made to include in the tables those variables of greatest present engineering interest and application. In addition, other variables were included which would be relevant to checking the relative analytical validity of other theories or variables which were of scientific interest and could conceivably be required for engineering in the future. Variables have been included which describe the detailed kinematics of the waves and also which represent, e.g., the integrated effect of the flow on a structural member.

It is not possible to assemble in concise tabular form all variables that could be of engineering use. It is feasible to tabulate the dimensionless drag force for all vertical piling extending from the bottom up to a certain level. It would not be feasible, however, to concisely tabulate the total drag force on members with all possible inclinations relative to a vertical.

Forty sets of dimensionless wave conditions were selected for tabulation. Each case is characterized by values of h/L_o and H/L_o . The parameter h/L_o , ranged from 0.002 to 2.0 and covered the relative depth range from shallow to deep water. The parameter H/L_o included wave steepness ratios: 0.25, 0.5, 0.75, and 1.0 of the breaking wave steepness for each of the 10 h/L_o values tabulated. Figure 23 shows the dimensionless wave conditions selected for tabulation and also indicates the referencing notation for the cases.

All tabulated variables are presented in dimensionless form. The description of these variables is presented in the following paragraphs and in Tables D, E, and F, where generally the following are included: the equation for the variable, the dimensionless form of the variable, an equation number for reference purposes, and the table number in the wave tables. To reduce confusion, it should be noted that the tables presented in this report are denoted by letters; the wave tables are identified by Roman numerals.

Variables Presented in Tabular Form

Three classes of variables are tabulated: (1) Internal field variables, depending on θ and S , (2) Variables depending on θ only, and (3) Overall variables which have a single value for the entire wave, for example the wavelength.

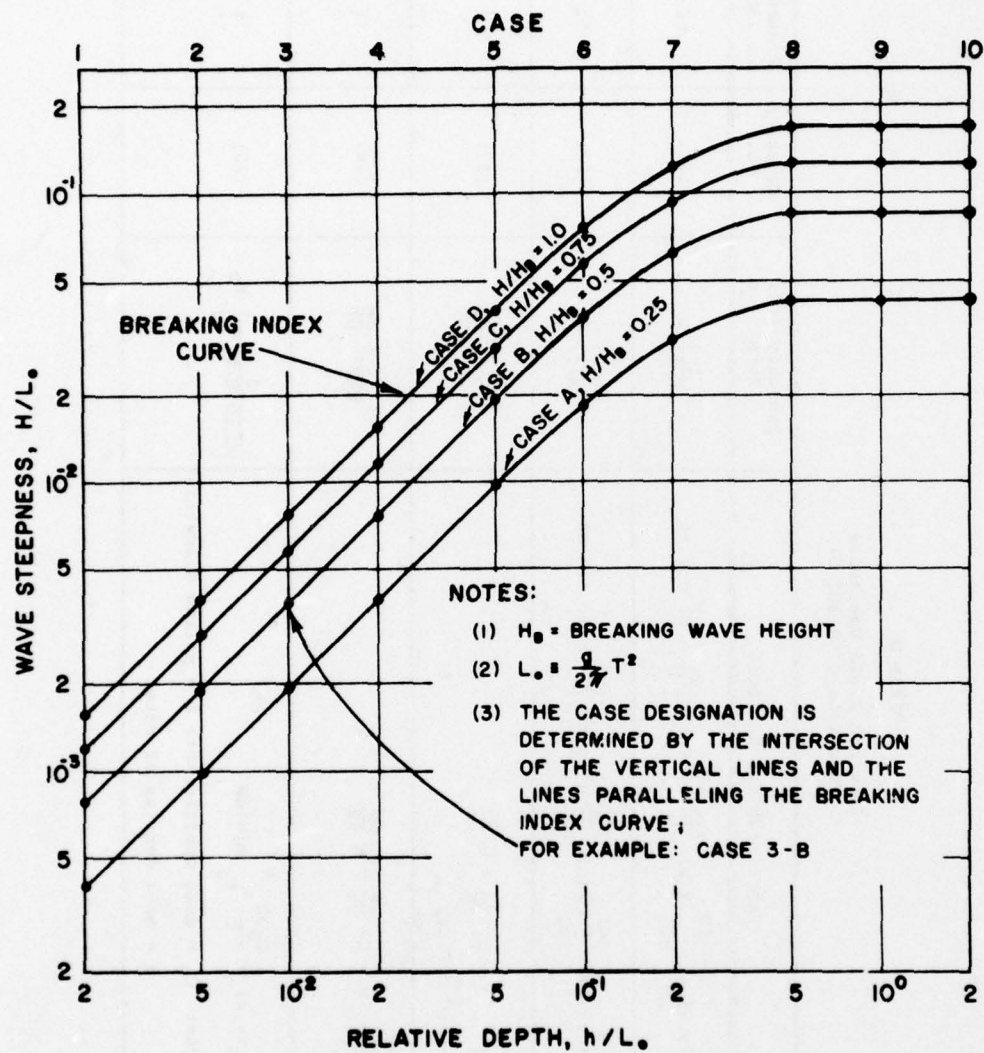


Figure 23. Wave characteristics selected for tabulation

TABLE D
Internal Field Variables
(Functions of θ and S)

Variable	Expression for Variable	Dimensionless Form	Equation No.	Presented in Table
Horizontal Water Particle Velocity, $u(\theta, S)$	$u(\theta, S) = - \sum_{n=1}^{NN} X(n) \left(\frac{2\pi}{L} n \right) \cosh \left(\frac{2\pi}{L} n S \right) \cos n\theta$	$\left(\frac{1}{H/T} \right) u$	(21)	I
Vertical Water Particle Velocity, $w(\theta, S)$	$w(\theta, S) = - \sum_{n=1}^{NN} X(n) \left(\frac{2\pi}{L} n \right) \sinh \left(\frac{2\pi}{L} n S \right) \sin n\theta$	$\left(\frac{1}{H/T} \right) w$	(22)	II
Horizontal Water Particle Acceleration, $\frac{Du}{Dt}$	$\frac{Du}{Dt} = (u - C) \frac{\partial u}{\partial x} + w \frac{\partial u}{\partial z}$ Note: $C \equiv L/T$	$\left(\frac{1}{H/T^2} \right) \frac{Du}{Dt}$	(23)	III
Vertical Water Particle Acceleration, $\frac{Dw}{Dt}$	$\frac{Dw}{Dt} = (u - C) \frac{\partial w}{\partial x} + w \frac{\partial w}{\partial z}$	$\left(\frac{1}{H/T^2} \right) \frac{Dw}{Dt}$	(24)	IV
Drag Force Component up to a Level, S , $F_D(\theta, S)$	$F_D(\theta, S) = \frac{C_D \rho D}{2} \int_0^S u u ds$ Note: C_D = drag coefficient; D = piling diameter; ρ = mass density of water	$\left(\frac{1}{C_D \rho D (H/T)^2 h} \right) F_D$	(25)	V

TABLE D—Continued

Variable	Expression for Variable	Dimensionless Form	Equation No.	Presented in Table
Inertia Force Component up to a Level, S, $F_I(\theta, S)$	$F_I(\theta, S) = \frac{C_M \rho V D^2}{4} \int_0^S \frac{Du}{Dt} ds'$ Note: C_M = inertia coefficient	$\left(\frac{C_M \rho V D^2 (H/T^2) h}{4} \right) F_I$	(26)	VI
Drag Moment Component up to a Level, S, $M_D(\theta, S)$	$M_D(\theta, S) = \frac{C_D \rho D}{2} \int_0^S s' u u ds'$	$\left(\frac{C_D \rho D (H/T^2) h^2}{2} \right) M_D$	(27)	VII
Inertia Moment Component up to a Level, S, $M_I(\theta, S)$	$M_I(\theta, S) = \frac{C_M \rho V D^2}{4} \int_0^S s' \frac{Du}{Dt} ds'$	$\left(\frac{C_M \rho V D^2 (H/T^2) h^2}{4} \right) M_I$	(28)	VIII
Dynamic Pressure Component $P_D(\theta, S)$	$P_D(\theta, S) = \gamma \bar{Q} - \frac{\rho}{2} ((u - c)^2 + w^2) + \frac{\rho}{2} c^2$ Note: γ = specific weight of water $\equiv \rho g$; Q is defined in Equation 8; \bar{Q} is the average value of Q	$\left(\frac{2}{\gamma H} \right) P_D$	(29)	IX

TABLE 2
Variables Depending on θ Only

Variable	Expression for Variable	Dimensionless Form	Equation No.	Presented in Table
Water Surface Displacement, $\eta(\theta)$	$\eta(\theta) = \frac{T}{L} \psi_n - \frac{T}{L} \sum_{n=1}^{NM} x(n) \sinh \left(\frac{2\pi}{L} n(h+n) \right) \cos(n\theta)$	$\left(\frac{1}{H} \right) \eta(\theta)$	(30)	I - IX
Total Drag Force Component, $F_D(\theta)$	Same as Eq. (25), except upper limit is $h + n(\theta)$	$\left(\frac{2}{C_{DP} D^2 (H/T)^2 H} \right) F_D$	(31)	V (labeled "Surface")
Total Inertia Force Component, $F_I(\theta)$	Same as Eq. (26), except upper limit is $h + n(\theta)$	$\left(\frac{4}{C_{MP} D^2 (H/T)^2 H} \right) F_I$	(32)	VI (labeled "Surface")
Total Drag Moment Component, $M_D(\theta)$	Same as Eq. (27), except upper limit is $h + n(\theta)$	$\left(\frac{2}{C_{DP} D^2 (H/T)^2 H^2} \right) M_D$	(33)	VII (labeled "Surface")
Total Inertia Moment Component, $M_I(\theta)$	Same as Eq. (28) except upper limit is $h + n(\theta)$	$\left(\frac{4}{C_{MP} D^2 (H/T)^2 H^2} \right) M_I$	(34)	VIII (labeled "Surface")
Kinematic Free Surface Boundary Condition Error, $\epsilon_1(\theta)$	$\epsilon_1(\theta) = \frac{\partial \eta}{\partial x} - \frac{w}{u - C}$	Expression given is in dimensionless form	(35)	X Item 1 Linear Theory Item 2 Stream Function Theory
Dynamic Free Surface Boundary Condition Error, $\epsilon_2(\theta)$	$\epsilon_2(\theta) = Q(\theta) - \bar{Q}$ Note: $\bar{Q} = \bar{Q}(\theta)$	$\left(\frac{1}{H} \right) \epsilon_2$	(36)	X Item 3, Linear Theory Item 4, Stream Function Theory

TABLE F
Overall Variables
(Do Not Depend on θ or S)

Variable	Expression for Variable	Dimensionless Form	Equation No.	Presented in Table
Wave Length, L	L is determined from Stream function solution (no explicit expression)	$\left(\frac{2\pi}{gT}\right) L$	(37)	XI Item 1
Average Potential Energy, PE	$PE = \frac{\gamma}{4\pi} \int_0^{2\pi} \eta^2(\theta) d\theta$	$\left(\frac{8}{\gamma H^2}\right) PE$	(38)	XI Item 2
Average Kinetic Energy, KE	$KE = \frac{\rho}{4\pi} \int_0^{2\pi} \int_0^{h+\eta} (u^2 + w^2) ds d\theta$	$\left(\frac{8}{\gamma H^2}\right) KE$	(39)	XI Item 3
Average Total Energy, TE	$TE = PE + KE$	$\left(\frac{8}{\gamma H^2}\right) TE$	(40)	XI Item 4
Average Total Energy Flux, F_{TE}	$F_{TE} = \frac{1}{2\pi} \int_0^{2\pi} \int_0^{h+\eta} u \left(p_D + \rho g z + \frac{\rho}{2} (u^2 + w^2) \right) ds d\theta$	$\left(\frac{8}{\gamma H^2 L/T}\right) F_{TE}$	(41)	XI Item 5
Group Velocity, C_G	$C_G = \frac{F_{TE}}{TE}$	$\left(\frac{1}{L/T}\right) C_G$	(42)	XI Item 6
Average Momentum M	$M = \frac{1}{2\pi} \int_0^{2\pi} \int_0^{h+\eta} \rho u ds d\theta$	$\left(\frac{8L/T}{\gamma H}\right) M$	(43)	XI Item 7

TABLE F—Continued

Variable	Expression for Variable	Dimensionless Form	Equation No.	Presented in Table
Average Momentum Flux, in Wave Direction, F_{mx}	$F_{mx} = \frac{1}{2\pi} \int_0^{2\pi} \int_0^{h+\eta} (P_D + \rho u^2) ds d\theta$	$\left(\frac{g}{VH^2} \right) F_{mx}$	(44)	XI Item 8
Average Momentum Flux, Transverse to Wave Direction F_{my}	$F_{my} = \frac{1}{2\pi} \int_0^{2\pi} \int_0^{h+\eta} P_D ds d\theta$	$\left(\frac{g}{VH^2} \right) F_{my}$	(45)	XI Item 9
Root-Mean-Square (RMS) and Maximum (Max) Kinematic Free Surface Boundary Condition Errors, $\sqrt{\epsilon_1}$ and $ \epsilon_1 _{\max}$	See Eq. (35)	Expression Given is in Dimensionless Form	(46)	XI Items 10 & 12
RMS and Max Dynamic Free Surface Boundary Condition Errors, $\sqrt{\epsilon_2}$ and $ \epsilon_2 _{\max}$	See Eq. (36)	$\left(\frac{1}{H} \right) \sqrt{\epsilon_1}$ and $\left(\frac{1}{H} \right) \epsilon_2 _{\max}$	(47)	XI Items 11 & 13
Kinematic Free Surface Breaking Parameter, β_1	$\beta_1 = \frac{u}{C}$, u evaluated at $\left(\theta = 0^\circ \right)$ $\left(S = h + \eta \right)$	Expression Given is in Dimensionless Form	(48)	XI Item 14
Dynamic Free Surface Breaking Parameter β_2	$\beta_2 = -\frac{1}{g} \frac{Dy}{Dt}$, $\frac{Dy}{Dt}$ evaluated at $\left(\theta = 0^\circ \right)$ $\left(S = h + \eta \right)$	Expression Given is in Dimensionless Form	(49)	XI Item 15

Note: In addition to values tabulated, the results include combined refraction/shoaling effects over idealized bathymetry; these results are presented in graphical form and will be described later.

Internal Field Variables Depending on θ and S

The internal field variables are tabulated at equally spaced dimensionless distances above the bottom, i.e., at S/h values of 0, 0.1, 0.2 . . . up to and including the free surface, and at θ values of 0° , 10° , 20° , 30° , 50° , 75° , 100° , 130° , 180° . Figure 24 shows a sample presentation of the dimensionless horizontal velocity component field.

A description of the entries in Figure 24 will serve to familiarize the reader with most of the features of the tables. The first row lists the phase angles (θ) in degrees. The second row lists the dimensionless wave profile (η/H) at the corresponding phase angles. The percent values listed beneath the η/H values are the differences between the Stream-function and Airy Theories, defined as:

$$\text{Percent} = \frac{\text{Stream-function} - \text{Airy}}{\text{Stream-function}} \times 100 \text{ percent}$$

The main body (remaining portion) of the table lists the dimensionless horizontal water particle velocities. The row labeled "Surface" represents the dimensionless velocities evaluated at the free surface; the percentage differences for velocities are calculated as defined above for the profile. The remaining part of the table represents the dimensionless velocities and percentage differences evaluated on a grid of $(\theta, S/h)$. The lack of entries for the higher S/h and higher θ values (right side of page) results from the wave profile in the trough region being lower than in the crest region (left side of page). Two additional comments pertaining to the percentage values will complete the description of the sample table. A percentage difference value of exactly 100 percent implies that the Stream-function profile occurred at a $(\theta, S/h)$ value, however, the Airy profile was lower than the particular S/h at the phase angle, θ , i.e., this grid point was not "covered" by the Airy profile. For example, this is the case at $\theta = 0^\circ$, $S/h = 1.5$ and 1.6 and $\theta = 180^\circ$, $S/h = 0.8$ and 0.9 . Finally, the asterisks indicate that the percentage differences were not calculated because the Stream-function value was less than 5 percent of the maximum Stream-function value. This avoided the tabulation of very large percentages which would have been the result of division by a small number.

A brief description of each of the tabulated internal field variables is presented below.

Horizontal Water Particle Velocity Component, $u(\theta, S)$

The horizontal water particle velocity component, $u(\theta, S)$, is defined by Equation (21). (The equations for the tabulated functions are presented in Tables D, E, and F.) The values $u'(\theta, S)$ tabulated, are presented (Table I) in the following dimensionless form:

$$u'(\theta, S) = \frac{u(\theta, S)}{(H/T)}$$

CASE 4-D										
TABLE 1-DIMENSIONLESS HORIZONTAL VELOCITY COMPONENT FIELD.....DEFINED IN EQUATION (21)										
TIME=	0.0	10.0	20.0	30.0	50.0	70.0	100.0	130.0	160.0	
ETA/HEIGHT=	0.009 4.3.7E	0.583 15.5E	0.264 -65.4E	0.101 -326.7E	-0.085 681.4E	-0.101 227.7E	-0.110 21.0E	-0.112 -242.0E	-0.111 -30.6.7E	
SURFACE	10.009 51.9E	12.419 24.1E	5.421 -80.3E	1.040 -347.1E	-0.093 000000E	-1.036 245.1E	-1.700 15.9E	-1.700 -273.2E	-1.700 -306.0E	
S/DEP Time1.0	10.167 100.0E									
S/DEP Time1.5	10.533 100.0E									
S/DEP Time1.4	10.137 30.7E	11.004 21.4E								
S/DEP Time1.3	13.042 32.3E	11.246 17.3E								
S/DEP Time1.2	12.919 20.0E	10.560 13.6E	5.427 -88.3E							
S/DEP Time1.1	12.043 22.9E	10.030 10.0E	5.437 -82.0E							
S/DEP Time1.0	11.094 10.9E	9.535 6.0E	5.427 -81.1E	2.046 -203.0E						
S/DEP Time0.9	10.655 10.1E	9.104 3.3E	5.403 -40.9E	2.266 -241.7E	-0.069 000000E	-1.030 242.0E	-1.700 13.2E	-1.700 100.0E	-1.700 100.0E	
S/DEP Time0.8	10.113 12.5E	8.734 0.3E	5.370 -44.2E	2.445 -213.2E	-0.723 000000E	-1.003 242.0E	-1.700 13.7E	-1.700 -273.2E	-1.700 100.0E	
S/DEP Time0.7	9.457 9.3E	8.420 -2.0E	5.324 -46.7E	2.592 -192.7E	-0.614 000000E	-1.079 243.6E	-1.700 14.2E	-1.700 -273.2E	-1.700 -307.1E	
S/DEP Time0.6	9.270 6.4E	8.155 -4.9E	5.497 -40.5E	2.709 -177.7E	-0.510 000000E	-1.096 246.5E	-1.700 14.7E	-1.700 -270.1E	-1.700 -306.1E	
S/DEP Time0.5	8.906 3.0E	7.936 -7.0E	5.462 -40.4E	2.803 -160.5E	-0.423 000000E	-1.037 245.2E	-1.700 15.0E	-1.700 -267.3E	-1.700 -302.3E	
S/DEP Time0.4	8.722 1.7E	7.760 -0.0E	5.431 -40.4E	2.875 -149.3E	-0.351 000000E	-1.021 245.0E	-1.700 15.3E	-1.700 -265.4E	-1.700 -370.2E	
S/DEP Time0.3	8.535 -0.0E	7.620 -10.2E	5.406 -40.4E	2.920 -122.9E	-0.296 000000E	-1.000 246.0E	-1.700 15.5E	-1.700 -263.7E	-1.700 -370.0E	
S/DEP Time0.2	8.404 -1.2E	7.531 -11.3E	5.367 -40.4E	2.965 -140.5E	-0.256 000000E	-1.000 247.0E	-1.700 15.7E	-1.700 -262.0E	-1.700 -370.1E	
S/DEP Time0.1	8.326 -2.0E	7.475 -11.9E	5.375 -40.4E	2.997 -140.2E	-0.233 000000E	-1.003 247.2E	-1.700 16.0E	-1.700 -261.9E	-1.700 -370.1E	
S/DEP Time0.0	8.300 -2.2E	7.456 -12.1E	5.372 -40.5E	2.994 -140.5E	-0.225 000000E	-1.001 247.3E	-1.700 15.0E	-1.700 -261.7E	-1.700 -373.7E	

Figure 24. Example output for dimensionless horizontal velocity component field

Vertical Water Particle Velocity Component, $w(\theta, S)$

The vertical water particle velocity component, $w(\theta, S)$, is defined by Equation (22). The dimensionless values tabulated (Table II), $w'(\theta, S)$, are defined by:

$$w'(\theta, S) = \frac{w(\theta, S)}{(H/T)}$$

Horizontal Water Particle Acceleration, Du/Dt

The horizontal water particle acceleration, Du/Dt' is defined in terms of the velocity components as presented in Equation (23). Note that the tabulated values represent the total (or material, substantial, etc.) acceleration consisting of the sum of the local and advective contributions. The dimensionless values tabulated (Table III), Du'/Dt' , are defined by:

$$\frac{Du'}{Dt'} = \frac{1}{(H/T^2)} \frac{Du}{Dt}$$

Vertical Water Particle Acceleration, Dw/Dt

The vertical water particle acceleration, defined in Equation (24), is tabulated (Table IV) in the following dimensionless form:

$$\frac{Dw'}{Dt'} = \frac{1}{(H/T^2)} \frac{Dw}{Dt}$$

Drag Force Component, $F_D(\theta, S)$

The drag force component up to a certain elevation, S , is defined by Equation (25) and tabulated (Table V) in dimensionless form as:

$$F'_D = \left(\frac{2}{C_{D\rho D(H/T)^2 h} \right) F_D$$

Inertia Force Component, $F_I(\theta, S)$

The inertia force component up to a certain elevation, S , is defined by Equation (26) and tabulated (Table VI) in dimensionless form as:

$$F'_I = \left(\frac{4}{C_{M\rho\pi D^2(H/T^2)h} \right) F_I$$

Drag Moment Component, $M_D(\theta, S)$

The drag moment component about the bottom due to wave pressures acting on a vertical member extending up to an elevation, S , is presented as Equation (27) and presented (Table VII) in dimensionless form as:

$$M'_D = \left(\frac{2}{C_D \rho D (H/T)^2 h^2} \right) M_D$$

Inertia Moment Component, $M_I(\theta, S)$

The inertia moment component about the bottom due to wave pressures acting on a vertical member extending up to an elevation S , is defined in Equation, (28) and presented (Table VIII) in dimensionless form as:

$$M'_I = \left(\frac{4}{C_M \rho \pi D^2 (H/T^2) h^2} \right) M_I$$

Dynamic Pressure Component, $p_D(\theta, S)$

The dynamic pressure component, defined by Equation, (29) is tabulated (Table IX) in dimensionless form as:

$$p'_D = \left(\frac{2}{\gamma H} \right) p_D$$

This completes the description of the field variables (depending on θ and S) that are included in the tables.

Variables Depending on θ Only

Water Surface Displacement, $\eta(\theta)$

The water surface displacement is defined in Equation (30), and tabulated (Tables I through IX) in dimensionless form as:

$$\eta' = \left(\frac{1}{H} \right) \eta$$

Total Drag Force Component, $F_D(\theta)$

The total drag force component is defined by Equation (25) with the upper limit taken to be $h + \eta(\theta)$, and is tabulated (Table V, labeled "SURFACE") in dimensionless form as:

$$F'_D = \left(\frac{2}{C_D \rho D (H/T)^2 h} \right) F_D$$

Total Inertia Force Component, $F_I(\theta)$

The total inertia force component is defined by Equation (26) with the upper limit taken to be $h + \eta(\theta)$, and is tabulated (Table VI, labeled "SURFACE") in dimensionless form as:

$$F_I' = \left(\frac{4}{C_M \rho \pi D^2 (H/T^2) h} \right) F_I$$

Total Drag Moment Component, $M_D(\theta)$

The total drag moment component is defined by Equation (27) with the upper limit taken to be $h + \eta(\theta)$ and is tabulated (Table VII, labeled "SURFACE") in dimensionless form as:

$$M_D' = \left(\frac{2}{C_D \rho D (H/T)^2 h^2} \right) M_D$$

Total Inertia Moment Component, $M_I(\theta)$

The total inertia moment component is defined by Equation (28) with an upper limit of $h + \eta(\theta)$ and is tabulated (Table VIII, labeled "SURFACE") in dimensionless form as:

$$M_I' = \left(\frac{4}{C_M \rho \pi D^2 (H/T^2) h^2} \right) M_I$$

Kinematic Free Surface Boundary Condition Error, $\epsilon_1(\theta)$

The kinematic free surface boundary condition error is defined by Equation (35). This variable, as defined, is in dimensionless form and is tabulated in Table X:

Item 1, Linear Wave Theory

Item 2, Stream-Function Theory

Dynamic Free Surface Boundary Condition Error, $\epsilon_2(\theta)$

The dynamic free surface boundary condition error is defined by Equation (36) and is tabulated (Table X) in the following dimensionless form:

$$\epsilon_2' = \left(\frac{1}{H} \right) \epsilon_2$$

with

Item 3, Linear Wave Theory

Item 4, Stream-Function Theory

This completes the presentation of variables depending on θ only.

Overall Variables (do not depend on θ or S)

Wavelength, L

For the Stream-function theory, there is no definable expression for the wavelength. Rather the wavelength is determined as a part of the numerical solution as described in Appendix I. The dimensionless wavelength is presented (Table XI, Item 1) in the following dimensionless form:

$$L' = \left(\frac{2\pi}{gT^2} \right) L$$

Average Potential Energy, PE

The average potential energy is defined by Equation (38) and is tabulated (Table XI, Item 2) in dimensionless form as:

$$PE' = \left(\frac{8}{\gamma H^2} \right) PE$$

Note that the dimensionless form is defined to be 0.5 for the linear (Airy) wave theory.

Average Kinetic Energy, KE

The average kinetic energy is defined by Equation (39), and is also tabulated (Table XI, Item 3) in dimensionless form as:

$$KE' = \left(\frac{8}{\gamma H^2} \right) KE$$

As for the dimensionless potential energy, the dimensionless value for the linear (Airy) wave theory is 0.5.

Average Total Energy, TE

The average total energy is simply the sum of the potential and kinetic energy contributions [Equation (40)], and is tabulated in dimensionless form (Table XI, Item 4) such that the difference from unity is an indication of the deviation from the linear wave theory.

$$TE' = \left(\frac{8}{\gamma H^2} \right) TE$$

Average Total Energy Flux, F_{TE}

The average total energy flux is defined by Equation (41), and is tabulated (Table XI, Item 5) in dimensionless form as:

$$F'_{TE} = \left(\frac{8}{\gamma H^2} \frac{L}{T} \right) F_{TE}$$

Group Velocity, C_G

The group velocity is defined as the ratio of total energy flux to total energy [Equation (42)] and is presented (Table XI, Item 6) in dimensionless form as:

$$C'_G = \left(\frac{1}{L/T} \right) C_G$$

The dimensionless group velocity is defined such that for linear wave theory the shallow and deepwater values are 1.0 and 0.5, respectively.

Average Momentum, M

The total average momentum is defined by Equation (43) and is presented (Table XI, Item 7) in dimensionless form as:

$$M' = \left(\frac{8 L/T}{\gamma H^2} \right) M$$

The dimensionless momentum is defined such that for linear wave theory the result is unity. Note that mass transport velocity, $U = [M/\rho h]$ is proportional to the average momentum.

Average Momentum Flux in Wave Direction, F_{m_x}

The total average momentum flux in the wave direction is defined by Equation (44) and is tabulated (Table XI, Item 8) in the following dimensionless form:

$$F'_{m_x} = \left(\frac{8}{\gamma H^2} \right) F_{m_x}$$

The above definition reduces to 1.5 and 0.5 for linear wave theory for shallow and deepwater waves, respectively.

Average Momentum Flux Transverse to Wave Direction, F_{m_y}

The total average momentum flux in a direction perpendicular to the wave advance direction is needed to define the radiation stress tensor, (discussed by Bowen 1969), is defined by Equation (45), and is tabulated (Table XI, Item 9) in the following dimensionless form:

$$F'_{m_y} = \left(\frac{8}{\gamma H^2} \right) F_{m_y}$$

For linear wave theory, the above definition reduces to 0.5 and 0.0 for shallow and deepwater waves, respectively.

Kinematic Free Surface Boundary Condition Errors, ϵ_1

The kinematic free surface boundary condition error is defined in dimensionless form by Equation (35) and the root-mean-square (RMS) and maximum values are tabulated (Table XI, Items 10 and 12) as defined by Equation (46).

Dynamic Free Surface Boundary Condition Errors, ϵ_2

The dynamic free surface boundary condition error is defined by Equation (36) and is represented in the following dimensionless form:

$$\epsilon_2^I = \frac{\epsilon_2}{H}$$

The RMS and maximum values are tabulated (Table XI, Items 11 and 13) as defined by Equation (47).

Kinematic Free Surface Breaking Parameter, β_1

The kinematic free surface breaking parameter is tabulated (Table XI, Item 14) as defined by Equation (48) (dimensionless form).

Dynamic Free Surface Breaking Parameter, β_2

The dynamic free surface breaking parameter is tabulated (Table XI, Item 15) as defined by Equation (49) in dimensionless form.

Variables Presented in Graphical Form—Combined Effect of Shoaling and Refraction

In addition to developing the tabulated values previously described, the study included the development of the combined effect of shoaling and refraction for nonlinear waves advancing toward shore with a deepwater direction, α_o , over bathymetry characterized by straight and parallel contours.

For linear wave theory, it is possible to separate the shoaling and refraction effects, because neither wave celerity, C (governing refraction), nor group velocity, C_G (governing energy flux), is dependent on wave height. For nonlinear waves, both celerity and group velocity at a certain location depend on wave height as well as wave period and water depth. The shoaling-refraction effects for nonlinear waves are therefore not separable, and the combined effect depends on the deepwater wave steepness, H_o/L_o , as well as the local relative depth.

Because the shoaling-refraction results are not readily presented in tabular form, graphs are presented as Figures 25, through 29 for deepwater wave directions, α_o of 0° , 10° , 20° , 40° , and 60° . A brief description of the use of these graphs follows. A wave with a deepwater direction α_o , will propagate toward shore such that the local H/L_o will fall along a curve characterized by the deepwater value H_o/L_o . At any particular relative depth, h/L_o , the local wave steepness H/L_o and direction α are read from the ordinate

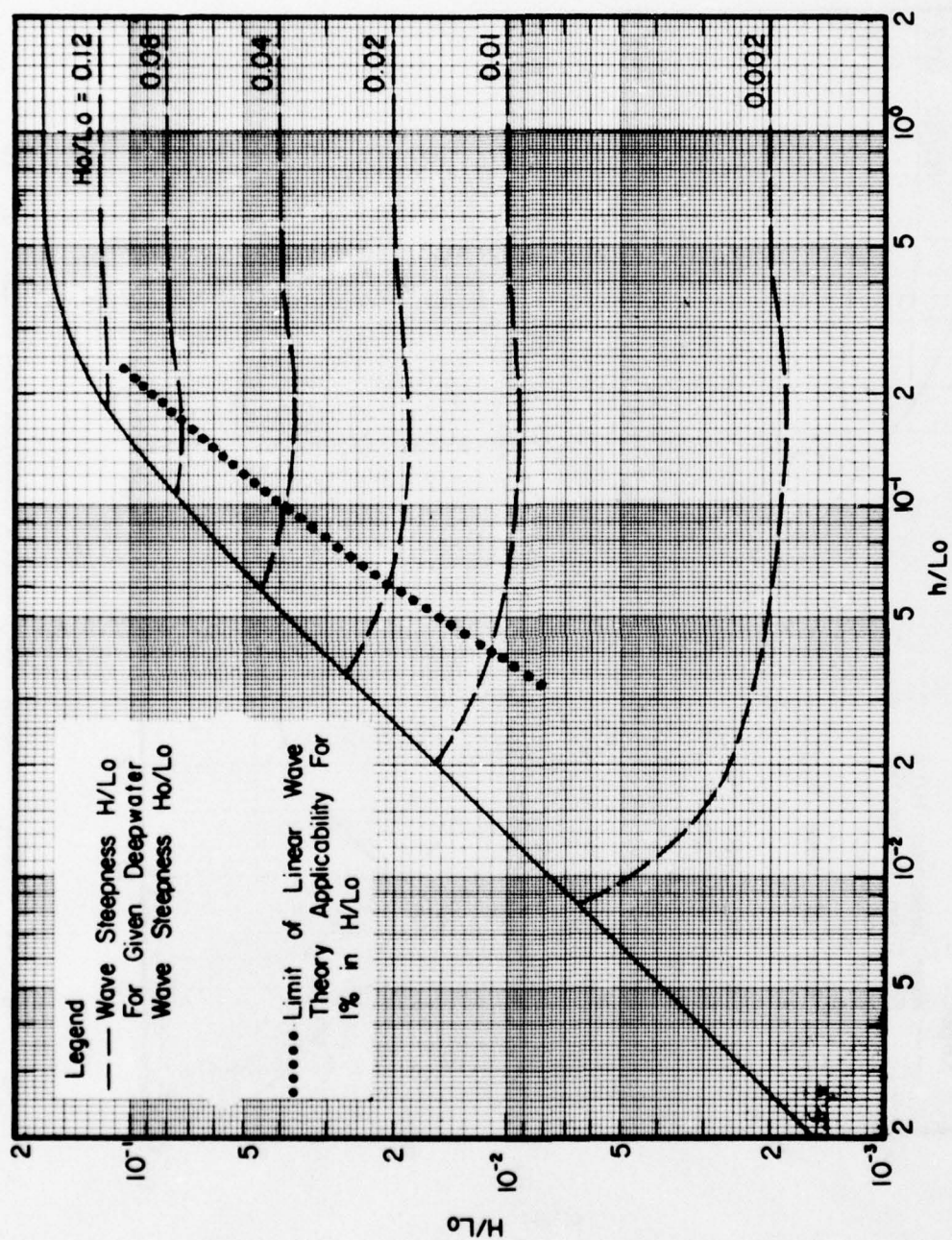


Figure 25. Combined shoaling-refraction for a deepwater wave direction, $\alpha_0 = 0^\circ$

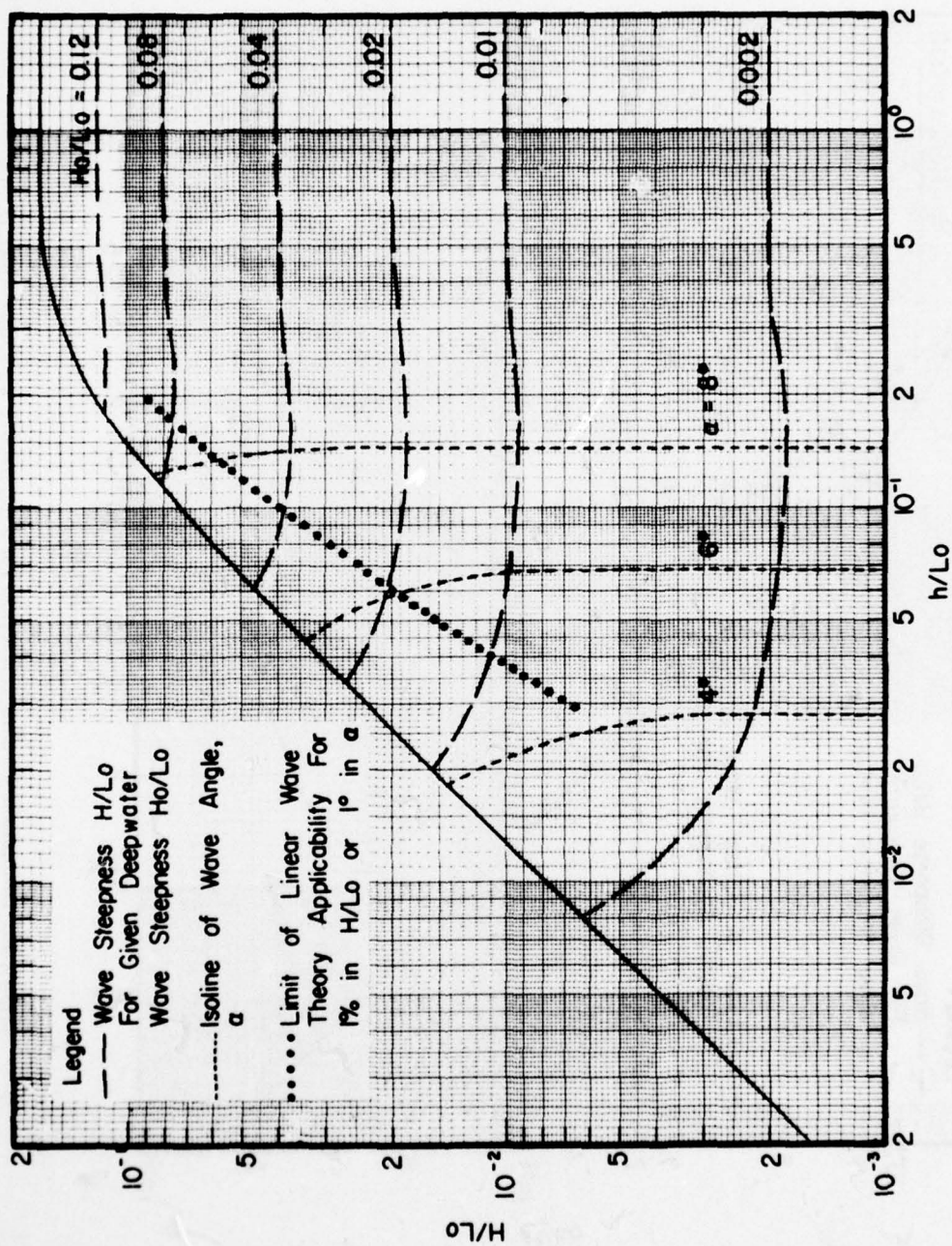


Figure 26. Combined shoaling-refraction for a deepwater wave direction, $\alpha_0 = 10^\circ$

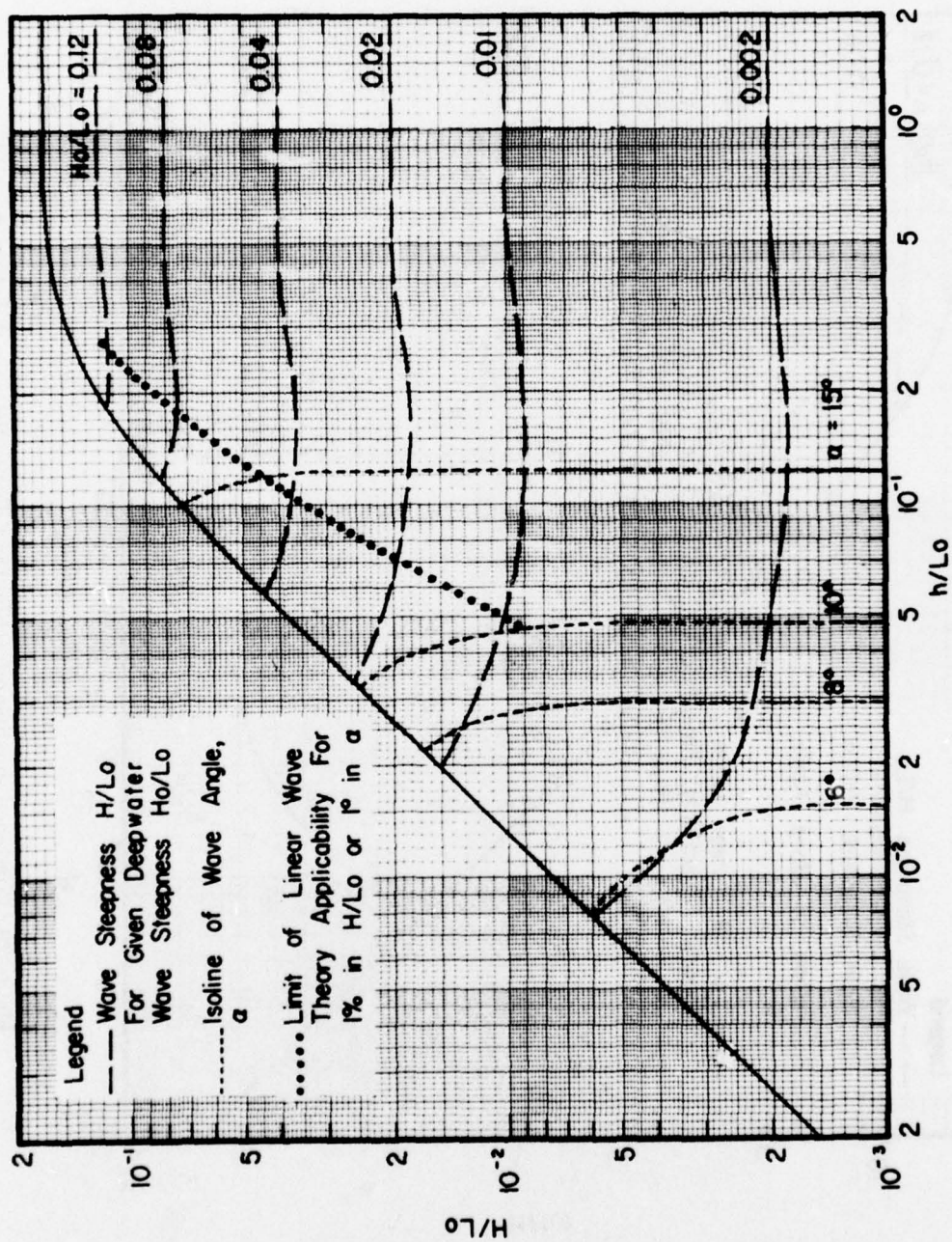


Figure 27. Combined shoaling-refraction for a deepwater wave direction, $\alpha_0 = 20^\circ$

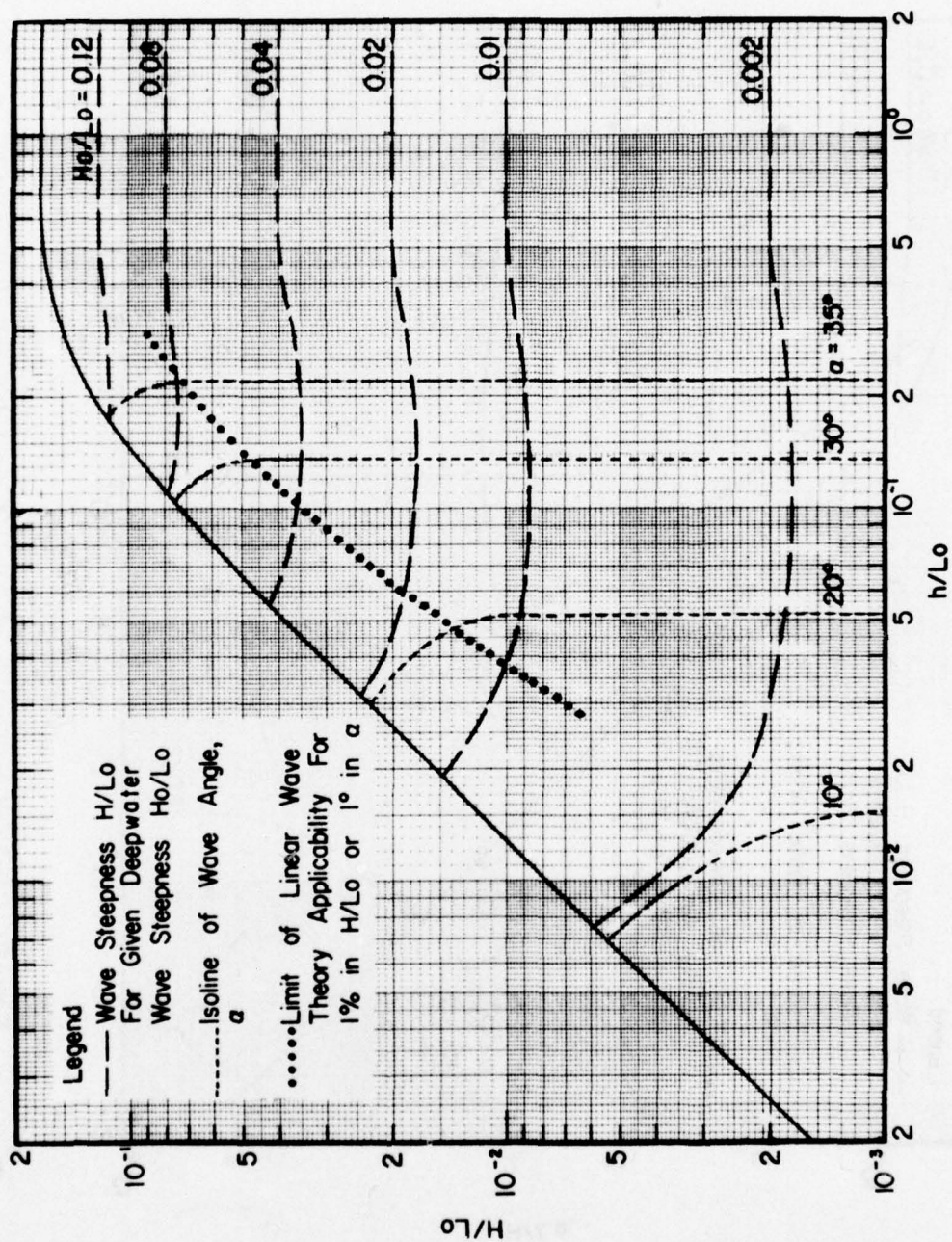


Figure 28. Combined shoaling-refraction for a deepwater wave direction, $\alpha_0 = 40^\circ$

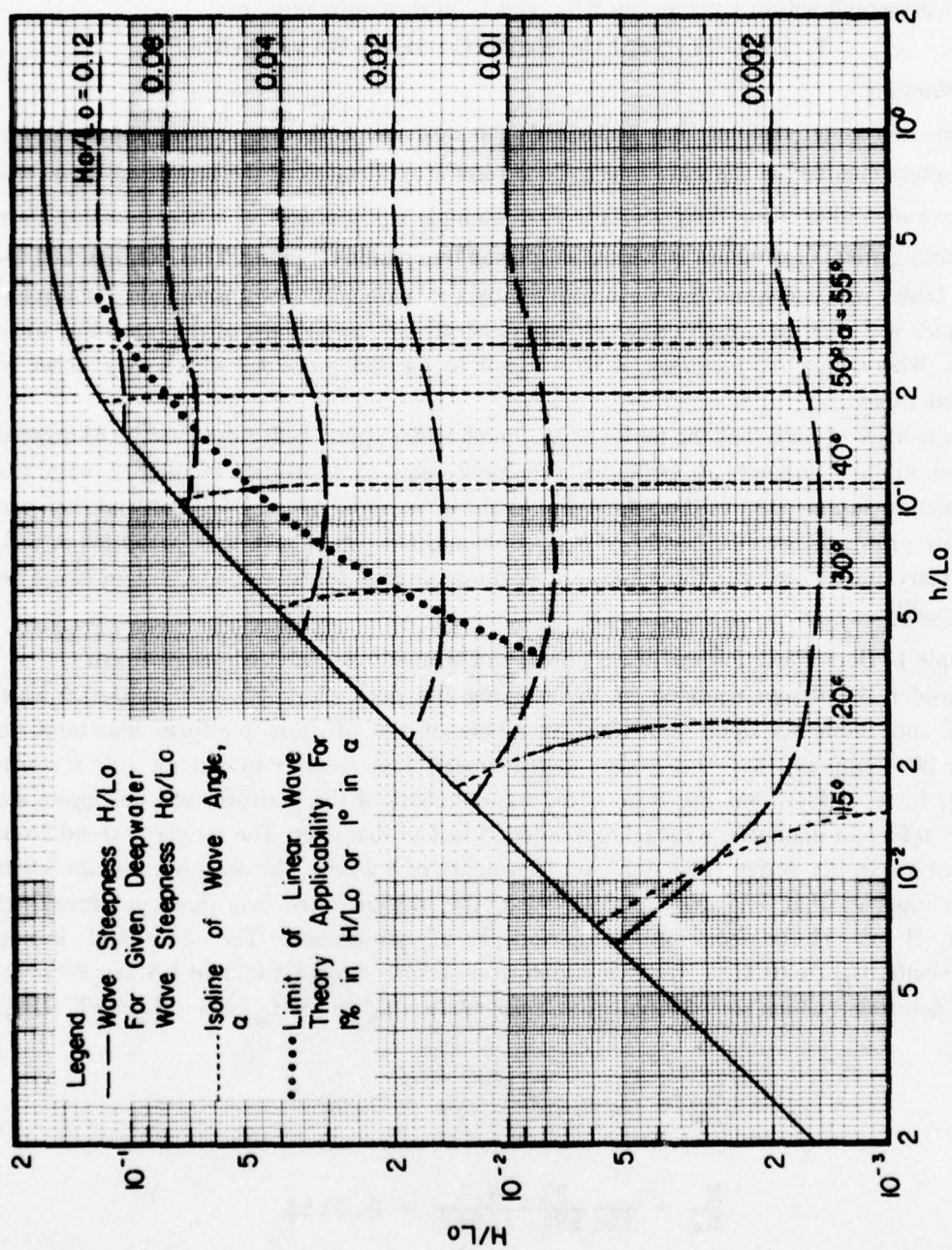


Figure 29. Combined shoaling-refraction for a deepwater wave direction, $\alpha_0 = 60^\circ$

and interpolated from the appropriate isolines, respectively. The region to the lower right of the line of dots indicates the region where use of the linear theory agrees with the nonlinear results presented within 1 percent in H/L_o and 1° in wave direction, α .

V. EXAMPLES ILLUSTRATING USE OF WAVE TABLES

Introduction

The preceding chapter has described the formats and the various dimensionless parameters included in the wave tables. To aid in the application of the tables, examples will be presented illustrating their use. The first example is a problem of a near-breaking wave interacting with an offshore structure supported by cylindrical piling. This example will use those tables which contain the wave profile and the wave forces and moments. Additional examples will then be presented which will illustrate the use of most of the remaining wave tables. Where possible, examples were selected to parallel problems which may occur in offshore design.

It is worthy of note that the tables have a much wider applicability than can be illustrated by the limited number of examples presented here. A thorough familiarity with the information summarized in the tables should aid in an understanding of them and their use in many problems involving water-wave phenomena. The examples will be presented in U.S. Customary units; however the tables are in dimensionless form, and any system could be used readily.

Example 1—Deck Elevation and Wave Forces and Moments on an Offshore Platform

Consider the design problem of determining the deck elevation and horizontal wave forces and moments upon individual members of the offshore platform illustrated in Figure 30. Suppose that the design depth (mean low water + maximum tide + storm surge), h , is 41 feet, and the main structural members of the platform and outriggers are pilings 6 feet in diameter, with piling fenders 3 feet in diameter. The fenders extend from 4.1 feet above the design stillwater level to a depth of 8.2 feet. The outriggers are 20.5 feet high. Suppose that analysis indicates that the design wave will have a (breaking) height, H , of 31.78 feet and a period, T , of 20 seconds. The drag and inertia coefficients, C_D and C_M , for this structure are assumed to be 1.05 and 1.5, respectively.

To determine which set of tables to use, calculate h/L_o and H/L_o , where $L_o \equiv gT^2/(2\pi)$,

$$\frac{h}{L_o} = \frac{41}{(5.12)(20)^2} = 0.02$$

$$\frac{H}{L_o} = \frac{31.78}{(5.12)(20)^2} = 0.0155$$

In this and most subsequent examples in this chapter, the tables for Case 4-D will be used (see Figure 23). A sample table set for Case 4-D is included as Appendix III.

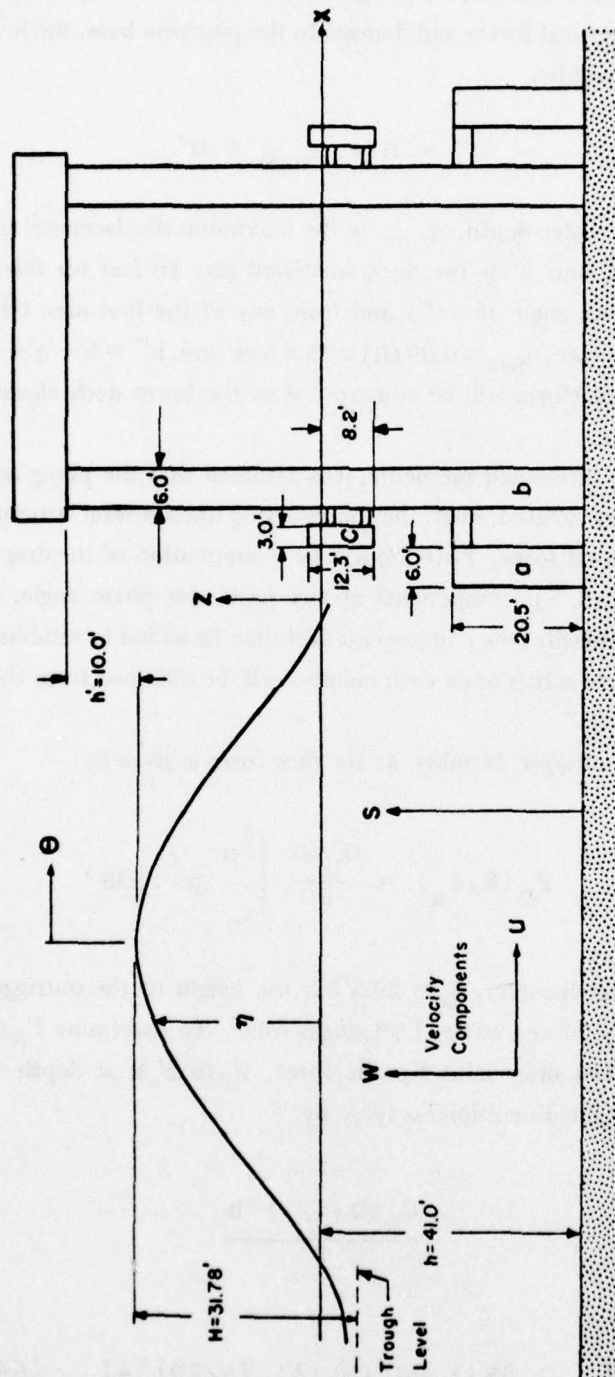


Figure 30. Definition sketch, wave approaching platform

Deck Elevation

To ensure that the deck is above the design crest elevation; thereby avoiding unnecessarily large horizontal and vertical forces and damage to the platform base, the height of the lower elevation of the deck will be:

$$h'' = h + \eta_{max} + h'$$

where h is the design water depth, η_{max} is the maximum displacement of the wave above design stillwater level, and h' is the deck freeboard (say 10 feet for this problem). η_{max} will occur at zero phase angle ($\theta = 0^\circ$) and from any of the first nine tables, $\eta/H = 0.89$ for $\theta = 0^\circ$. Therefore, $\eta_{max} = 0.89(H) = 28.3$ feet and $h'' = h + \eta + h' = 41 + 28.3 + 10 = 79.3$ feet. The platform will be constructed so the lower deck elevation will be 79.3 feet above the bottom.

In determining the forces and moments, it is assumed that the piling are sufficiently far apart to be considered isolated. First, the forces acting upon several structural members will be determined. The total force, $F_T(\theta, S)$, will be a summation of the drag force, $F_D(\theta, S)$, and inertia force, $F_I(\theta, S)$, components at any particular phase angle. Each component will be presented graphically; the components will then be added to establish the total force, and the maximum force acting upon each member will be obtained from the graph.

Forces on Member "a"

In the case of the outrigger, Member a, the drag force is given by:

$$F_D(\theta, S_a) = \frac{C_D \rho D}{2} \int_0^{S_a} u |u| ds'$$

where D is the piling diameter, $S_a (= 20.5')$ is the height of the outrigger above bottom, and $\rho =$ mass density of sea water, 1.99 slugs/foot³. To determine $F_D(\theta, S_a)$, select the tabulated dimensionless drag value for the force, $F'_D(\theta, S_a)$, at depth $S_a/h = 0.5$ from Table V and multiply the dimensionless force by:

$$\frac{C_D \rho D (H/T)^2 h}{2}$$

$$\frac{C_D \rho D (H/T)^2 h}{2} = \frac{1.05 (1.99) (6) (31.78/20)^2 41}{2} = \begin{bmatrix} 648.9 \text{ lbs} \\ 0.6489 \text{ kips} \end{bmatrix}$$

The inertia force on Member a is given by:

$$F_I(\theta, S_a) = \frac{C_M \rho \pi D^2}{4} \int_0^{S_a} \frac{Du}{Dt} ds'.$$

To determine $F_I(\theta, S_a)$, select the tabulated value of the dimensionless inertia force, $F_I'(\theta, S)$, for a relative depth $S_a/h = 0.5$ from Table VI and multiply the dimensionless force by:

$$\frac{C_M \rho \pi D^2 (H/T^2) h}{4} = \begin{cases} 274.9 \text{ lbs} \\ 0.2749 \text{ kips} \end{cases}$$

The total force will be determined by summation of $F_I(\theta, S_a)$ and $F_D(\theta, S_a)$ at each phase angle, θ . The force calculations are summarized in Table G and the forces are plotted in Figure 31.

TABLE G
Horizontal Wave Forces on Member "a"

$\theta(^{\circ})$	0	10	20	30	50	75	100	130	180
F_D'	36.31	29.00	14.60	4.30	-0.04	-1.14	-1.54	-1.62	-1.60
$F_D(\text{kips})$	23.56	18.81	9.47	2.79	-0.03	-0.74	-1.00	-1.05	-1.04
F_I'	0.0	22.59	36.36	36.63	17.25	3.76	0.67	0.12	0.0
$F_I(\text{kips})$	0.0	6.21	10.00	10.07	4.74	1.03	0.18	0.03	0.0
$F_T(\text{kips})$	23.56	25.02	19.47	12.86	4.71	0.29	-0.82	-1.02	-1.04

Forces on Member "b"

Next, consider the horizontal forces acting on the main support piling. In this case, the forces are integrated from 0 to $h + \eta(\theta)$. To determine $F_D(\theta)$, multiply the tabulated

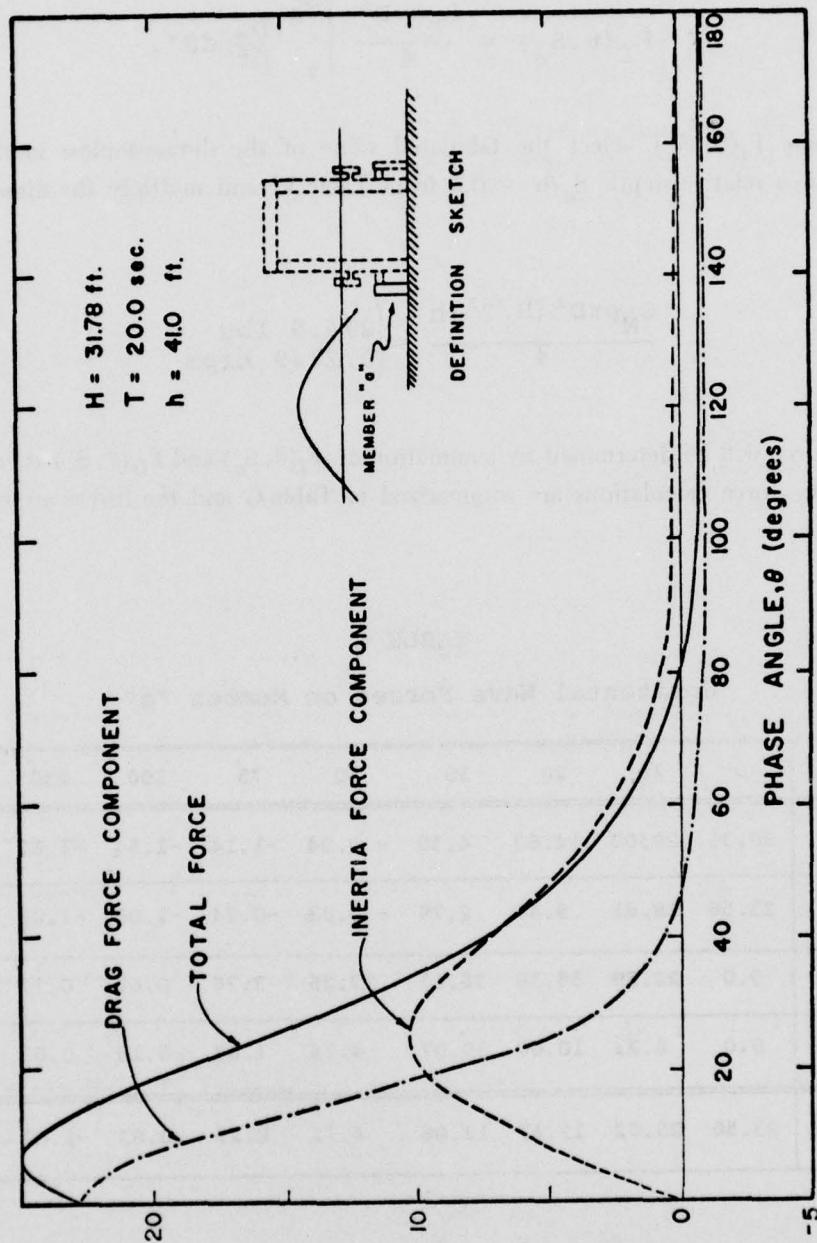


Figure 31. Horizontal wave forces on member "a"

value for the dimensionless total drag force, $F'_D(\theta)$ (indicated "Surface" in Table V) by the same constant as for Member a, i.e.,

$$\frac{C_D \rho D (H/T)^2 h}{2} = 0.6849 \text{ kips}$$

Similarly, $F_I(\theta)$ is found by multiplying the tabulated value, $F'_I(\theta)$, indicated "Surface" in Table VI by:

$$\frac{C_M \rho \pi D^2 (H/T^2) h}{4} = 0.2749 \text{ kips}$$

The calculated forces are summarized in Table H and are plotted in Figure 32.

TABLE H
Horizontal Wave Forces on Member "b"

$\theta(^{\circ})$	0	10	20	30	50	75	100	130	180
F'_D	242.39	119.80	37.00	7.72	-0.25	-2.19	-2.84	-2.95	-2.92
$F_D(\text{kips})$	157.3	77.7	24.0	5.0	-0.2	-1.4	-1.8	-1.9	-1.9
F'_I	0.0	112.13	113.47	84.55	30.12	6.08	1.03	0.27	0.0
$F_I(\text{kips})$	0.0	30.8	31.2	23.2	8.3	1.7	0.3	0.1	0.0
$F_T(\text{kips})$	157.3	108.5	55.2	28.2	8.1	0.3	-1.5	-1.8	-1.9

Forces on Member "c"

Finally, consider structural Member c, the fender. The computation for this member is a combination of the two previous methods since it is sometimes over-topped by the wave. The forces are integrated from $S_{c1} = 32.8$ ft to $S_{c2} = 45.1$ ft; therefore, the force acting on

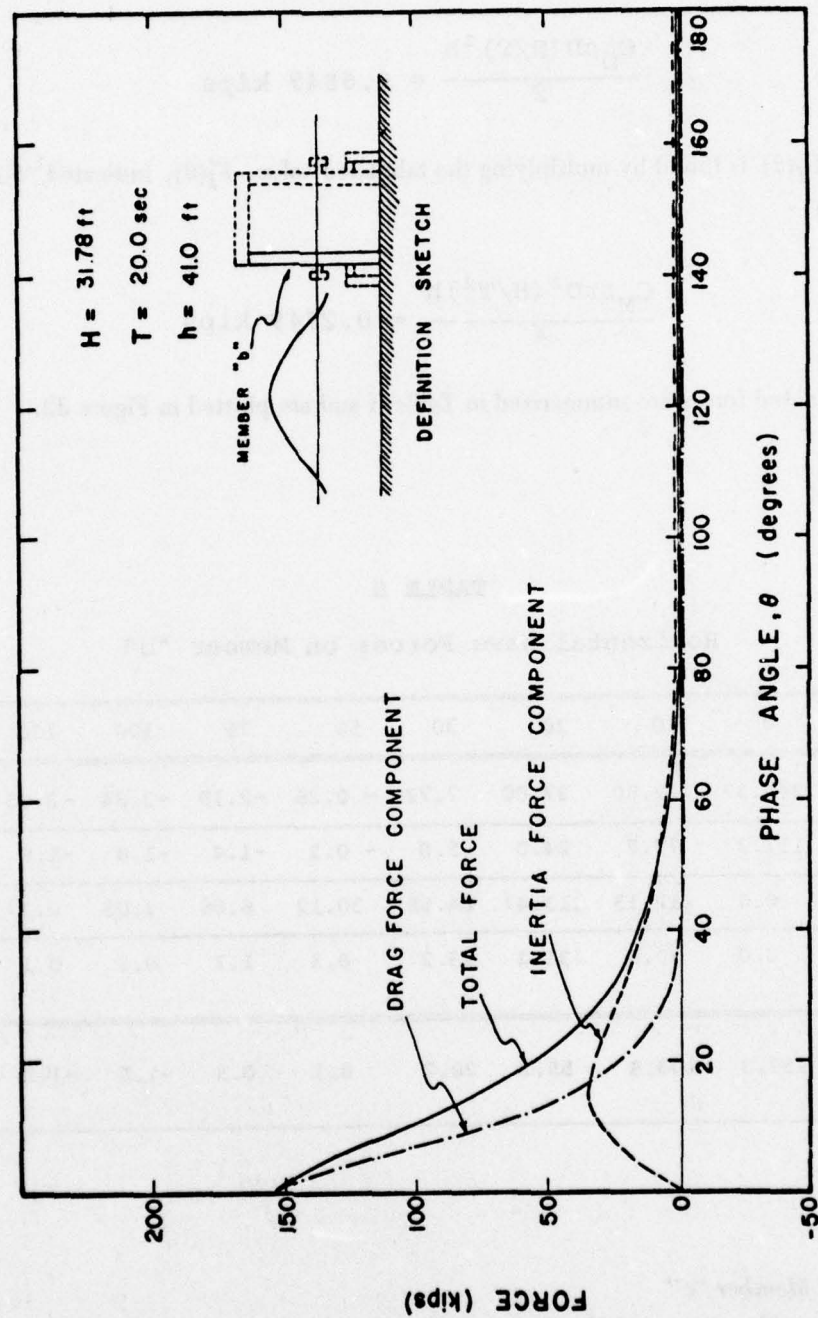


Figure 32. Horizontal wave forces on member "b"

an imaginary piling up to the bottom of the fender is subtracted from a similar term for the top of the fender. The dimensionless forces are obtained by subtracting the dimensionless force components pertaining to the bottom of the member from those pertaining to the top. If the top of the member is submerged, the value at $S'_{c2} = 1.1$ should be used; for times that the top is not submerged, the value indicated "Surface" should be employed for S'_{c2} . Note that the selection of the proper value for the member upper elevation follows readily from the tables; the values at $S'_{c2} = 1.1$ are used at phase angles where they are tabulated ($0 \leq \theta \leq 20^\circ$) and the values labeled "Surface" are used for the remaining phase angles ($30^\circ \leq \theta \leq 180^\circ$).

Summarizing, for each phase angle, the net dimensionless force components on Member c are obtained by:

$$F'_{D_N} = F'_{D_U} - F'_{D_L}$$

$$F'_{I_N} = F'_{I_U} - F'_{I_L}$$

where the subscripts, N, U and L indicate net, upper and lower. The dimensionalizing constant for drag force for the member is calculated (recalling that $D = 3'$)

$$\frac{C_D \rho D (H/T)^2 h}{2} = 0.3245 \text{ kips}$$

and for the inertia force component

$$\frac{C_M \rho \pi D^2 (H/T^2) h}{4} = 0.0687 \text{ kips}$$

The required calculations are summarized in Table I and the results are shown in Figure 33.

The maximum horizontal wave-induced forces are now available for the design wave, and may be used in further design analysis. They are summarized in Table J.

Moments on Member "a"

The moments due to the wave forces acting on the structure are also essential in design. For any member, the moment about the mudline is defined as:

$$\begin{aligned} M_T(\theta) &= \int_{S_1}^{S_2} S \, dF_T(\theta, S) = \int_{S_1}^{S_2} S \, dF_D(\theta, S) + \int_{S_1}^{S_2} S \, dF_I(\theta, S) \\ &= M_D(\theta) + M_I(\theta) \end{aligned}$$

TABLE I
Horizontal Wave Forces on Member "c"

$\theta (^{\circ})$	0	10	20	30	50	75	100	130	150
F_{D_U}'	99.73	75.87	33.17	7.72	- 0.25	-2.19	-2.84	-2.95	-2.92
F_{D_L}'	63.34	49.68	23.72	6.40	- 0.14	-1.87	-2.48	-2.59	-2.56
$F_{D_N}' =$ $F_{D_U}' - F_{D_L}'$	36.39	26.19	9.45	1.32	- 0.11	-0.32	-0.36	-0.36	-0.36
F_D (kips)	11.81	8.50	3.07	0.43	- 0.04	-0.10	-0.12	-0.12	-0.12
F_{I_U}'	0.0	65.78	96.88	84.55	30.12	6.08	1.03	0.27	0.0
F_{I_L}'	0.0	40.55	62.97	60.49	26.23	5.53	0.96	0.22	0.0
$F_{I_N}' =$ $F_{I_U}' - F_{I_L}'$	0.0	25.23	33.91	24.06	3.89	0.55	0.07	0.05	0.0
F_I (kips)	0.0	1.73	2.33	1.65	0.27	0.04	0.0	0.0	0.0
F_T (kips)	11.81	10.23	5.40	2.08	0.23	-0.06	-0.11	-0.11	-0.12

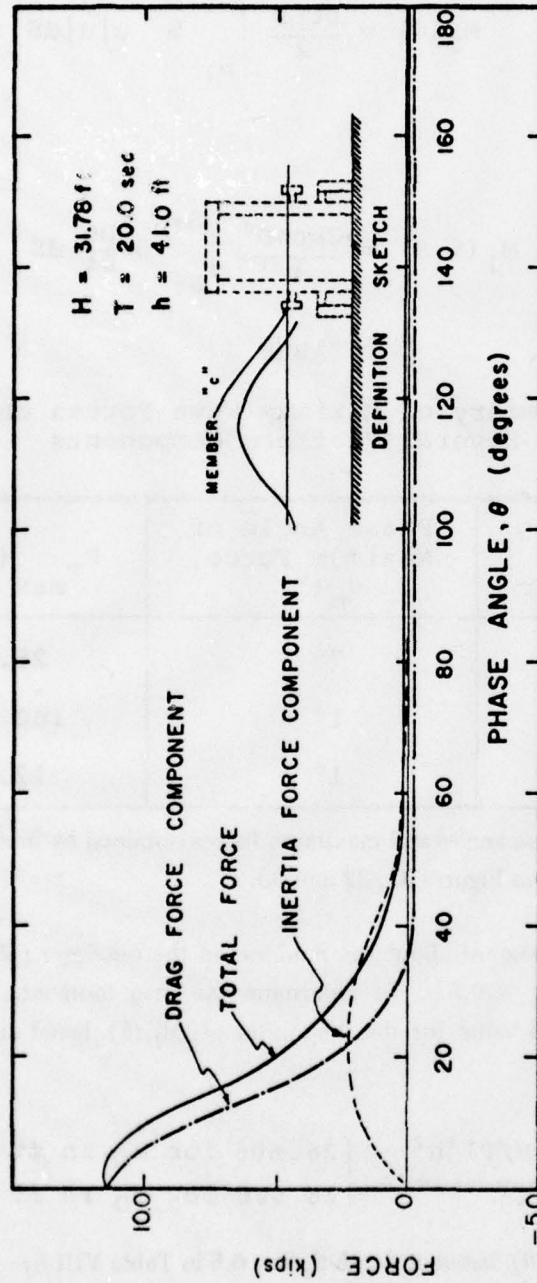


Figure 33. Horizontal wave forces on member "c"

where

$$M_D(\theta) = \frac{\rho C_D D}{2} \int_{S_1}^{S_2} s |u| ds$$

and

$$M_I(\theta, S) = \frac{C_M \rho \pi D^2}{4} \int_{S_1}^{S_2} s \frac{Du}{Dt} ds$$

TABLE J

Summary of Maximum Wave Forces on
Several Platform Components

Member	Phase Angle of Maximum Force, θ_m (°)	$F_{T_{max}}$ (kips)
a	7°	25.1
b	1°	160
c	1°	12.3

Note: Phase angles and maximum forces obtained by interpolation
from Figures 31, 32 and 33.

Consider the total moment about the mudline on the outrigger (Member a). In this case $S_1 = 0$, and $S_2 = S_a = 0.5 h$. To determine the drag moment, $M_D(\theta)$, multiply the dimensionless tabulated value for the drag moment, $M'_D(\theta)$, listed at depth $S_a/h = 0.5$ in Table VII, by:

$$\frac{C_D \rho D (H/T)^2 h^2}{2} = \begin{cases} 26,606 \text{ for } M_D \text{ in ft-lbs} \\ 26.606 \text{ for } M_D \text{ in ft-kips} \end{cases}$$

Similarly, multiply $M'_I(\theta)$ listed at depth $S_a/h = 0.5$ in Table VIII by:

$$\frac{C_M \rho \pi D^2 (H/T^2) h^2}{4} = \begin{cases} 11,272 \text{ for } M_I \text{ in ft-lbs} \\ 11.272 \text{ for } M_I \text{ in ft-kips} \end{cases}$$

to obtain $M_I(\theta)$. These moments are added to obtain $M_T(\theta)$, as shown in Table K and Figure 34.

TABLE K
Wave Moments (About Mudline) on Member "a"

$\theta(^{\circ})$	0	10	20	30	50	75	100	130	180
M'_D	9.31	7.40	3.67	1.05	- 0.01	- 0.29	- 0.39	- 0.40	- 0.40
M_D (ft-kips)	247.7	196.9	97.6	27.9	- 0.3	- 7.7	-10.4	-10.6	-10.6
M'_I	0.0	5.85	9.32	9.26	4.25	0.92	0.16	0.03	0.0
M_I (ft-kips)	0.0	65.9	105.1	104.4	47.9	10.4	1.8	0.3	0.0
M_T (ft-kips)	247.7	262.8	202.7	132.3	47.6	+ 2.7	- 8.6	-10.3	-10.6

Moments on Member "b"

Next consider the moment on the main structural piling (Member b). The limits of integration are from 0 to $h + \eta(\theta)$. Therefore, take the tabulated values labeled "Surface" from Table VII, $[M'_D(\theta)]$, and Table VIII, $[M'_I(\theta)]$, and multiply by:

$$\frac{C_D \rho D (H/T)^2 h^2}{2} = 26.606 \text{ for } M_D \text{ in ft-kips}$$

and

$$\frac{C_M \rho \pi D^2 (H/T^2) h^2}{4} = 11.272 \text{ for } M_I \text{ in ft-kips}$$

in order to obtain $M_D(\theta)$ and $M_I(\theta)$. The two moments are added to obtain $M_T(\theta)$ as indicated in Table L and plotted in Figure 35.

Moments on Member "c"

The fender has the same limits of integration for moment calculation as for the force calculation and is determined in a similar manner. However, the tabulated moments, $M'_D(\theta, S)$, and $M'_I(\theta, S)$, are taken from Tables VII and VIII. The total moment acting on the fender is found by: $M_T(\theta) = M_D(\theta) + M_I(\theta)$. The calculations are summarized in Table M and are plotted in Figure 36.

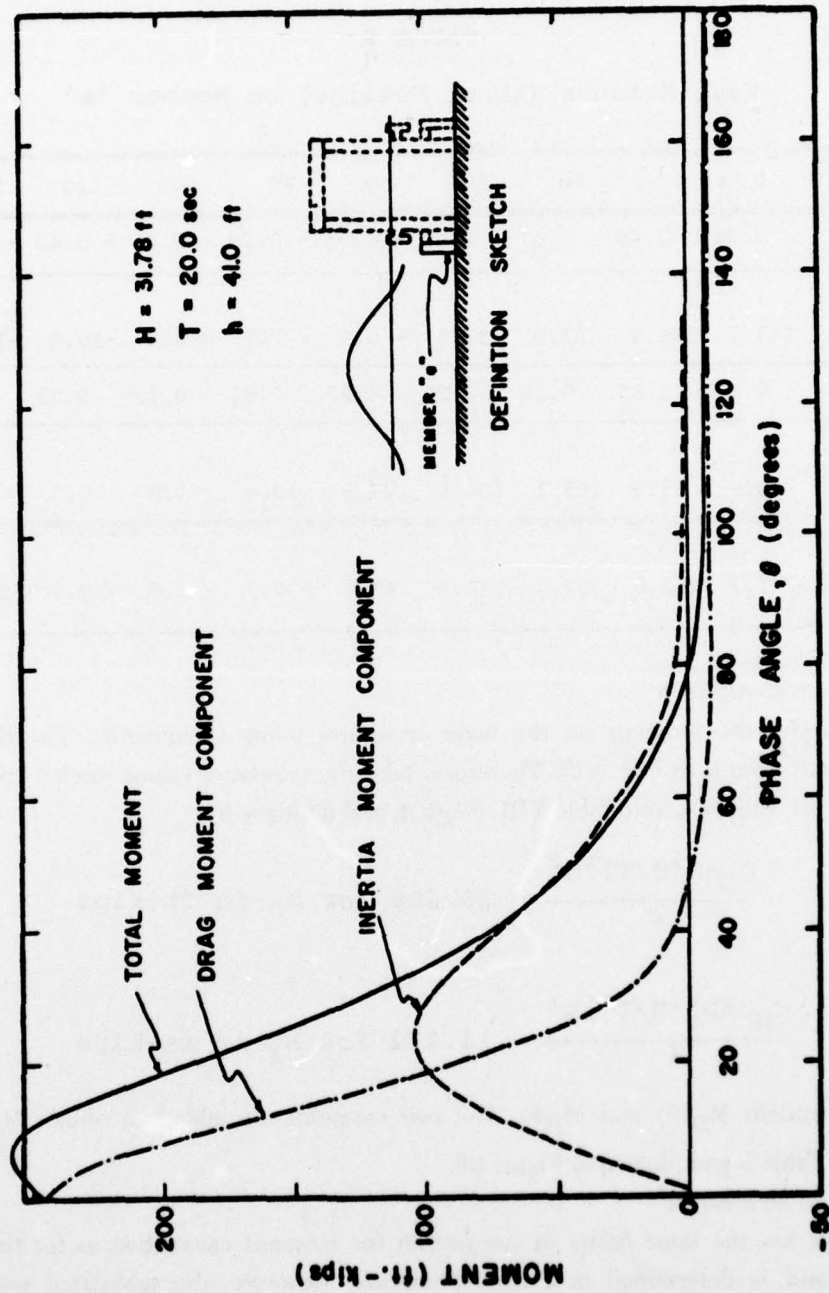


Figure 34. Wave moments on member "a"

TABLE L

Wave Moments (About Mudline) on Member "b"

$\theta(^{\circ})$	0	10	20	30	50	75	100	130	180
M'_D	268.1	102.6	23.0	3.6	- 0.2	- 1.0	- 1.3	- 1.3	- 1.3
M_D (ft-kips)	7133	2730	612	96	- 5	-27	-35	-35	-35
M'_I	0.0	101.7	78.5	47.5	13.5	2.5	0.4	0.1	0.0
M_I (ft-kips)	0.0	1146	885	535	152	28	5	1	0.0
M_T (ft-kips)	7133	3876	1497	631	147	1	-30	-34	-35

TABLE M

Wave Moments (About Mudline) on Member "c"

$\theta(^{\circ})$	0	10	20	30	50	75	100	130	180
M'_{DU}	61.94	46.01	18.59	3.63	- 0.18	-1.04	-1.31	-1.35	-1.33
M'_{DL}	27.04	20.94	9.61	2.40	- 0.08	-0.77	-1.00	-1.04	-1.02
$M'_{DN} = M'_{DU} - M'_{DL}$	34.90	25.07	8.98	1.23	- 0.10	-0.27	-0.31	-0.31	-0.31
M_D (ft-kips)	464	334	119	16	- 1	-4	-4	-4	-4
M'_{IU}	0.0	41.87	59.20	47.47	13.45	2.52	0.40	0.14	0.0
M'_{IL}	0.0	17.66	26.76	24.82	10.04	2.05	0.34	0.10	0.0
$M'_{IN} = M'_{IU} - M'_{IL}$	0.0	24.21	32.44	22.65	3.41	0.47	0.06	0.04	0.0
M_I (ft-kips)	0.0	68	91	64	10	1	0	0	0.0
M_T (ft-kips)	464	402	210	80	9	-3	-4	-4	-4

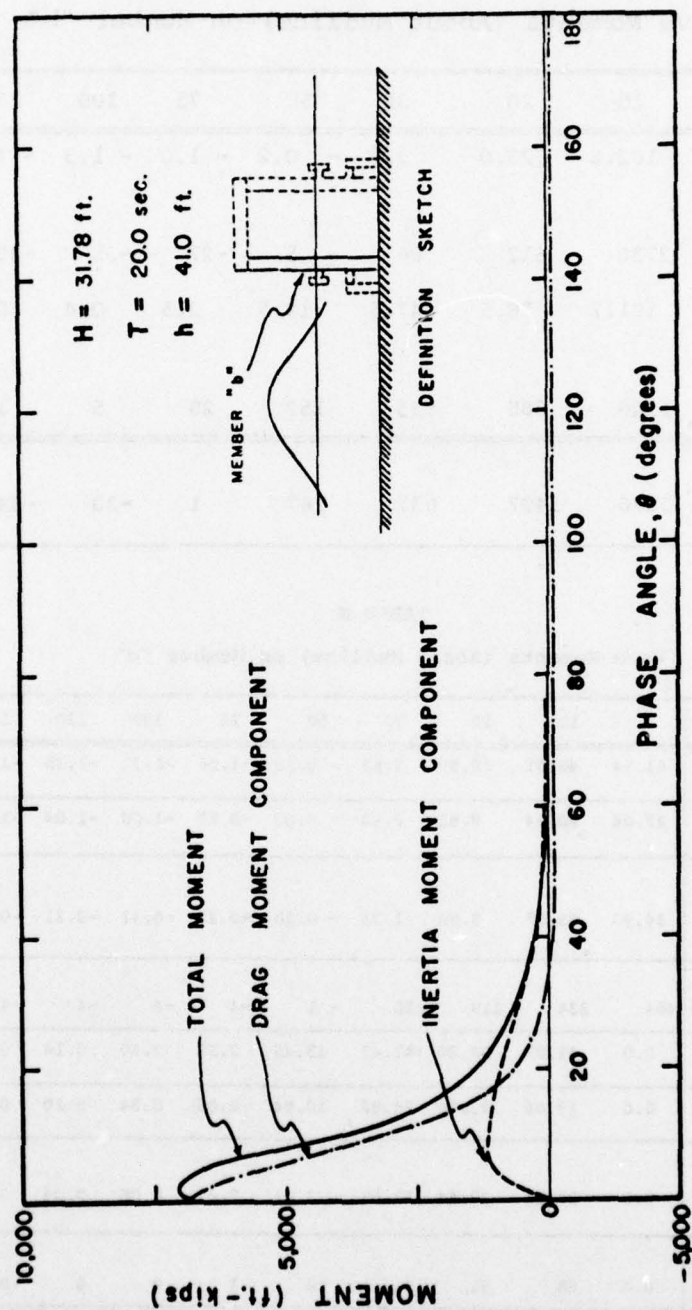


Figure 35. Wave moments on member "b"

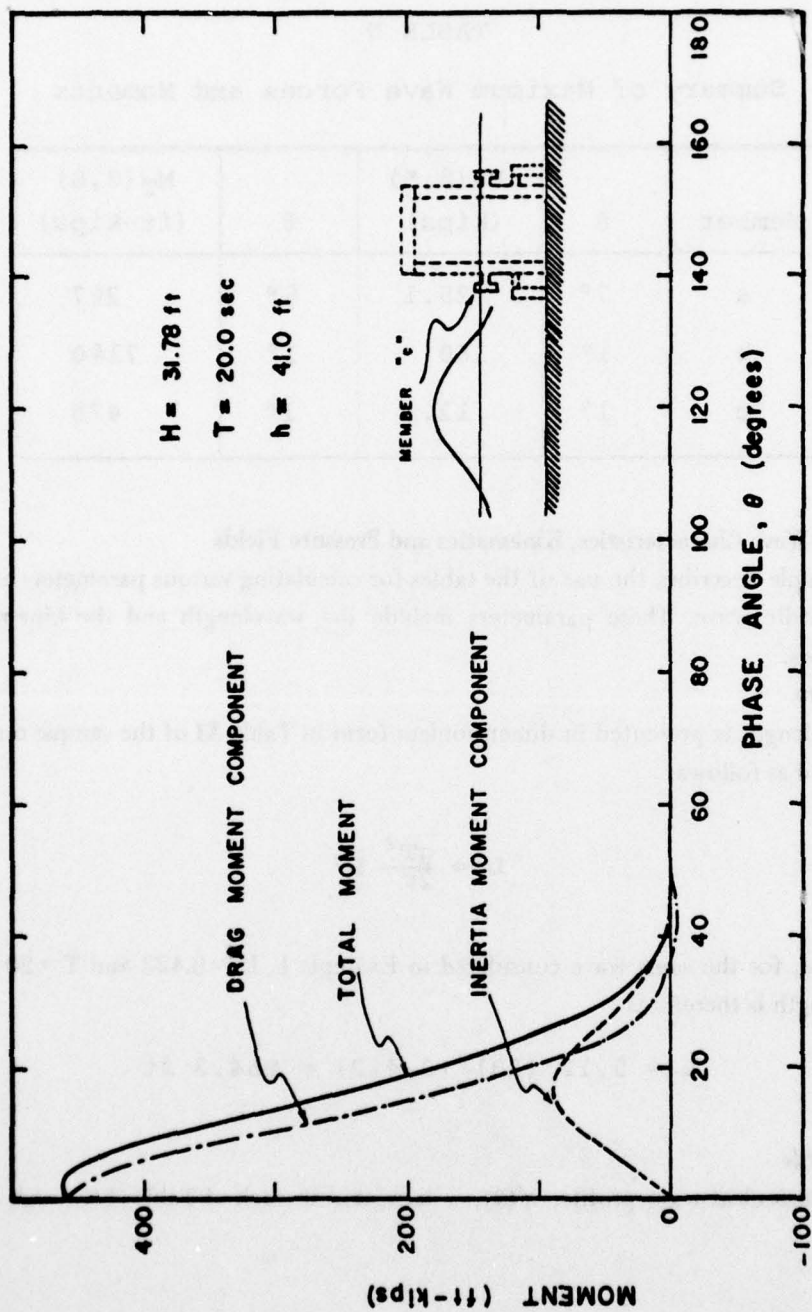


Figure 36. Wave moments on member "c"

The maximum calculated forces and moments on the three platform members due to the design wave are summarized in Table N.

TABLE N
Summary of Maximum Wave Forces and Moments

Member	θ	$F_T(\theta, S)$ (kips)	θ	$M_T(\theta, S)$ (ft-kips)
a	7°	25.1	5°	267
b	1°	160	1°	7140
c	1°	12.3	1°	475

Example 2—Wave Characteristics, Kinematics and Pressure Fields

This example describes the use of the tables for calculating various parameters associated with a periodic wave. These parameters include the wavelength and the kinematic and pressure fields.

Wavelength

The wavelength is presented in dimensionless form in Table XI of the sample output and is determined as follows:

$$L = \frac{gT^2}{2\pi} L'$$

For example, for the same wave considered in Example 1, $L' = 0.422$ and $T = 20$ seconds. The wavelength is therefore:

$$L = 5.12 (20)^2 (0.422) = 864.3 \text{ ft}$$

Wave Profile

The dimensionless wave profile, $\eta'(\theta)$, is tabulated in each of Tables I through IX and is defined as:

$$\eta'(\theta) = \frac{\eta(\theta)}{H}$$

therefore

$$\eta(\theta) = \eta'(\theta) \cdot H$$

The wave profile calculation for Case 4-D is summarized in Table O and is plotted in Figure 37. Note that η is an even function of θ .

Water Particle Kinematics

The water particle kinematics will be calculated for Case 4-D as presented in the sample output. These kinematics will be calculated for mid-depth (i.e., 20.5 feet above the bottom). The dimensionless forms of these variables are presented in Tables I through IV of the sample output. The dimensionless water particle velocities are defined as:

$$u'(\theta, S) \equiv \frac{u(\theta, S)}{H/T}$$

and

$$w'(\theta, S) \equiv \frac{w(\theta, S)}{H/T}$$

and the dimensionless water particle total accelerations are defined as:

$$\left(\frac{Du}{Dt}\right)' \equiv \frac{\frac{Du}{Dt}}{H/T^2}$$

and

$$\left(\frac{Dw}{Dt}\right)' \equiv \frac{\frac{Dw}{Dt}}{H/T^2}$$

Note that these are functions of θ and S , however, for convenience, the dependence has not been indicated in the above expressions. The calculations of the water particle velocities and accelerations over the range $0^\circ < \theta < 180^\circ$, are also summarized in Table O and plotted in Figure 37.

It will be noted that in the tables of wave functions, the variables are only presented for phase angles ranging between 0° and 180° . All of the variables are either symmetrical or antisymmetrical about a phase angle of 0° . The variables that are symmetrical include: the water surface profile, the horizontal component of water particle velocity and the vertical

TABLE O
Calculated Wave Profile, Kinematics, and Dynamic Pressure (All Kinematics and
Dynamic Pressure Calculated at Mid-Depth)

Variable	Dimensionalizing Constant	$\theta(^{\circ})$									
		0	10	20	30	50	75	100	130	180	
η' $\eta(\text{ft})$	$H = 31.78 \text{ ft}$	0.89 28.28	0.58 18.43	0.28 8.90	0.10 3.18	- 0.06 - 1.90	- 0.10 - 3.18	- 0.11 - 3.50	- 0.11 - 3.50	- 0.11 - 3.50	
u' $u(\text{ft}/\text{sec})$	$H/T = 31.78/20$ $= 1.589 \text{ ft}/\text{sec}$	8.97 14.25	7.94 12.62	5.46 8.68	2.80 4.45	- 0.42 - 0.67	- 1.54 - 2.45	- 1.76 - 2.80	- 1.80 - 2.86	- 1.79 - 2.84	
w' $w(\text{ft}/\text{sec})$	Same as for u , $= 1.589 \text{ ft}/\text{sec}$	0.0 0.0	1.46 2.32	2.14 3.40	1.95 3.10	0.81 1.29	0.17 0.27	0.03 0.05	0.01 0.02	0.0 0.0	
$\frac{Du'}{Dt}$ $\frac{Du}{Dt}(\text{ft}/\text{sec}^2)$	$H/T^2 = 31.78/(20)^2$ $= 0.07945$ ft/sec^2	0.0 0.0	51.89 4.12	80.18 6.37	76.41 6.07	32.40 2.57	6.73 0.53	1.16 0.09	0.28 0.02	0.0 0.0	
$\frac{Dw'}{Dt}$ $\frac{Dw}{Dt}(\text{ft}/\text{sec}^2)$	Same as for $\frac{Du}{Dt}$, $= 0.07945$ ft/sec^2	-39.21 -3.11	-25.66 - 2.03	2.27 0.18	21.80 1.73	18.01 1.43	4.04 0.32	1.04 0.08	0.04 0.00	- 0.28 - 0.02	
P'_D $P_D(\text{lb}/\text{ft}^2)$	$\frac{\gamma H}{2} = \frac{(64)(31.78)}{2}$ $= 1017 \text{ lb}/\text{ft}^2$	1.030 1048	0.930 946	0.673 684	0.372 378	- 0.035 - 36	- 0.189 -192	- 0.221 -225	- 0.226 -230	- 0.225 -229	

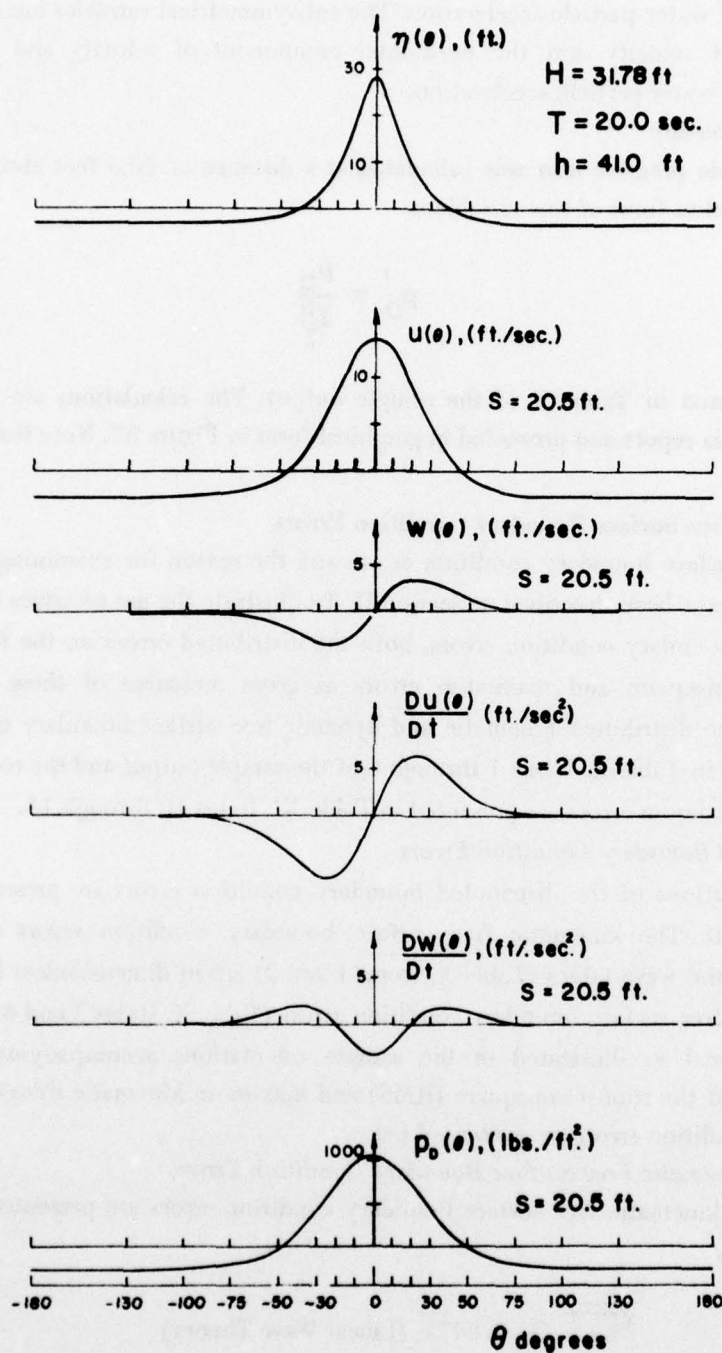


Figure 37. Example calculations of wave profile, kinematics and dynamic pressure

component of water particle acceleration. The antisymmetrical variables include the vertical component of velocity and the horizontal component of velocity and the horizontal component of water particle acceleration.

Dynamic Pressure

The dynamic pressure also was calculated at a distance of 20.5 feet above the bottom. The dimensionless form of this variable is:

$$p_D' = \frac{p_D}{\gamma H} \frac{1}{2}$$

and is presented in Table IX of the sample output. The calculations are summarized in Table O of this report and presented in graphical form in Figure 37. Note that p_D is an even function of θ .

Example 3—Free Surface Boundary Condition Errors

The free surface boundary condition errors and the reason for examining and tabulating these errors have been described in Section II. To illustrate the use of tables to calculate the free surface boundary condition errors, both the distributed errors on the free surface and the root-mean-square and maximum errors as gross measures of these errors will be presented. The distributed kinematic and dynamic free surface boundary condition errors are presented in Table X, Items 1 through 4 of the sample output and the root-mean-square errors and maximum errors are presented in Table XI, Items 10 through 13.

Distributed Boundary Condition Errors

The calculations of the distributed boundary condition errors are presented in Table P and Figure 38. The kinematic free surface boundary condition errors as defined and presented in the wave tables (Table X, Items 1 and 2) are in dimensionless form. However, the dynamic free surface boundary condition errors (Table X, Items 3 and 4 of wave tables) are dimensional as illustrated in the sample calculations accompanying Table P. The calculations of the root-mean-square (RMS) and maximum kinematic dynamic free surface boundary condition errors are presented below.

Overall Kinematic Free Surface Boundary Condition Errors

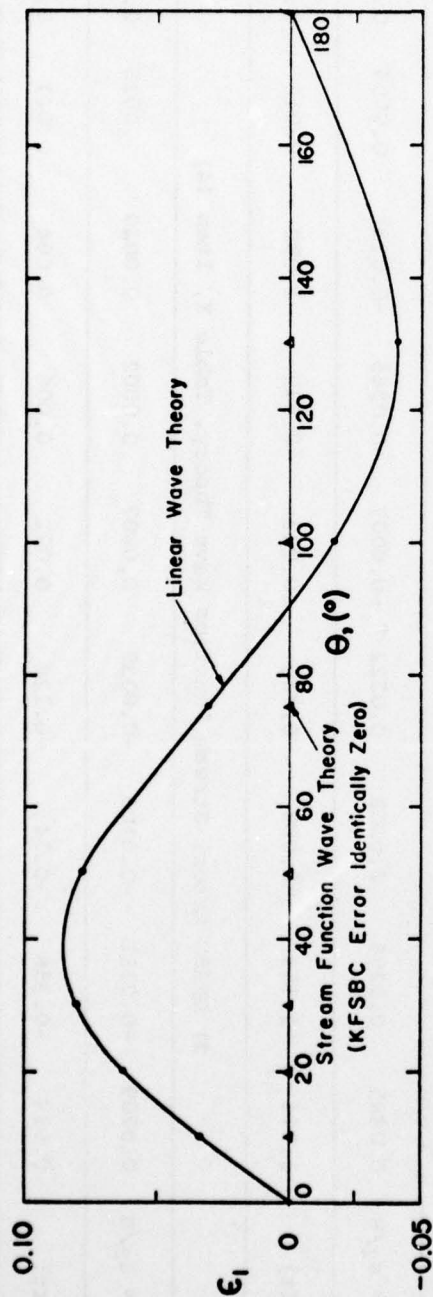
The RMS kinematic free surface boundary condition errors are presented as Item 10 in Table XI, i.e.,

$$\sqrt{\epsilon_1^2} = 0.0475 \text{ (Linear Wave Theory)}$$

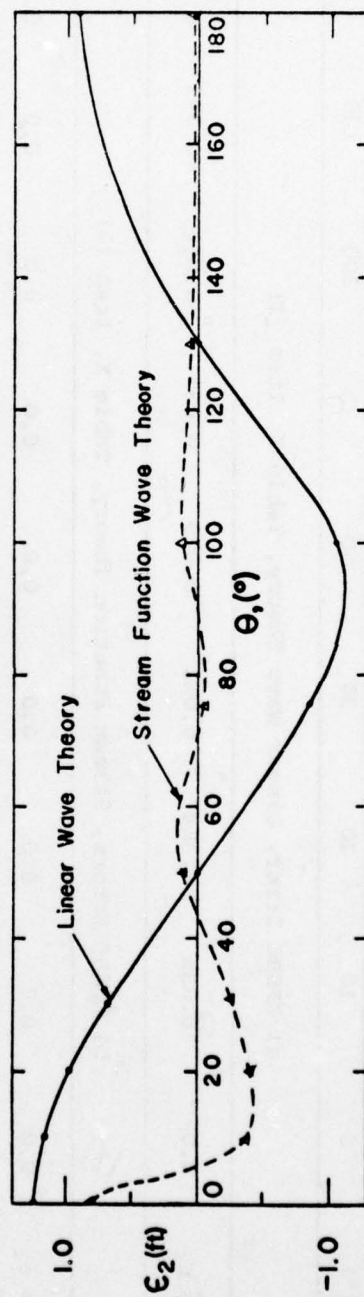
$$\sqrt{\epsilon_1^2} = 0.0 \text{ (Stream-function Wave Theory)}$$

TABLE P
Free Surface Boundary Condition Errors

$\theta(^{\circ})$	0	10	20	30	50	75	100	130	180
a) KFSBC Error, Linear Wave Theory, Table X, Item (1)									
$\epsilon'_1 = \epsilon_1$	0.0	0.035	0.064	0.081	0.079	0.032	-0.018	-0.042	0.0
b) KFSBC Errors, Stream Function Theory, Table X, Item (2)									
$\epsilon'_1 = \epsilon_1$	0.0	0.0	0.0	0.0	0.0	0.0	0.0	0.0	0.0
c) DFSBC Errors, Linear Wave Theory, Table X, Item (3)									
$\epsilon'_2 = \epsilon_2/H$	0.0385	0.0366	0.0309	0.0222	-0.0007	-0.0265	-0.0331	0.0004	0.0284
$\epsilon_2(\text{ft})$	1.224	1.163	0.982	0.706	-0.022	-0.842	-1.052	0.013	0.903
d) DFSBC Error, Stream Function Wave Theory, Table X, Item (4)									
$\epsilon'_2 = \epsilon_2/H$	0.0289	-0.0112	-0.0108	-0.0039	0.0007	0.0002	0.0020	.0013	0.0003
$\epsilon_2(\text{ft})$	0.918	-0.356	-0.343	-0.124	0.022	0.006	0.064	0.041	0.010



a) Distribution of Kinematic Free Surface Boundary Condition Error



b) Distribution of Dynamic Free Surface Boundary Condition Error

Figure 38. Free surface boundary condition errors

The maximum KFSBC error is obtained from Item 12 of Table XI,

$$|\epsilon_1|_{\max} = 0.0856 \quad (\text{Linear Wave Theory})$$

$$|\epsilon_1|_{\max} = 0.0 \quad (\text{Stream-function Wave Theory})$$

Overall Dynamic Free Surface Boundary Condition Errors

The RMS DFSBC errors are presented in dimensionless form as Item 11 in Table XI, i.e.,

$$\left. \begin{aligned} \sqrt{\epsilon_2^2}/H &= 0.0241 \\ \sqrt{\epsilon_2^2} &= 0.765 \text{ ft} \end{aligned} \right\} \quad (\text{Linear Wave Theory})$$

$$\left. \begin{aligned} \sqrt{\epsilon_2^2}/H &= 0.0048 \\ \sqrt{\epsilon_2^2} &= 0.153 \text{ ft} \end{aligned} \right\} \quad (\text{Stream-function Wave Theory})$$

The maximum DFSBC errors, obtained from Table XI, Item 13 are:

$$\left. \begin{aligned} \frac{|\epsilon_2|_{\max}}{H} &= 0.0385 \\ |\epsilon_2|_{\max} &= 1.224 \text{ ft} \end{aligned} \right\} \quad (\text{Linear Wave Theory})$$

$$\left. \begin{aligned} \frac{|\epsilon_2|_{\max}}{H} &= 0.0289 \\ |\epsilon_2|_{\max} &= 0.918 \text{ ft} \end{aligned} \right\} \quad (\text{Stream-function Wave Theory})$$

In the interpretation of the boundary condition errors in accordance with the discussion in Section II, if the boundary condition errors for any given theory were found to be generally better than for the Stream-function theory, then it could be concluded that at least the analytical validity of that wave theory would be better, and (as discussed earlier) there is evidence that the analytical wave theory is a good indicator of the experimental validity (or of the wave phenomenon in nature).

AD-A048 881

FLORIDA UNIV GAINESVILLE COASTAL AND OCEANOGRAPHIC --ETC F/G 8/3
EVALUATION AND DEVELOPMENT OF WATER WAVE THEORIES FOR ENGINEERI--ETC(U)
NOV 74 R 6 DEAN

DACW72-67-C-0009

UNCLASSIFIED

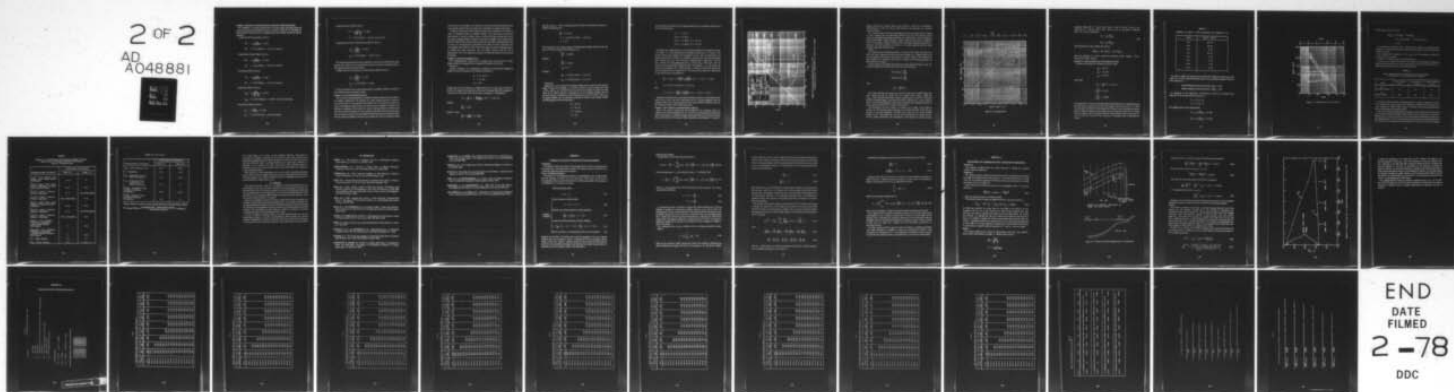
TR-14

CERC-SR-1-VOL-1

NL

2 OF 2

AD
A048881



END
DATE
FILMED
2-78
DDC

Example 4—Calculation of Energy, Momentum, and Energy and Momentum Fluxes

The tabulations of average potential, kinetic, and total energy and energy fluxes and average momentum and momentum fluxes are presented in Table XI. The calculation of these quantities in dimensional form is straightforward and will simply be presented without discussion.

Average Potential Energy (Table XI, Item 2)

$$PE' = \frac{PE}{(\gamma H^2/8)} = 0.213$$

$$PE = 0.213(8080) = 1721 \text{ ft-lb/ft}^2$$

Average Kinetic Energy (Table XI, Item 3)

$$KE' = \frac{KE}{(\gamma H^2/8)} = 0.254$$

$$KE = 0.254(8080) = 2052 \text{ ft-lb/ft}^2$$

Total Energy (Table XI, Item 4)

$$TE' = \frac{TE}{(\gamma H^2/8)} = 0.467$$

$$TE = 0.467(8080) = 3773 \text{ ft-lb/ft}^2$$

Energy Flux (Table XI, Item 5)

$$F'_{TE} = \frac{F_{TE}}{\left(\frac{\gamma H^2}{8} \frac{L}{T}\right)} = 0.447$$

$$F_{TE} = 0.447(349166) = 156077 \text{ ft-lbs/(ft-sec)}$$

Group Velocity (Table XI, Item 6)

$$C_G' = \frac{C_G}{(L/T)} = 0.957$$

$$C_G = 0.957(43.21) = 41.36 \text{ ft/sec}$$

Average Momentum (Table XI, Item 7)

$$M' = \frac{M}{\left(\frac{\gamma H^2}{8} \frac{T}{L}\right)} = 0.505$$

$$M = 0.505(187) = 94.42 \text{ lb-sec/ft}^2$$

Average Momentum Flux in Wave Direction (Table XI, Item 8)

$$F'_{m_x} = \frac{F_{m_x}}{\left(\frac{\gamma H^2}{8}\right)} = 0.603$$

$$F_{m_x} = 0.603(8080) = 4872 \text{ lb/ft}$$

The average momentum flux has been recognized in recent years as an important dynamic quantity and is related to wave setup within the surf zone and also is an important factor in the longshore transport of littoral material.

Average Momentum Flux Transverse to Wave Direction (Table XI, Item 9)

$$F'_{m_y} = \frac{F_{m_y}}{\left(\frac{\gamma H^2}{8}\right)} = 0.156$$

$$F_{m_y} = 0.156(8080) = 1260$$

From the momentum flux components presented, it is possible to obtain any component of the radiation stress tensor (Bowen, 1969).

Example 5—Free Surface Breaking Parameters

The free surface breaking parameters as defined by Equations (48) and (49) are based on two stability considerations. The kinematic free surface breaking parameter is defined in terms of the speed of a water particle on the surface at the crest relative to the wave form speed. If this parameter should equal unity, then the wave is regarded as unstable due to kinematic considerations. The dynamic free surface breaking parameter is defined as the ratio of the vertical acceleration of a water particle on the surface at the wave crest relative to the acceleration of gravity. The interpretation is that if this parameter should equal unity, then the pressure immediately under the crest would be zero and if the parameter should

exceed unity, then according to the equations of motion, the pressure beneath the wave crest would be negative which is unrealistic and would indicate an unstable water surface.

It should be noted that the theory employed in the study is composed of a finite series of terms. To adequately define an instability formally, it may be necessary to extend the representation to include an infinite number of terms. The results presented here for the free surface breaking parameters should be interpreted accordingly. For the sample output (Case 4-D, Table XI, Item 14) shows that the kinematic free surface breaking parameters for the linear and Stream-function representations are 0.429 and 0.733, respectively. The corresponding values (Table XI, Item 15) for the dynamic free surface breaking parameter are 0.0409 and 0.286, respectively. The wave height associated with this case is approximately 0.78 of the depth and according to the McCowan criterion, the wave would be breaking.

Example 6—Combined Shoaling-Refraction

The shoaling-refraction results were not tabulated, but are presented for various deepwater directions in graphical form as Figures 25 through 29 of this report.

Example 6-a

Consider a deepwater wave propagating over bathymetry characterized by straight and parallel contours; the deepwater wave conditions considered are:

$$H_0 = 11.52 \text{ ft}$$

$$T = 15 \text{ sec}$$

$$\alpha_0 = 40^\circ$$

Suppose that we wish to find the wave height and direction in a water depth of 30 feet and also the wave height, water depth and wave direction at breaking. Figure 28 is applicable for a deepwater wave direction of 40° . The deepwater wavelength L_0 is calculated as:

$$L_0 = \frac{g}{2\pi} T^2 = \frac{32.17}{6.2832} (15)^2 = 1152 \text{ ft}$$

therefore

$$\frac{H_0}{L_0} = 0.01$$

and for $h = 30 \text{ ft}$

$$\frac{h}{L_0} = \frac{30}{1152} = 0.0260$$

The line for $H_o/L_o = 0.01$ is simply followed to the left to the intersection with $h/L_o = 0.0260$. At this intersection,

$$\frac{H}{L_o} = 0.0119$$

$$H = (0.0119)(1152) = 13.71 \text{ ft}$$

$$\alpha \approx 17^\circ$$

The second part of the example requires the breaking depth, height and angle. For this, the $H_o/L_o = 0.01$ curve intersects the breaking curve at:

$$\frac{h_B}{L_o} = 0.0190$$

therefore

$$\frac{H_B}{L_o} = 0.0147$$

$$\alpha_B = 17^\circ$$

therefore

$$H_B = 0.0147(1152) = 16.9 \text{ ft}$$

$$h_B = 0.0190(1152) = 21.9 \text{ ft}$$

Example 6-b

Suppose that a wave is observed in transitional depths and it is desired to determine the height at deep water, breaking, or any depth of interest. For this example, the values of H/L_o and h/L_o are calculated from the observed wave height and period and water depth. If the observed direction corresponds to one of the graphs available, then one proceeds as before in Example 6-a. If the observed point is not in accordance with any of the graphs available, then an interpolative procedure is required. As an example, consider the following observed wave characteristics

$$H = 20 \text{ ft}$$

$$h = 60 \text{ ft}$$

$$T = 12 \text{ sec}$$

$$\alpha = 11^\circ$$

and it is desired to calculate the wave height and direction in a water depth of 40 feet. From the observed information

$$L_0 = 737.3$$

$$H/L_0 = 0.0271$$

$$h/L_0 = 0.0814 \quad (h = 60 \text{ ft})$$

$$h/L_0 = 0.0542 \quad (h = 40 \text{ ft})$$

Examining the available figures, it is seen that the deepwater wave direction is between 10° and 20° . As a close approximation, the problem is solved for $\alpha_0 = 10^\circ$ and $\alpha_0 = 20^\circ$, and the desired results obtained by interpolation. For $\alpha_0 = 10^\circ$, from Figure 26, a line passing through $H/L_0 = 0.0271$, $h/L_0 = 0.0814$ is sketched with the same approximate shape as those for $H_0/L_0 = 0.02$ and 0.04 to determine $H/L_0 = 0.033$ and $\alpha = 6.2^\circ$ for $h/L_0 = 0.0542$. The corresponding values for $\alpha_0 = 20^\circ$ are $H/L_0 = 0.031$ and $\alpha = 12^\circ$. The procedure is shown graphically in Figure 39 for $\alpha_0 = 10^\circ$. Because for $\alpha_0 = 10^\circ$ and 20° , the α values corresponding to $h/L_0 = 0.0814$ and $H/L_0 = 0.0271$ are 6.8° and 13° respectively, and the desired α for these conditions is 11° , the values of H/L_0 and α for $h = 40$ feet may be determined by linear interpolation as:

$$\frac{H}{L_0} = 0.033 + \frac{(.031 - .033)}{(13^\circ - 6.8^\circ)} (11^\circ - 6.8^\circ) = 0.032$$

or

$$H = (737.3)(0.032) = 23.6 \text{ ft}$$

and

$$\alpha = 6.2^\circ + \frac{(12^\circ - 6.2^\circ)}{(13^\circ - 6.8^\circ)} (11^\circ - 6.8^\circ) = 10.1^\circ$$

Dissipative mechanisms such as percolation and bottom friction are not included in these results, and in many cases these mechanisms will be of greater significance than the nonlinear effects on the celerity and group velocity which represent the difference between the results presented here and the linear wave theory.

Example 7—Use of Tables for Nontabulated Wave Conditions

Most of the previous examples have been presented for wave conditions which were available as one of the 40 tabulated cases, i.e., Case 4-D. It is anticipated that the tabulations will be used primarily for preliminary design, and therefore that the 40 cases may provide adequate information for this purpose without interpolation. Final design of, for example, a

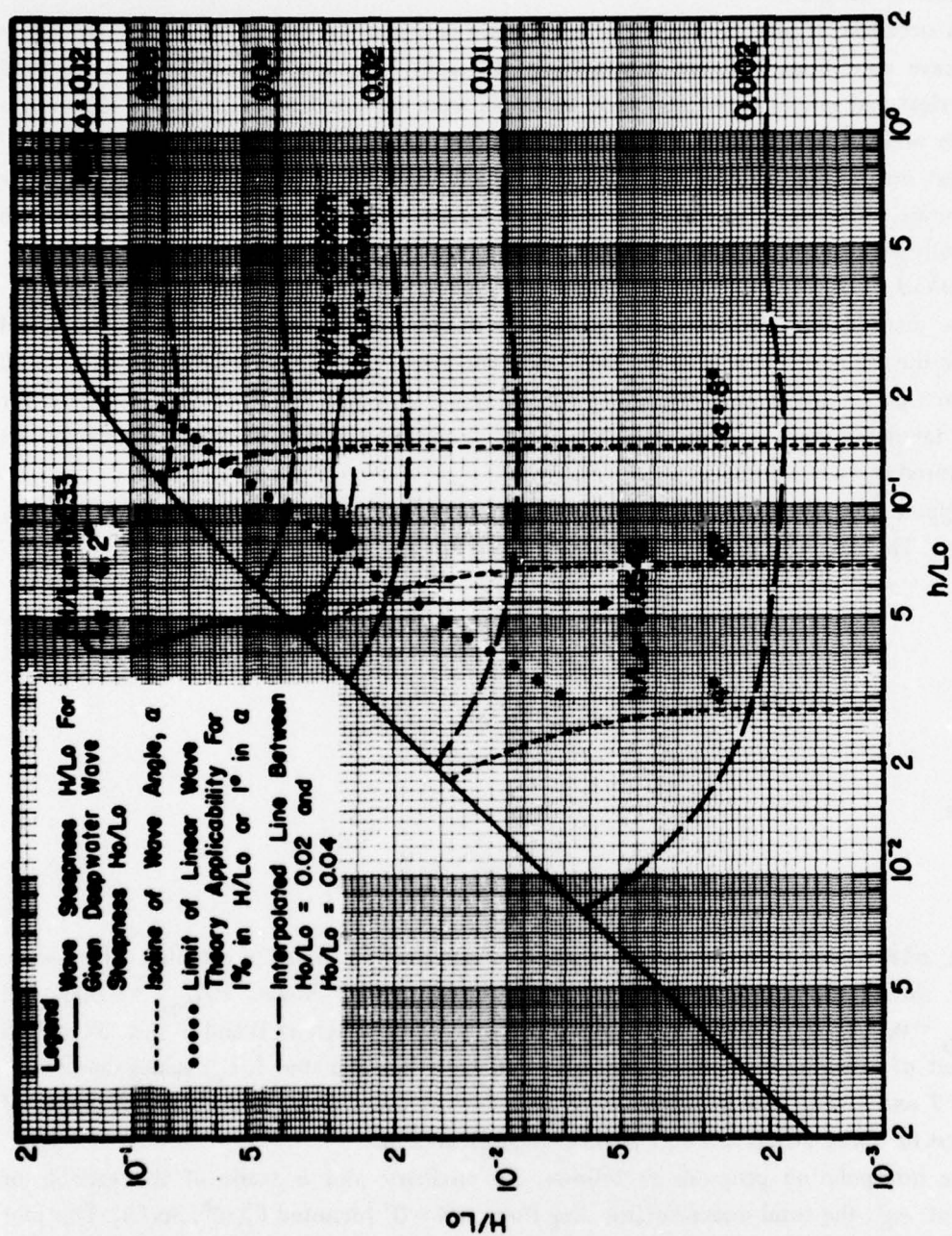


Figure 39. Example 6-b, shoaling-refraction for $\alpha_0 = 10^\circ$.
Interpolation from $h/L_0 = 0.0814$ and $H/L_0 = 0.0271$ to $h/L_0 = 0.0542$

platform supported by battered piling would probably be carried out by establishing a Stream-function or other wave theory representation for the particular wave conditions selected for design.

On occasion, it may be desired to interpolate between the cases presented in the tables for wave conditions that are substantially different from any of the 40 cases. Several numerical and graphical interpolation methods were explored with a goal of obtaining a simple method which yielded reasonably accurate results. Because most wave variables of interest are nonlinear, numerical schemes which used linear interpolation proved to be inaccurate. The best procedure was found to be a simple graphical procedure which generally yields results within 5 percent.

Method

The method uses the tabulated parameters of interest for the H/H_B values above and below the value of interest at the two lower and two higher h/L_o tabulated values; in all for each parameter desired, the interpolated value is based on values of that parameter for eight tabulated wave conditions. The method is outlined in the following paragraphs and illustrated by two examples.

Suppose that the wave height, period, and water depth selected for design are H_D , T_D , and h_D . The design wave steepness and relative depth are calculated as:

$$\text{Wave Steepness: } \frac{H_D}{L_{oD}}$$

$$\text{Relative Depth: } \frac{h_D}{L_{oD}}$$

where

$$L_{oD} = \frac{g}{2\pi} T_D^2$$

The relative depth and wave steepness are plotted on Figure 40 to establish which wave cases should be used for design. For the example shown, $H/L_{oD} = 0.086$ and $h/L_{oD} = 0.313$. This point falls between H/H_B values denoted as B and C (i.e., 50 and 75 percent of breaking heights, respectively) and between tabulated h/L_o values denoted as Cases 7 and 8. The interpolation would therefore be based on the tabulated parameter of interest for Cases 6-B, 6-C, 7-B, 7-C, 8-B, 8-C, 9-B, and 9-C.

The interpolation proceeds as follows. An auxiliary plot is made of the variable of interest, e.g., the total dimensionless drag force at $\theta = 0^\circ$ [denoted $F'_D(0^\circ, \text{Surf.})$]. This plot provides a continuous distribution of $F'_D(0^\circ, \text{Surf.})$ versus h/L_o for relative breaking heights B and C. Interpolated F'_D values are then obtained from the auxiliary plot for the h/L_o design value (0.313). The interpolation for the design wave steepness requires

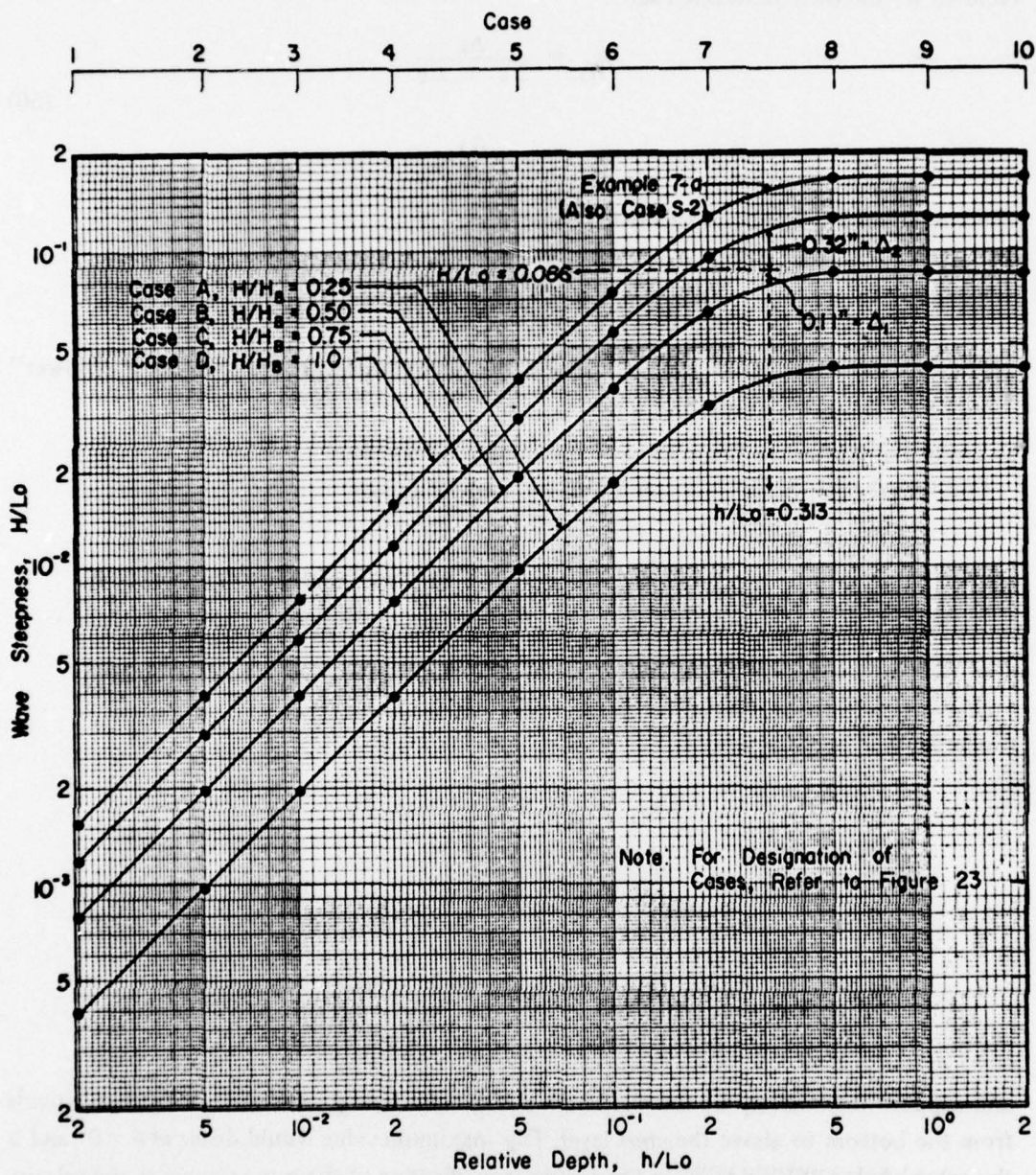


Figure 40. Interpolation aid

measuring (Figure 40) the vertical linear distance from the B and C lines to the design H/L_o of interest; denote these values, Δ_1 and Δ_2 , respectively. Weighting factors, W , are then established as:

$$W_L = \frac{\Delta_2}{\Delta_1 + \Delta_2}$$

$$W_U = \frac{\Delta_1}{\Delta_1 + \Delta_2}$$
(50)

The interpolated F'_D value is finally determined as:

$$(F'_D)_D = W_L (F'_D)_L + W_U (F'_D)_U$$

where the subscripts, D, L and U outside the parentheses denote: "Design," "Lower" (Case B), and "Upper" (Case C).

Example 7-a—Numerical Illustration of Interpolation Procedure

Consider the following wave conditions selected for design

$$H_D = 44 \text{ ft}$$

$$T_D = 10 \text{ sec}$$

$$h_D = 160 \text{ ft}$$

which yield

$$L_{oD} = \frac{g}{2\pi} T^2 = 512 \text{ ft}$$

$$\frac{h_D}{L_{oD}} = 0.313$$

$$\frac{H_D}{L_{oD}} = 0.0859$$

and suppose that we require the maximum dimensionless drag force on a piling that extends from the bottom to above the crest level. This maximum value would occur at $\theta = 0^\circ$ and is the value labeled "SURFACE" in the tabulations. Plotting of the wave steepness and relative depth on Figure 40 indicates that the design values are spanned by Cases 7-B, 7-C, 8-B and 8-C. In accordance with the preceding section the values of $F'_D(0^\circ, \text{Surf.})$ for Cases 6-B, 6-C, 7-B, 7-C, 8-B, 8-C, 9-B, and 9-C are required for interpolation and are summarized in Table Q.

TABLE Q

Summary of $F'_D(0^\circ, \text{Surf.})$ Required for Example 7-a

Case	$F'_D(0^\circ, \text{Surf.})$
6-B	22.37
6-C	28.79
7-B	8.60
7-C	11.31
8-B	2.71
8-C	3.53
9-B	1.33
9-C	1.72

The values in Table Q are presented as an auxiliary plot in Figure 41. Interpolation at the design h/L_o of 0.313 yields the following values of F'_D for relative breaking of 50 and 75 percent respectively.

Relative Breaking of 50 percent (Line B): $(F'_D)_L = 4.90$

Relative Breaking of 75 percent (Line C): $(F'_D)_U = 6.10$

To interpolate to the design H/L_o , the distances Δ_1 and Δ_2 are measured from Figure 40. For this example, these are found to be:

$$\Delta_1 = 0.11 \text{ in}$$

$$\Delta_2 = 0.32 \text{ in}$$

The weighting values are then (Equation 50)

$$w_L = \frac{\Delta_2}{\Delta_1 + \Delta_2} = 0.744$$

$$w_U = \frac{\Delta_1}{\Delta_1 + \Delta_2} = 0.256$$

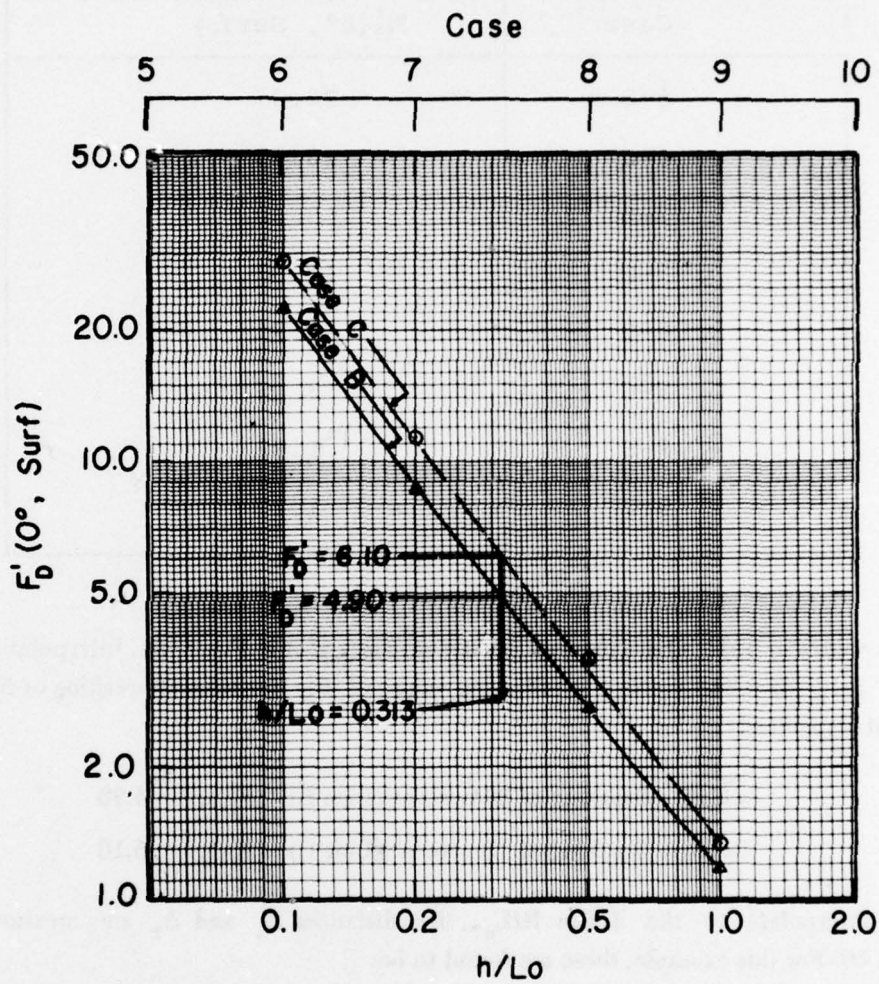


Figure 41. Auxiliary plot of F'_D for example 7a

and the interpolated value of F'_D is:

$$\begin{aligned}(F'_D)_D &= w_L (F'_D)_L + w_U (F'_D)_U \\ &= (0.744)(4.90) + (0.256)(6.10) \\ &= 5.21\end{aligned}$$

To evaluate this interpolated value, a Stream-function solution was developed for the conditions of interest, and F'_D from the actual solution was found to be 5.04 or a difference of about 3.4 percent.

More comprehensive evaluations of the accuracy of the interpolation method are presented in the next example.

Example 7-b—Assessment of the Interpolation Method

To present a more extensive evaluation of the accuracy of the interpolation method, two special cases (one shallow-water and one deepwater) were selected for evaluation. The wave characteristics for these two cases are presented in Table R.

TABLE R
Wave Characteristics Selected for Accuracy
Evaluation of Interpolation Method

Case	Wave Height, H (ft)	Wave Period, T (sec)	Water Depth, h (ft)
S-1 (Shallow Water)	19	20	30
S-2 (Deep Water)	44	10	160

Using the procedure described, interpolated values of a number of quantities of interest were developed and compared with values obtained by Stream-function solutions at the wave conditions of interest. Table S presents a summary of the percentage differences between the solution and interpolated values.

As an overall statement regarding the interpolation, it is noted that Table S indicates that the procedure presented generally provides results which are within 5 percent; however, differences up to 10 percent could occur. One final comment concerning the consistency of the tabulated values is in order. In preparing the auxiliary plots, it was usually found that a line could be drawn through the four points within 2 to 3 percent, except for the breaking

TABLE S

Summary of Percentage Differences Between Values
Determined by Stream Function Solutions
and by Interpolation

Dimensionless Variable ^a	Percentage Difference ^b	
	Case S-1	Case S-2
$u'(0^\circ, 0.5)$; Horiz. Vel. Comp., Zero Phase Angle, Mid-Depth	+3.9	<1
$F_D'(0^\circ, \text{Surf})$, Max. Drag Force Component, Acting Over Entire Depth	+6.7	+3.4
$F_I'(10^\circ, \text{Surf})$, Inertia Force Component	+1.3	Not Evaluated
$F_I'(75^\circ, \text{Surf})$, Inertia Force Component	Not Evaluated	-3.9
$M_D'(0^\circ, \text{Surf})$, Max. Drag Moment Component About Mudline	+4.5	+3.6
$M_I'(10^\circ, \text{Surf})$, Inertia Moment Component	+2.2	Not Evaluated
$M_I'(75^\circ, \text{Surf})$, Inertia Moment Component	Not Evaluated	-3.7
$p_D'(0^\circ, 0.5)$, Dynamic Pressure Component, Zero Phase Angle, Mid-Depth	<1	-2.4
$p_D'(180^\circ, 0.5)$, Dynamic Pressure Component, Trough Phase Position, Mid-Depth	<1	-2.8
L' , Wave Length	1.1	<1
TE' , Total Energy	-4.6	-3.7

TABLE S—Continued

Dimensionless Variable ^a	Percentage Difference ^b	
	Case S-1	Case S-2
F'_{TE} , Total Energy Flux	-4.2	+3.5
M' , Momentum	-4.1	-2.2
F'_{m_x} , Momentum Flux in Wave Direction	-3.7	-2.6
F'_{m_y} , Momentum Flux Transverse to Wave Direction	-1.7	<1
KFSBP, Kinematic Free Surface Breaking Parameter	8.4	+4.4
DFSBP, Dynamic Free Surface Breaking Parameter	1.4	<1

^aRefer to Tables D, E, and F for a more complete description of the dimensionless variables.

^bPercentage Difference $\equiv \frac{\text{Interpolated Value} - \text{Stream-function Solution}}{\text{Stream-function Solution}} \times 100 \text{ Percent}$

wave height, $H/H_B = 1.0$ in which case the maximum deviations could amount to ± 5 percent. The probable explanation for this deviation is that: (1) the calculated wave heights for the tabulated cases were allowed to deviate from the desired values by 1 percent, and (2) the different orders to represent different cases could cause a difference in kinematics of 1 to 2 percent. The effects noted above could conceivably amount to deviations of ± 5 percent for those variables which are inherently nonlinear, e.g., drag forces or wave breaking parameters.

This completes the section illustrating the use of the wave tables. It should be recognized, however, that only the more simple examples have been presented and that the tables can be effectively applied to the solution of situations which are considerably broader and more complex than those examined in this section.

VI. SUMMARY

This report presents the results of an investigation which has demonstrated that the Stream-function wave theory provides a generally better representation of periodic wave phenomena than other wave theories examined. As a result of this indication, tables have been prepared, based on the Stream-function wave theory, that include parameters which should be an aid in preliminary offshore design. The tables also include parameters which are presently of greatest interest to researchers.

Because of its simplicity, the linear wave theory is widely used for many calculations over all ranges of relative depth. This study has identified that, for a number of variables, there are substantial differences between the linear and Stream-function wave theories. Although this point has not been amplified in this report, inspection of the tables will substantiate this conclusion. The identification of these differences should be of assistance in planning experimental programs to provide definitive research results.

If the set of tables is extensively applied, as is hoped, undoubtedly the users will note shortcomings, omissions or develop recommendations directed toward the improved usefulness, applicability, or efficiency of the tables. The author would welcome information of this type so that future work may benefit by as wide a range of user's needs as possible.

VII. REFERENCES

- BOWEN, A. J., "The Generation of Longshore Currents on a Plane Beach," *Journal of Marine Research*, Vol. 27, No. 2, p. 209, May, 1969.
- BRETSCHNEIDER, C. L., "Selection of Design Waves for Offshore Structures," *Transactions, American Society of Civil Engineers*, Paper No. 3026, 1960.
- CHAPPELEAR, J. E., "Direct Numerical Calculation of Wave Properties," *Journal of Geophysical Research*, Vol. 66, No. 2, pp. 501-508, February, 1961.
- DEAN, R. G., "Stream Function Representation of Nonlinear Ocean Waves," *Journal of Geophysical Research*, Vol. 70, No. 18, pp. 4561-4572, September, 1965.
- DEAN, R. G., 1968a, "Relative Validity of Water Wave Theories," *Proceedings, ASCE Specialty Conference on Civil Engineering in The Oceans*, San Francisco, pp. 1-30, 1968. (Also published in *Waterways and Harbors Journal, American Society of Civil Engineers*, pp. 105-119, February, 1970).
- DEAN, R. G., 1968b, "Breaking Wave Criteria: A Study Employing a Numerical Wave Theory," *Proceedings 11th International Conference on Coastal Engineering*, London, Ch. 8, pp. 108-123, 1968.
- DEAN, R. G., and LE MEHAUTE, B., "Experimental Validity of Water Wave Theories," Paper presented at the 1970 ASCE Structural Engineering Conference, Portland, Oregon, April 8, 1970.
- DIVOKY, D., LE MEHAUTE, B., and LIN, A., "Breaking Waves on Gentle Slopes," *Journal of Geophysical Research*, Vol. 75, No. 9, pp. 1681-1692, March, 1970.
- IPPEN, A.T., (Editor), *Estuary and Coastline Hydrodynamics*, McGraw-Hill, Chs. 1 and 2, pp. 1-132, 1966.
- KEULEGAN, G. H., and PATTERSON, G. W., "Mathematical Theory of Irrotational Translation Waves," RP 1272, National Bureau of Standards, Washington, D.C., 1940.
- LAITONE, E. V., "The Second Approximation to Cnoidal and Solitary Waves," *Journal of Fluid Mechanics*, Vol. 9, Part 3, pp. 430-444, November, 1960.
- LE MEHAUTE, B., DIVOKY, D., and LIN, A., "Shallow Water Waves: A Comparison of Theory and Experiment," *Proceedings 11th International Conference on Coastal Engineering*, Ch. 7, pp. 86-107, 1968.

LE MEHAUTE, B., and WEBB, L. M., "Periodic Gravity Waves Over a Gentle Slope at a Third Order of Approximation," *Proceedings Ninth Conference on Coastal Engineering*, Ch. 2, pp. 23-40, 1964.

MICHELL, J. H., "On the Highest Waves in Water," *Philosophical Magazine*, Vol. 36, No. 5, pp. 430-435, 1893.

MUNK, W. H., "The Solitary Wave and Its Application to Surf Problems," *Annals New York Academy of Science*, Vol. 51, pp. 376-424, 1949.

REID, R. O., and BRETSCHNEIDER, C. L., "Surface Waves and Offshore Structures," *Texas A & M Research Foundation*, Technical Report, October, 1953.

SKJELBREIA, L., and HENDRICKSON, J. A., "Fifth Order Gravity Wave Theory," *Proceedings Seventh Conference on Coastal Engineering*, Ch. 10, pp. 184-196, 1961.

VON SCHWIND, J. J., and REID, R. O., "Characteristics of Gravity Waves of Permanent Form," *Journal of Geophysical Research*, Vol. 77, No. 3, pp. 420-433, January, 1972.

APPENDIX I

NUMERICAL SOLUTION OF STREAM FUNCTION PARAMETERS

Introduction

This appendix outlines the method of determining numerical values for the parameters in the general form of the Stream-function solution. The numerical solution requires the use of a reasonably high-speed, large memory computer.

Review of Problem Formulation

The problem of a two-dimensional, periodic wave propagating in water of uniform depth has been discussed in Section II of the main body of this report. If the water is incompressible and the motion irrotational, then the following boundary value problem can be established for an "arrested" wave system.

Differential Equation (DE):

$$\nabla^2 \psi = 0 \quad (I-1)$$

Bottom Boundary Condition (BBC):

$$w = 0, \quad z = -h \quad (I-2)$$

Kinematic Free Surface Boundary Condition (KFSBC):

$$\frac{\partial \eta}{\partial x} = \frac{w}{u - C}, \quad z = \eta(x) \quad (I-3)$$

Dynamic Free Surface Boundary Condition (DFSBC):

$$\eta + \frac{1}{2g} \left[(u - C)^2 + w^2 \right] - \frac{C^2}{2g} = Q, \quad z = \eta(x) \quad (I-4)$$

Motion is periodic in x with spatial periodicity of the wavelength, L . (I-5)

Equations (I-1 through I-5) represent the common formulation for all of the classical nonlinear water wave problems in which it is assumed that the wave propagates without change of form and a reference coordinate system has been chosen that travels with the wave form. For a specified wave height, water depth and wave period, the goal then is to determine as exactly as possible a solution to the formulation.

Stream-function Solution

The general form of the Stream-function solution is:

$$\psi(x, z) = \frac{L}{T} z + \sum_{n=1}^{NN} X(n) \sinh \left(\frac{2\pi n}{L} (h + z) \right) \cos \left(\frac{2\pi n}{L} x \right) \quad (I-6)$$

The water displacement, η , is determined by setting $z = \eta$ in Equation (I-6)

$$\eta = \frac{T}{L} \psi_{\eta} - \frac{T}{L} \sum_{n=1}^{NN} X(n) \sinh \left(\frac{2\pi n}{L} (h + \eta) \right) \cos \left(\frac{2\pi n}{L} x \right) \quad (I-7)$$

where ψ_{η} is the (constant) value of the Stream-function on the free surface. The velocity components are defined by:

$$u - C = - \frac{\partial \psi}{\partial z} \quad (I-8)$$

$$w = + \frac{\partial \psi}{\partial x} \quad (I-9)$$

In continuing the quest to determine a solution that satisfies Equations (I-1) to (I-5) as faithfully as possible, it is noted that for arbitrary values of: ψ_{η} , L , and the $X(n)$'s, the Stream-function solution *exactly* satisfies all of the requirements of the formulation except the DFSBC, Equation (I-4). All of the effort can therefore be directed to determining these "free" variables such that they represent the specified wave height and also "best" satisfy Equation (I-4). The approach employed is numerical iteration, in which a trial solution is regarded as available and at each step of the iteration; the "free" variables are modified to improve the solution.

As a preliminary step, an error is defined in the one remaining unsatisfied boundary condition,

$$E = \frac{1}{J} \sum_{j=1}^J (Q_j - \bar{Q})^2 \quad (I-10)$$

where the Q_j 's represent equally spaced (in θ) values of the quantity in Equation (I-4), and \bar{Q} represents the average of the Q_j 's. If, for example, $J = 41$, and the free variables

could be adjusted so that E was very small, then the associated solution would provide a good fit to the complete formulation at these 41 points, and computations have shown that the fit or other phase angles would be comparably good. The problem therefore has evolved into one of minimizing the total error E . The procedure used is a least-squares procedure, which requires formally that

$$\frac{\partial E}{\partial L} = 0 \quad (I-11)$$

$$\frac{\partial E}{\partial X(n)} = 0 \quad (I-12)$$

(The parameter ψ_η is not determined by the least-squares procedure, but is selected such that the mean water level is not changed by the other variables selected. This will be discussed later.) Examination of Equations (I-11) and (I-12) further will indicate that the usual least-squares procedure is not applicable, because the error is not defined as a quadratic function of the unknowns. This problem then falls in the category of a nonlinear least-squares problem.

The problem was linearized as follows. Suppose that at the k^{th} iteration, a trial solution is available. The objective is to select changes in the unknowns such that the errors will be reduced. If this were a linear least-squares problem, only one iteration would be required. Expressing the quantity Q in terms of small changes in the unknowns (to be determined at the k^{th} iteration).

$$Q_j^{k+1} = Q_j^k + \sum_{n=1}^{NN} \frac{\partial Q_j^k}{\partial X(n)} \Delta X(n) + \frac{\partial Q_j^k}{\partial L} \Delta L \quad (I-13)$$

where

$$\frac{\partial Q}{\partial X(n)} = \frac{\partial Q}{\partial \eta} \frac{\partial \eta}{\partial X(n)} + \frac{\partial Q}{\partial u} \frac{\partial u}{\partial X(n)} + \frac{\partial Q}{\partial w} \frac{\partial w}{\partial X(n)} \quad (I-14)$$

$$\frac{\partial Q}{\partial L} = \frac{\partial Q}{\partial \eta} \frac{\partial \eta}{\partial L} + \frac{\partial Q}{\partial u} \frac{\partial u}{\partial L} + \frac{\partial Q}{\partial w} \frac{\partial w}{\partial L} + \frac{\partial Q}{\partial C} \frac{\partial C}{\partial L} \quad (I-15)$$

where the $\partial Q/\partial \eta$, $\partial Q/\partial u$ are obtained from Equation (I-4) and the $\partial \eta/\partial X(n)$, $\partial u/\partial X(n)$, etc., are obtained from Equations, (I-7), (I-8), etc.

Rewriting the least-squares procedure in terms of the unknowns: ΔL and $\Delta X(n)$

$$\frac{\partial E}{\partial \Delta L} = 0 \quad (I-16)$$

$$\frac{\partial E}{\partial \Delta X(n)} = 0, \quad n = 1 \dots NN \quad (I-17)$$

Equations (I-16) and (I-17) represent a set of $NN + 1$ linear simultaneous equations in terms of the $NN + 1$ unknowns. After each iteration, the water surface is recalculated, by iteration, from Equation (I-7) and ψ_η is redetermined such that

$$\int_0^L \eta \, dx = 0 \quad (I-18)$$

which can be expressed in integral form as:

$$\psi_\eta = \frac{2}{L} \int_0^{L/2} x(n) \sinh \left(\frac{2\pi n}{L} (h + \eta) \right) \cos \left(\frac{2\pi n}{L} x \right) dx \quad (I-19)$$

where, in the computations, a Simpson's rule approximation to Equation (I-19) is used.

One complete iteration comprises a simultaneous solution for ΔL and the $\Delta K(n)$'s and a redetermination of ψ_η . Successive iterations involve exactly the same procedure, and the iterations can be terminated when successive reductions in the error E are small. Numerical instabilities can occur, especially near breaking wave conditions, and one effective procedure in these cases is to apply only a fraction of the ΔL and $\Delta X(n)$'s specified by the least-squares solution.

One final comment should be directed toward the problem of establishing the desired wave height. Although it is possible to develop more sophisticated procedures which converge on the wave height, the procedure followed here was simply to conduct successive runs until the wave height was within an acceptable limit (1 percent) of the desired height.

APPENDIX II

DEVELOPMENT OF COMBINED SHOALING-REFRACTION COEFFICIENTS

Introduction

This appendix describes briefly the method employed to calculate the combined shoaling-refraction coefficients.

Background

The shoaling-refraction coefficients developed are valid for a bathymetry characterized by straight and parallel bottom contours and for a wave system which suffers no energy losses. The two principles employed are Snell's Law and the concept that there is no energy flux across a wave ray, see Figure II-1.

Snell's Law governs refraction and relates the wave propagation speed, C , to the wave direction, α ,

$$\frac{\sin \alpha_1}{C_1} = \text{Const}_1 = \frac{\sin \alpha_2}{C_2} \quad (\text{II-1})$$

in which the subscripts pertain to any arbitrary depths.

The requirement that no energy is propagated across wave rays may be written as:

$$\left(F_{TE} \cos \alpha \right)_1 = \left(F_{TE} \cos \alpha \right)_2 = \text{Const}_2 \quad (\text{II-2})$$

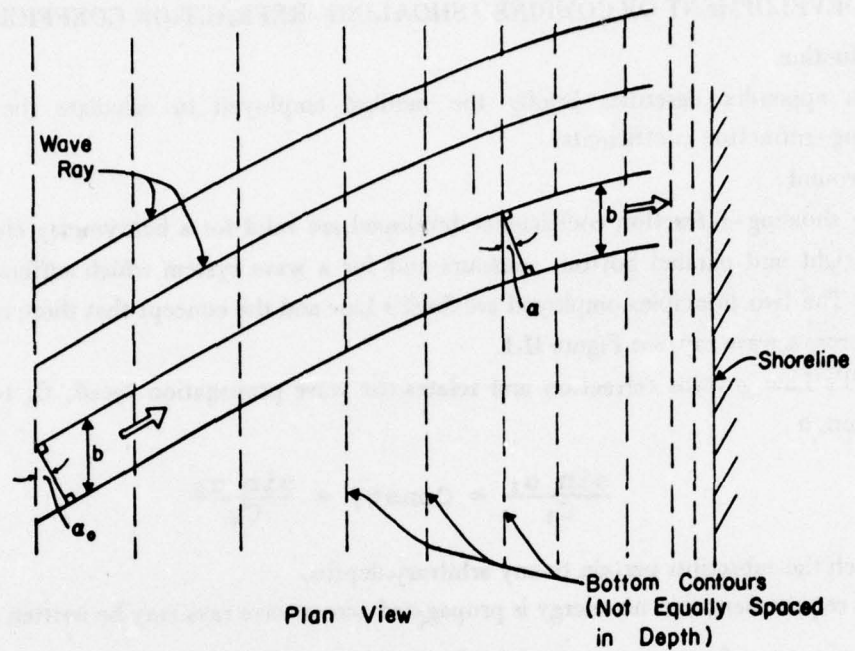
in which F_{TE} represents the energy flux per unit width in the direction of wave propagation and the $\cos \alpha$ term represents the width between adjacent wave rays. The F_{TE} term could be expressed as the product of the wave energy density, TE , and the group velocity, C_G , although this will not be helpful in the effort here. For linear wave theory, it is possible to separate the refraction and shoaling effects because neither the celerity, C , (governing refraction) nor the group velocity, C_G (governing shoaling) depend on wave height. For our case, inspection of Equations (II-1) and (II-2) will show that the two phenomena are coupled through the dependency of C and C_G on the wave height.

Method

The method employed here utilizes the dimensionless energy flux, F'_{TE} (Table XI, Item 5) and the dimensionless wavelength, L' (Table XI, Item 1), where

$$F'_{TE} = \frac{F_{TE}}{\gamma \frac{H^2}{8} \frac{L}{T}}$$

$$L' = \frac{L}{(gT^2/2\pi)}$$



Refraction Over Bathymetry Characterized By
Straight and Parallel Contours

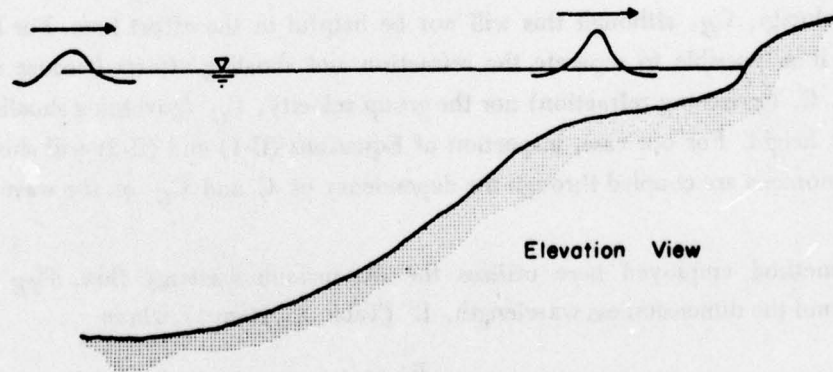


Figure II-1. Definition sketch for shoaling-refraction considerations

Equation (II-1) can be rewritten in terms of the dimensionless quantities as:

$$\frac{2\pi}{gT_1} \frac{\sin \alpha_1}{L'_1} = \frac{2\pi}{gT_2} \frac{\sin \alpha_2}{L'_2} = \text{Const}_1 \quad (\text{II-3})$$

However since the period is conserved, i.e., $T_1 = T_2$

$$\frac{\sin \alpha_1}{L'_1} = \frac{\sin \alpha_2}{L'_2} = \text{Const}_3 \quad (\text{II-4})$$

The energy flux relationship, Equation (II-2) can be expressed as:

$$\frac{\gamma}{8T} \left(\frac{gT^2}{2\pi} \right)^3 \left(\frac{H}{L_0} \right)^2 F'_{TE} L' \cos \alpha = \text{Const}_2$$

or recognizing that the period is conserved

$$\left(\frac{H}{L_0} \right)^2 F'_{TE} L' \cos \alpha = \text{Const}_4 \quad (\text{II-5})$$

Equations (II-4) and (II-5) describe the shoaling-refraction process in terms of available dimensionless parameters, and were solved as described in the following paragraphs.

Solution

It was found convenient to characterize a particular incoming deepwater wave by the direction, α_0 , and deepwater steepness, H_0/L_0 . The problem is to determine wave steepnesses at other relative depths h/L_0 such that Equations (II-4) and (II-5) are satisfied recalling that L' and F'_{TE} both depend on h/L_0 and H/L_0 . For each relative depth, h/L_0 , four values of L' and F'_{TE} are available (for $H/H_B = 0.25, 0.5, 0.75$, and 1.0 , c.f. Figure 23) whereas a continuous distribution is required for the purpose here. For each relative depth, h/L_0 , continuous distributions were obtained by fitting straight lines between the four available points; for $H/H_B = 0$, it was assumed that the simple linear wave theory applied, see Figure II-2 for an example for $h/L_0 = 0.02$.

For given H_0/L_0 and α_0 , the constants in Equations (II-4) and (II-5) are defined. The wave steepness H/L_0 and direction α at any relative depth are determined by iteration of the two following equations.

$$\alpha^{k+1} = \sin^{-1} \left[(L')^k \frac{\sin \alpha_0}{L'_0} \right] \quad (\text{II-6})$$

$$\frac{H}{L_0}^{k+1} = \left[\frac{(H_0/L_0)^2 (F'_{TE})_0 L'_0 \cos \alpha_0}{(F'_{TE})^k (L')^k \cos \alpha^k} \right]^{1/2} \quad (\text{II-7})$$

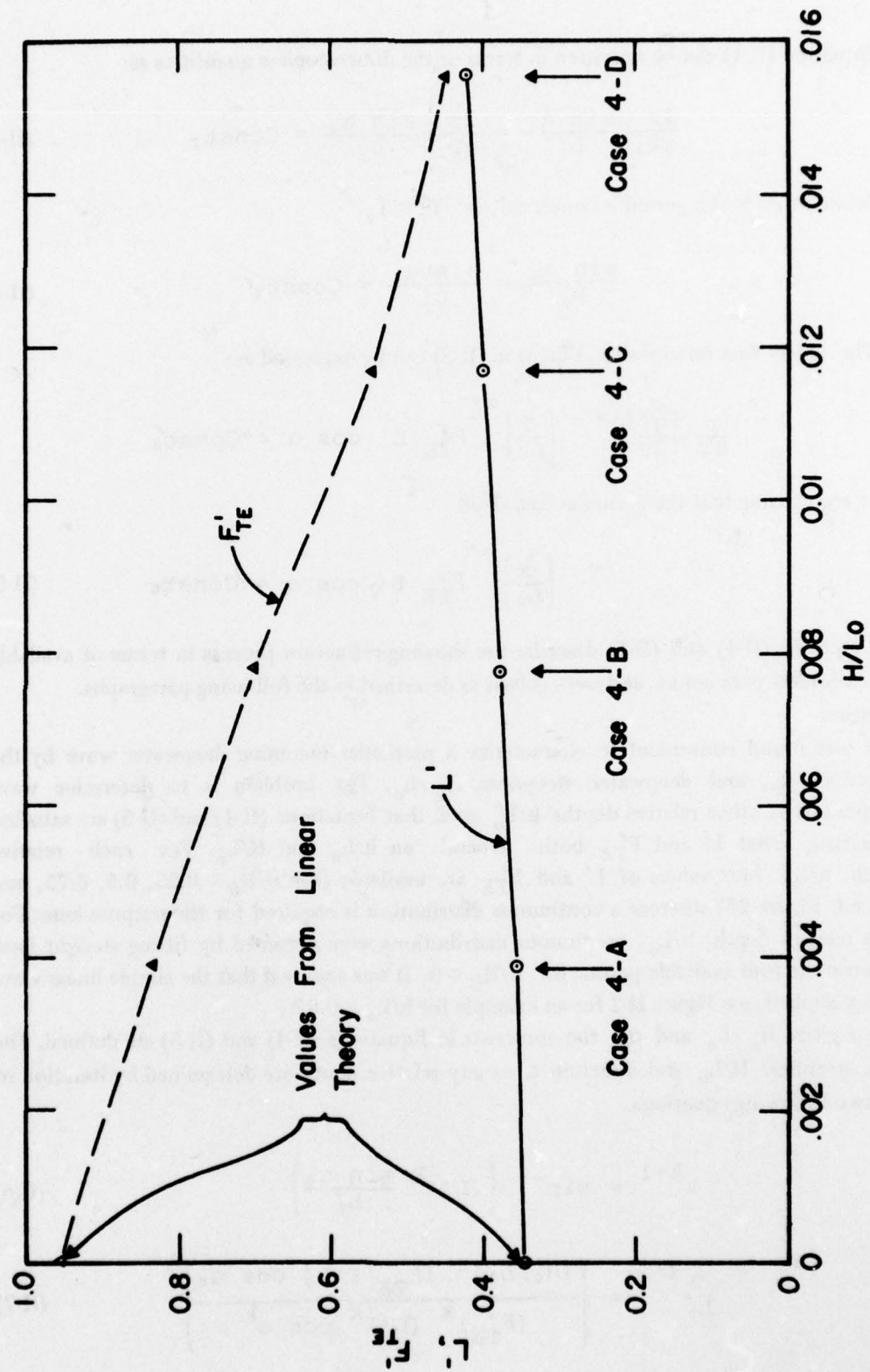


Figure II-2. Variation of F'_{TE} and L' as employed in shoaling-refraction development for $h/L_0 = 0.02$

in which the superscript $k + 1$ denotes the $(k + 1)^{th}$ iteration and applies to the improved estimates of α and H/L_o . Once these estimates are known, the parameters with the k subscripts on the right hand sides of Equations (II-8) and (II-9) are calculated and improved estimates of α and H/L_o are determined, etc. The procedure was initiated in deep water and the wave steepness and direction calculated at the remaining nine values of relative depth advancing shoreward or until breaking was indicated. At each relative depth, the iteration converged very rapidly with three or four iterations usually sufficient. For the first iteration at a relative depth, the initial value for wave steepness was taken as the final value for the preceding (greater) relative depth.

The shoaling-refraction results are presented in graphical form, for $\alpha_o = 0^\circ, 10^\circ, 20^\circ, 40^\circ$, and 60° in Figures 25, 26, 27, 28, and 29, respectively. A description of these tables is presented in Section IV and two examples illustrating their application are given in Section V.

APPENDIX III

SAMPLE SET OF WAVE TABLES FOR CASE 4-D

CASE 4-D
11TH ORDER STREAM FUNCTION WAVE THEORY

DEFINITIONS

H = WAVE HEIGHT
T = WAVE PERIOD
DPT = WATER DEPTH
LO = DEEP WATER WAVE LENGTH, CALCULATED FROM LINEAR WAVE THEORY, $LO = (G/6.28318) * T^2 * 0.02$
L = WAVE LENGTH
PSI = VALUE OF STREAM FUNCTION ON THE FREE SURFACE
G = GRAVITATIONAL CONSTANT
X(N) = NTH STREAM FUNCTION COEFFICIENT

WAVE CHARACTERISTICS

H/LO = 0.015553 DPT/LO = 0.020000

M/DPT = 0.777652

L/LO = 0.422461 PSI/(G*H*T) = -0.002296

LISTING OF DIMENSIONLESS STREAM FUNCTION COEFFICIENTS

X(1)/(H*T*G) = -0.342650E-01
X(2)/(H*T*G) = -0.123201E-01
X(3)/(H*T*G) = -0.499400E-02
X(4)/(H*T*G) = -0.201803E-02
X(5)/(H*T*G) = -0.708020E-03
X(6)/(H*T*G) = -0.298070E-03
X(7)/(H*T*G) = -0.998972E-04
X(8)/(H*T*G) = -0.343591E-04
X(9)/(H*T*G) = -0.108353E-04
X(10)/(H*T*G) = -0.304493E-05
X(11)/(H*T*G) = -0.465501E-06

TABLE 1-9 HORIZONTAL VELOCITY COMPONENT FIELD... COPIES IN EQUATION (21)

YTD TON	Q-0	10-0	20-0	30-0	50-0	75-0	100-0	125-0	100-0
OTAPAGE (CONT)	0-000 4-0 75	0-003 15-00	0-004 -0-0 15	0-101 -35-0 75	-0-005 001-1 15	-0-101 257-0 75	-0-110 21-0 5	-0-112 -24-0 45	-0-111 -30-0 75
WATERAGE	10-000 01-00	12-010 04-10	0-021 -0-0 05	1-000 -30-7 15	-0-003 0000000	-1-000 200-1 15	-1-700 12-00	-1-700 -273-2 5	-1-700 -30-0 05
1/2000 Tons 1-0	10-107 100-00								
1/2000 Tons 1-5	1-123 10-00								
1/2000 Tons 1-0	10-137 30-0 75	11-000 01-00							
1/2000 Tons 1-3	12-042 30-20	11-040 17-20							
1/2000 Tons 1-2	12-010 20-00	10-000 13-00	0-027 -0-0 20						
1/2000 Tons 1-1	12-043 23-00	10-030 10-00	0-037 -0-0 00						
1/2000 Tons 1-0	11-004 10-00	0-020 0-00	0-027 -0-1 15	2-000 -20-0 00					
1/2000 Tons 0-0	10-005 0-00	0-100 3-20	0-003 -0-0 20	2-004 -20-1 75	-0-005 0000000	-1-000 200-0 00	-1-700 13-20	-1-700 -273-2 5	-1-700 100-00
1/2000 Tons 0-5	10-113 12-00	0-750 0-20	0-070 -0-0 20	0-040 -213-0 00	0000000	-1-000 200-0 00	13-70	-1-700 -273-2 5	100-00
1/2000 Tons 0-7	0-007 0-00	0-020 -0-00	0-024 -0-0 75	2-002 -1-0 0 75	0000000	-1-000 200-0 00	14-20	-1-700 -273-2 5	-1-700 -30-7 15
1/2000 Tons 0-0	0-070 0-00	0-100 -0-00	0-007 -0-0 00	2-000 -177-0 00	-0-010 0000000	-1-000 200-0 00	14-70	-1-700 -273-2 5	-1-707 -30-0 10
1/2000 Tons 0-5	0-000 3-00	7-030 3-00	0-002 -0-0 00	2-003 -1-0 0 00	-0-023 0000000	-1-000 200-0 00	15-00	-1-700 -273-2 5	-1-700 -30-0 00
1/2000 Tons 0-0	0-002 1-75	7-040 -0-00	0-021 -0-0 00	2-070 -1-00 20	-0-001 0000000	-1-001 200-0 00	15-30	-1-700 -273-2 5	-1-700 -30-0 00
1/2000 Tons 0-3	0-030 -0-00	7-020 -0-00	0-004 -0-0 00	2-000 -1-0 0 00	-0-004 0000000	-1-000 200-0 00	15-00	-1-700 -273-2 5	-1-700 -30-0 00
1/2000 Tons 0-2	0-004 -1-20	7-031 -1-20	0-007 -0-0 00	2-005 -1-0 0 00	-0-006 0000000	-1-006 207-0 00	15-70	-1-700 -273-2 5	-1-701 -30-0 10
1/2000 Tons 0-1	0-004 -0-00	7-070 -1-10	0-075 -0-0 00	2-007 -1-00 00	-0-033 0000000	-1-003 207-0 00	15-00	-1-701 -273-2 5	-1-701 -30-0 10
1/2000 Tons 0-0	0-000 -0-20	7-004 -1-0 10	0-072 -0-0 00	2-004 -1-00 00	-0-025 0000000	-1-004 207-0 00	15-00	-1-701 -273-2 5	-1-701 -30-0 10

TABLE 11-DIMENSIONLESS VERTICAL VELOCITY COMPONENT FIELD...DEFINED IN EQUATION (22)

TIME	0.0	10.0	20.0	30.0	50.0	75.0	100.0	130.0	180.0
ETA/HEIGHT	0.009 43.7%	0.503 18.3%	0.204 -65.4%	0.101 -326.7%	-0.095 681.4%	-0.101 227.7%	-0.110 21.4%	-0.112 -232.4%	-0.111 -346.7%
SURFACE	0.0 0.00000	7.070 89.1%	6.715 77.0%	4.876 83.4%	1.430 -112.0%	6.273 0.00000	6.046 0.00000	6.012 0.00000	-0.000 0.00000
S/DEP TIME1.0	0.0 0.00000								
S/DEP TIME1.5	0.0 0.00000								
S/DEP TIME1.6	0.0 0.00000	6.530 88.2%							
S/DEP TIME1.3	0.0 0.00000	5.635 87.2%							
S/DEP TIME1.2	0.0 0.00000	4.085 86.4%	6.534 88.1%						
S/DEP TIME1.1	0.0 0.00000	4.170 88.4%	5.719 76.3%						
S/DEP TIME1.0	0.0 0.00000	3.906 84.8%	4.905 76.3%	4.106 82.5%					
S/DEP TIME0.9	0.0 0.00000	3.065 84.1%	4.316 77.7%	3.766 82.0%	1.364 -58.5%	6.269 0.00000	6.045 0.00000	6.012 0.00000	-0.000 0.00000
S/DEP TIME0.8	0.0 0.00000	2.601 83.4%	2.709 77.0%	3.244 81.6%	1.240 -51.9%	6.049 0.00000	6.043 0.00000	6.010 0.00000	-0.000 0.00000
S/DEP TIME0.7	0.0 0.00000	2.185 82.7%	3.169 76.4%	2.709 81.2%	1.104 -56.3%	6.025 0.00000	6.039 0.00000	6.000 0.00000	-0.000 0.00000
S/DEP TIME0.6	0.0 0.00000	1.609 82.2%	2.630 75.0%	2.370 68.0%	0.962 -47.0%	6.198 0.00000	6.035 0.00000	6.007 0.00000	-0.000 0.00000
S/DEP TIME0.5	0.0 0.00000	1.443 81.7%	2.143 75.4%	1.954 68.3%	0.812 -63.0%	6.169 0.00000	6.030 0.00000	6.005 0.00000	-0.000 0.00000
S/DEP TIME0.4	0.0 0.00000	1.162 81.3%	1.684 76.0%	1.549 68.2%	0.655 -43.9%	6.138 0.00000	6.025 0.00000	6.004 0.00000	-0.000 0.00000
S/DEP TIME0.3	0.0 0.00000	0.841 80.9%	1.245 74.6%	1.154 68.0%	0.496 -42.6%	6.108 0.00000	6.019 0.00000	6.003 0.00000	-0.000 0.00000
S/DEP TIME0.2	0.0 0.00000	0.503 80.7%	0.822 74.4%	0.765 68.0%	0.332 0.00000	6.071 0.00000	6.013 0.00000	6.002 0.00000	-0.000 0.00000
S/DEP TIME0.1	0.0 0.00000	0.274 80.0%	0.408 74.2%	0.382 59.7%	0.167 0.00000	6.035 0.00000	6.004 0.00000	6.001 0.00000	-0.000 0.00000
S/DEP TIME0.0	0.0 0.00000	0.0 0.00000	0.0 0.00000	0.0 0.00000	0.0 0.00000	6.0 0.00000	6.0 0.00000	6.0 0.00000	0.0 0.00000

TABLE III-DIMENSIONLESS HORIZONTAL ACCELERATION COMPONENT FIELD...DEFINED IN EQUATION (23)

TIME	0.0	10.0	20.0	30.0	50.0	75.0	100.0	130.0	180.0
ETA/MEIGHT	0.000 0.378	0.303 15.5E	0.304 -86.4E	0.101 -326.7E	-0.055 601.4E	-0.101 227.7E	-0.110 21.4E	-0.112 -202.4E	-0.111 -308.7E
SURFACE	0.0 0.000000	167.815 95.8E	165.513 90.4E	89.353 76.6E	22.552 -55.7E	4.026 0.000000	0.450 0.000000	0.490 0.000000	-0.000 0.000000
S/DEPTM=1.6	0.0 0.000000								
S/DEPTM=1.5	0.0 0.000000								
S/DEPTM=1.4	0.0 0.000000	155.000 95.5E							
S/DEPTM=1.3	0.0 0.000000	134.031 94.9E							
S/DEPTM=1.2	0.0 0.000000	116.203 94.5E	142.544 90.0E						
S/DEPTM=1.1	0.0 0.000000	101.376 93.6E	120.328 80.8E						
S/DEPTM=1.0	0.0 0.000000	86.966 92.8E	117.723 89.0E	87.724 77.6E					
S/DEPTM=0.9	0.0 0.000000	78.402 92.0E	107.624 86.2E	85.399 77.4E	24.251 -36.5E	4.194 0.000000	0.492 0.000000	0.480 0.000000	-0.000 0.000000
S/DEPTM=0.8	0.0 0.000000	69.695 91.1E	99.922 87.4E	82.971 77.1E	26.879 -31.2E	4.964 0.000000	0.702 0.000000	0.413 0.000000	-0.000 0.000000
S/DEPTM=0.7	0.0 0.000000	62.499 90.3E	91.511 86.5E	80.595 76.7E	29.087 -10.6E	5.621 0.000000	0.880 0.000000	0.159 0.000000	-0.000 0.000000
S/DEPTM=0.6	0.0 0.000000	56.617 89.4E	85.292 85.8E	78.381 76.4E	30.914 -3.0E	6.218 0.000000	1.032 0.000000	0.316 0.000000	-0.000 0.000000
S/DEPTM=0.5	0.0 0.000000	51.885 88.5E	80.180 85.0E	76.409 76.0E	32.395 2.7E	6.731 0.000000	1.158 0.000000	0.283 0.000000	-0.000 0.000000
S/DEPTM=0.4	0.0 0.000000	48.176 87.6E	76.098 84.3E	74.735 75.7E	33.562 6.8E	7.156 0.000000	1.260 0.000000	0.258 0.000000	-0.000 0.000000
S/DEPTM=0.3	0.0 0.000000	45.389 87.1E	72.988 83.8E	73.359 75.4E	34.440 9.7E	7.491 0.000000	1.339 0.000000	0.239 0.000000	-0.000 0.000000
S/DEPTM=0.2	0.0 0.000000	43.450 86.6E	70.799 83.4E	72.428 75.2E	35.032 11.6E	7.731 0.000000	1.396 0.000000	0.227 0.000000	-0.000 0.000000
S/DEPTM=0.1	0.0 0.000000	42.306 86.3E	69.500 82.1E	71.839 75.1E	35.414 12.8E	7.876 0.000000	1.439 0.000000	0.219 0.000000	-0.000 0.000000
S/DEPTM=0.0	0.0 0.000000	41.928 86.2E	69.269 83.0E	71.662 75.0E	35.533 13.1E	7.924 0.000000	1.491 0.000000	0.217 0.000000	-0.000 0.000000

CASE 4-0

TABLE 19-DIMENSIONLESS VERTICAL ACCELERATION COMPONENT FIELD...DEFINED IN EQUATION (24)

TIME	0.0	10.0	20.0	30.0	50.0	75.0	100.0	130.0	160.0
ETA/VELOCITY	0.000 0.375	0.503 15.50	0.304 -05.45	0.101 -320.75	-0.055 681.45	-0.101 227.75	-0.110 21.45	-0.112 -262.45	-0.111 -308.75
SURFACE	-115.500 06.25	-30.049 56.95	31.010 127.55	73.423 110.15	34.530 110.15	0.267 47.45	1.003 000000	-0.002 000000	-0.700 000000
S/DEPTIME=1.0	-123.444 100.00								
S/DEPTIME=1.5	-124.712 100.00								
S/DEPTIME=1.0	-120.045 00.00	-53.517 04.55							
S/DEPTIME=1.3	-113.549 00.00	-40.974 70.15							
S/DEPTIME=1.2	-104.774 04.75	-50.760 73.25	47.602 120.25						
S/DEPTIME=1.1	-95.105 00.00	-50.000 75.00	34.150 133.00						
S/DEPTIME=1.0	-85.320 00.35	-47.742 70.15	24.010 143.95	03.104 110.45					
S/DEPTIME=0.9	-75.505 00.00	-44.200 70.75	15.444 137.95	52.009 115.00	32.530 113.25	0.102 000000	1.003 000000	0.002 000000	-0.710 000000
S/DEPTIME=0.8	-65.923 00.75	-40.140 77.00	15.926 177.95	42.502 117.35	26.040 113.35	5.700 000000	1.044 000000	0.024 000000	-0.877 000000
S/DEPTIME=0.7	-56.044 00.45	-35.560 77.25	6.040 207.75	30.573 110.75	25.312 113.35	5.300 000000	1.443 000000	0.036 000000	-0.460 000000
S/DEPTIME=0.6	-47.765 00.15	-30.403 77.35	4.140 000000	27.721 120.15	21.050 113.75	4.700 000000	1.240 000000	0.041 000000	-0.363 000000
S/DEPTIME=0.5	-30.200 00.00	-25.044 77.45	2.272 000000	21.700 121.35	16.006 113.85	4.030 000000	1.037 000000	0.040 000000	-0.262 000000
S/DEPTIME=0.4	-20.040 00.45	-20.565 77.55	1.004 000000	16.613 122.55	14.369 113.95	3.304 000000	0.832 000000	0.030 000000	-0.212 000000
S/DEPTIME=0.3	-22.006 00.45	-15.432 77.65	0.405 000000	11.989 123.45	10.793 114.05	2.820 000000	0.436 000000	0.029 000000	-0.182 000000
S/DEPTIME=0.2	-15.200 00.35	-10.280 77.35	0.082 000000	7.773 124.15	7.195 114.15	1.700 000000	0.419 000000	0.020 000000	-0.090 000000
S/DEPTIME=0.1	-7.569 00.25	-5.143 000000	-0.014 000000	3.021 000000	3.574 000000	0.856 000000	0.210 000000	0.011 000000	-0.041 000000
S/DEPTIME=0.0	0.0 000000	0.0 000000	0.0 000000	0.0 000000	0.0 000000	0.0 000000	0.0 000000	0.0 000000	0.0 000000

CASE 4-9

TABLE V-DIMENSIONLESS DRAG FORCE COMPONENT FIELD.....DEFINED IN EQUATION (25)

TIME	0.0	10.0	20.0	30.0	50.0	70.0	100.0	130.0	160.0
ETA/WEIGHT	0.009 63.7E	0.003 15.5E	0.284 -66.6E	0.101 -386.7E	-0.009 681.0E	-0.101 227.7E	-0.110 21.6E	-0.112 -282.6E	-0.111 -386.7E
SURFACE	242.394 95.0E	110.799 12.1E	37.694 -155.2E	7.722 0.000E	-0.254 0.000E	-2.101 0.000E	-2.044 0.000E	-2.091 0.000E	-2.019 0.000E
1/DEPTIME1.0	200.482 104.0E								
1/DEPTIME1.5	176.432 106.0E								
1/DEPTIME1.4	154.349 29.4E	111.081 5.9E							
1/DEPTIME1.3	133.294 24.2E	98.411 0.4E							
1/DEPTIME1.2	115.203 20.0E	84.495 -3.4E	26.345 -124.1E						
1/DEPTIME1.1	96.729 16.1E	75.607 -7.0E	32.170 -128.6E						
1/DEPTIME1.0	84.133 12.5E	64.340 -15.3E	29.997 -121.9E	7.423 0.000E					
1/DEPTIME0.9	74.105 9.2E	57.628 -13.2E	26.843 -121.3E	6.957 0.000E	-0.207 0.000E	-2.134 0.000E	-2.790 0.000E	-2.090 0.000E	-2.077 0.000E
1/DEPTIME0.8	63.335 6.3E	49.678 -15.9E	22.721 -121.0E	6.400 0.000E	-0.143 0.000E	-1.873 0.000E	-2.480 0.000E	-2.586 0.000E	-2.560 0.000E
1/DEPTIME0.7	53.576 3.7E	42.324 -16.2E	20.639 -120.8E	5.744 0.000E	-0.097 0.000E	-1.620 0.000E	-2.165 0.000E	-2.263 0.000E	-2.241 0.000E
1/DEPTIME0.6	44.624 1.5E	39.444 -20.3E	17.597 -120.7E	5.040 0.000E	-0.044 0.000E	-1.374 0.000E	-1.851 0.000E	-1.939 0.000E	-1.922 0.000E
1/DEPTIME0.5	36.310 -9.4E	28.997 -22.0E	14.595 -120.6E	4.300 0.000E	-0.044 0.000E	-1.136 0.000E	-1.540 0.000E	-1.616 0.000E	-1.603 0.000E
1/DEPTIME0.4	28.695 -2.5E	22.864 -23.6E	11.629 0.000E	3.493 0.000E	-0.029 0.000E	-0.901 0.000E	-1.230 0.000E	-1.293 0.000E	-1.283 0.000E
1/DEPTIME0.3	21.658 -3.2E	16.931 -26.5E	8.693 0.000E	2.655 0.000E	-0.019 0.000E	-0.672 0.000E	-0.921 0.000E	-0.969 0.000E	-0.962 0.000E
1/DEPTIME0.2	13.893 -4.0E	11.193 0.000E	5.722 0.000E	1.781 0.000E	-0.011 0.000E	-0.446 0.000E	-0.616 0.000E	-0.646 0.000E	-0.642 0.000E
1/DEPTIME0.1	6.993 0.000E	5.548 0.000E	2.837 0.000E	0.895 0.000E	-0.005 0.000E	-0.222 0.000E	-0.307 0.000E	-0.323 0.000E	-0.321 0.000E
1/DEPTIME0.0	0.0 0.000E	0.0 0.000E	0.0 0.000E	0.0 0.000E	0.0 0.000E	0.0 0.000E	0.0 0.000E	0.0 0.000E	0.0 0.000E

TABLE VI—Dimensionless inertia force component fields...defined in equation (20)

115

TABLE VII-DIMENSIONLESS DRAG MOMENT COMPONENT FIELD.....DEFINED IN EQUATION (27)

TIME	0.0	10.0	20.0	30.0	50.0	75.0	100.0	130.0	180.0
ETA/HEIGHT=	0.000 03.7%	0.003 15.5%	0.204 -85.4%	0.101 -380.7%	-0.055 001.4%	-0.101 227.7%	-0.110 21.4%	-0.112 -102.4%	-0.111 -340.7%
SURFACE	200.000 70.0%	102.439 26.2%	23.042 -190.0%	3.424 00000%	-0.179 00000%	-1.001 00000%	-1.309 00000%	-1.309 00000%	-1.330 00000%
S/DEP Time1.4	213.007 100.0%								
S/DEP Time1.5	167.232 100.0%								
S/DEP Time1.4	130.000 30.7%	91.200 17.1%							
S/DEP Time1.3	102.377 30.0%	72.163 9.0%							
S/DEP Time1.2	70.041 20.0%	50.230 5.0%	22.243 -126.0%						
S/DEP Time1.1	61.030 23.7%	46.000 0.4%	10.903 -120.3%						
S/DEP Time1.0	47.440 10.2%	30.900 -3.9%	10.201 -122.0%	3.310 00000%					
S/DEP Time0.9	36.207 14.0%	27.707 -7.0%	10.204 00000%	2.079 00000%	-0.130 00000%	-0.090 00000%	-1.200 00000%	-1.310 00000%	-1.200 00000%
S/DEP Time0.8	27.044 11.0%	20.043 -11.0%	9.411 00000%	2.403 00000%	-0.000 00000%	-0.760 00000%	-0.900 00000%	-1.030 00000%	-1.030 00000%
S/DEP Time0.7	10.716 7.4%	10.425 -14.0%	7.209 00000%	1.907 00000%	-0.046 00000%	-0.570 00000%	-0.701 00000%	-0.702 00000%	-0.702 00000%
S/DEP Time0.6	13.402 0.3%	10.001 00000%	0.321 00000%	1.470 00000%	-0.006 00000%	-0.410 00000%	-0.507 00000%	-0.502 00000%	-0.500 00000%
S/DEP Time0.5	0.310 00000%	7.402 00000%	3.070 00000%	1.002 00000%	-0.014 00000%	-0.207 00000%	-0.300 00000%	-0.404 00000%	-0.400 00000%
S/DEP Time0.4	0.704 00000%	0.430 00000%	2.330 00000%	0.400 00000%	-0.007 00000%	-0.101 00000%	-0.240 00000%	-0.250 00000%	-0.204 00000%
S/DEP Time0.3	3.109 00000%	2.009 00000%	1.307 00000%	0.300 00000%	-0.003 00000%	-0.101 00000%	-0.130 00000%	-0.140 00000%	-0.140 00000%
S/DEP Time0.2	1.300 00000%	1.123 00000%	0.379 00000%	0.170 00000%	-0.001 00000%	-0.040 00000%	-0.001 00000%	-0.005 00000%	-0.004 00000%
S/DEP Time0.1	0.340 00000%	0.270 00000%	0.144 00000%	0.040 00000%	-0.002 00000%	-0.011 00000%	-0.010 00000%	-0.010 00000%	-0.010 00000%
S/DEP Time0.0	0.0 00000%	0.0 00000%	0.0 00000%	0.0 00000%	0.0 00000%	0.0 00000%	0.0 00000%	0.0 00000%	0.0 00000%

TABLE VIII-DIMENSIONLESS INERTIA MOMENT COMPONENT FIELD...DEFINED IN EQUATION (28)

TIME	3.0	10.0	20.0	30.0	50.0	75.0	100.0	130.0	180.0
ETA/HEIGHT	0.889 63.7%	0.983 15.5%	0.884 -65.4%	0.101 -326.7%	-0.095 681.4%	-0.101 227.7%	-0.110 21.4%	-0.112 -742.4%	-0.111 -348.7%
SURFACE	0.0 0.0000	101.722 94.0%	78.463 84.7%	47.457 63.3%	13.453 -91.6%	2.520 0.0000	0.401 0.0000	0.142 0.0000	-0.000 0.0000
S/DEPTIME1.6	0.0 0.0000								
S/DEPTIME1.5	0.0 0.0000								
S/DEPTIME1.4	0.0 0.0000	89.481 93.2%							
S/DEPTIME1.3	0.0 0.0000	89.908 92.4%							
S/DEPTIME1.2	0.0 0.0000	54.370 91.7%	74.826 87.9%						
S/DEPTIME1.1	0.0 0.0000	41.867 91.1%	59.188 87.3%						
S/DEPTIME1.0	0.0 0.0000	31.888 90.4%	46.232 86.7%	40.201 76.7%					
S/DEPTIME0.9	0.0 0.0000	23.049 89.6%	35.531 86.1%	31.974 76.4%	12.214 -6.0%	2.441 0.0000	0.395 0.0000	0.136 0.0000	-0.000 0.0000
S/DEPTIME0.8	0.0 0.0000	17.659 89.1%	26.755 85.5%	24.817 76.2%	17.040 -1.2%	2.053 0.0000	0.344 0.0000	0.098 0.0000	-0.000 0.0000
S/DEPTIME0.7	0.0 0.0000	12.704 88.5%	19.616 85.0%	18.681 76.0%	7.941 2.7%	1.626 0.0000	0.285 0.0000	0.049 0.0000	-0.000 0.0000
S/DEPTIME0.6	0.0 0.0000	8.835 88.0%	13.871 84.5%	13.514 75.7%	5.990 5.7%	1.272 0.0000	0.223 0.0000	0.048 0.0000	-0.000 0.0000
S/DEPTIME0.5	0.0 0.0000	5.852 87.5%	9.321 84.1%	9.257 75.5%	4.249 0.0000	0.916 0.0000	0.162 0.0000	0.031 0.0000	-0.000 0.0000
S/DEPTIME0.4	0.0 0.0000	3.401 0.0000	5.805 83.7%	5.856 75.4%	2.765 0.0000	0.603 0.0000	0.108 0.0000	0.019 0.0000	-0.000 0.0000
S/DEPTIME0.3	0.0 0.0000	1.964 0.0000	3.106 0.0000	3.246 0.0000	1.575 0.0000	0.347 0.0000	0.063 0.0000	0.010 0.0000	-0.000 0.0000
S/DEPTIME0.2	0.0 0.0000	0.854 0.0000	1.359 0.0000	1.441 0.0000	0.706 0.0000	0.157 0.0000	0.028 0.0000	0.004 0.0000	-0.000 0.0000
S/DEPTIME0.1	0.0 0.0000	0.211 0.0000	0.346 0.0000	0.359 0.0000	0.177 0.0000	0.030 0.0000	0.007 0.0000	0.001 0.0000	-0.000 0.0000
S/DEPTIME0.0	0.0 0.0000	0.0 0.0000	0.0 0.0000	0.0 0.0000	0.0 0.0000	0.0 0.0000	0.0 0.0000	0.0 0.0000	0.0 0.0000

TABLE 1X-DIMENSIONLESS DYNAMIC PRESSURE COMPONENT FIELD...DEFINED IN EQUATION (29)

TIME	0.0	10.0	20.0	30.0	50.0	70.0	100.0	130.0	160.0
ETA/HEIGHT	0.000 0.000	0.003 10.00	0.004 00.00	0.001 -00.00	-0.006 001.00	-0.001 007.00	-0.010 01.00	-0.012 -00.00	-0.011 -00.00
SURFACE	1.710 00.00	1.100 20.00	0.500 -00.00	0.211 -00.00	-0.112 070.00	-0.203 000.00	-0.225 00.00	-0.226 -00.00	-0.226 -00.00
S/DEP TH=1.0	1.000 100.00								
S/DEP TH=1.5	1.070 100.00								
S/DEP TH=1.0	1.000 100.00								
S/DEP TH=1.3	1.017 100.00								
S/DEP TH=1.2	1.040 100.00								
S/DEP TH=1.1	1.000 100.00								
S/DEP TH=1.0	1.000 100.00								
S/DEP TH=0.9	1.070 100.00								
S/DEP TH=0.8	1.130 100.00								
S/DEP TH=0.7	1.001 100.00								
S/DEP TH=0.6	1.000 100.00								
S/DEP TH=0.5	1.000 100.00								
S/DEP TH=0.4	1.000 100.00								
S/DEP TH=0.3	1.001 100.00								
S/DEP TH=0.2	1.000 100.00								
S/DEP TH=0.1	1.000 100.00								
S/DEP TH=0.0	1.000 100.00								

CASE 4-0
TABLE 2-VARIABLES DEPENDING ONLY ON PHASE ANGLE

THETA=	0.0	10.0	20.0	30.0	50.0	75.0	100.0	130.0	180.0
(1) DIMENSIONLESS KINEMATIC FREE SURFACE BOUNDARY CONDITION ERROR, LINEAR WAVE THEORY REPRESENTATION... DEFINED IN EQ.(35)									
SURFACE	0.0	0.035157	0.063467	0.080976	0.070797	0.032082	-0.018251	-0.042202	-0.080000
(2) DIMENSIONLESS KINEMATIC FREE SURFACE BOUNDARY CONDITION ERROR, STREAM FUNCTION THEORY REPRESENTATION... DEFINED IN EQ.(35)									
SURFACE	0.0	-0.000001	-0.000000	-0.000000	-0.000000	-0.000000	0.000000	0.000000	-0.000000
(3) DIMENSIONLESS DYNAMIC FREE SURFACE BOUNDARY CONDITION ERROR, LINEAR WAVE THEORY REPRESENTATION... DEFINED IN EQ.(36)									
SURFACE	0.038509	0.030640	0.030915	0.022104	-0.000722	-0.020406	-0.033132	0.000406	0.028376
(4) DIMENSIONLESS DYNAMIC FREE SURFACE BOUNDARY CONDITION ERROR, STREAM FUNCTION THEORY REPRESENTATION... DEFINED IN EQ.(37)									
SURFACE	0.020000	-0.011249	-0.010005	-0.003093	0.000660	0.000236	0.001999	0.001250	0.000322

CASE 4-0
TABLE XI-OVERALL WAVE PARAMETERS... DC NOT DEPEND ON PHASE ANGLE OR ELEVATION

(1) DIMENSIONLESS WAVE LENGTH... DEFINED IN EQUATION (37)	0.422 (17.0E)
(2) DIMENSIONLESS AVERAGE POTENTIAL ENERGY.... DEFINED IN EQUATION (38)	0.213 (-134.0E)
(3) DIMENSIONLESS AVERAGE KINETIC ENERGY.... DEFINED IN EQUATION (39)	0.256 (-101.0E)
(4) DIMENSIONLESS TOTAL AVERAGE ENERGY.... DEFINED IN EQUATION (40)	0.467 (-110.0E)
(5) DIMENSIONLESS TOTAL AVERAGE ENERGY FLUX.... DEFINED IN EQUATION (41)	0.447 (-110.1E)
(6) DIMENSIONLESS GROUP VELOCITY.... DEFINED IN EQUATION (42)	0.957 (-0.0E)
(7) DIMENSIONLESS TOTAL AVERAGE MOMENTUM.... DEFINED IN EQUATION (43)	0.505 (-90.5E)
(8) DIMENSIONLESS TOTAL AVERAGE MOMENTUM FLUX IN WAVE DIRECTION.... DEFINED IN EQUATION (44)	0.403 (-136.0E)
(9) DIMENSIONLESS TOTAL AVERAGE MOMENTUM FLUX TRANSVERSE TO WAVE DIRECTION... DEFINED IN EQUATION (45)	0.156 (-189.5E)

CASE 4-D

TABLE XI (CONTINUED) - CYBERBALL HAVE PARAMETERS... DO NOT DEPEND ON PHASE ANGLE OR ELEVATION

(10) DIMENSIONLESS ROOT MEAN SQUARE KINEMATIC FREE SURFACE BOUNDARY CONDITION ERROR.... DEFINED IN EQUATION (46)
 LINEAR 0.047488
 STREAM FUNCTION 0.000000

(11) DIMENSIONLESS ROOT MEAN SQUARE DYNAMIC FREE SURFACE BOUNDARY CONDITION ERROR.... DEFINED IN EQUATION (47)
 LINEAR 0.024001
 STREAM FUNCTION 0.004032

(12) DIMENSIONLESS MAXIMUM KINEMATIC FREE SURFACE BOUNDARY CONDITION ERROR.... DEFINED IN EQUATION (46)
 LINEAR 0.005603
 STREAM FUNCTION 0.000001

(13) DIMENSIONLESS MAXIMUM DYNAMIC FREE SURFACE BOUNDARY CONDITION ERROR.... DEFINED IN EQUATION (47)
 LINEAR 0.038509
 STREAM FUNCTION 0.028890

(14) DIMENSIONLESS KINEMATIC FREE SURFACE BREAKING PARAMETER.... DEFINED IN EQUATION (48)
 LINEAR 0.459147
 STREAM FUNCTION 0.732602

(15) DIMENSIONLESS DYNAMIC FREE SURFACE BREAKING PARAMETER.... DEFINED IN EQUATION (49)
 LINEAR 0.040894
 STREAM FUNCTION 0.286105